Transient Free Convection in Micropolar Fluid with Heat Generation and Constant Heat Flux

A Thesis
Submitted for the partial fulfillment of the degree of
Master of philosophy
In
Mathematics

By
Gazi Mamunar Rashid
Roll No. 1051501, January 2010

to

Department of Mathematics
Khulna University of Engineering & Technology
Khulna-9203, Bangladesh

December, 2012.

Dedication

To my beloved mother who always dream my success.

Declaration

I hereby declare that the thesis entitled "Transient Free Convection in Micropolar Fluid with Heat Generation and Constant Heat Flux" submitted for the partial fulfillment for the Master of philosophy degree is done by myself under the supervision of Professor Dr. Mohammad Arif Hossain as supervisor and is not submitted elsewhere for any other degree or diploma.

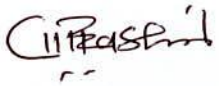

(Gazi Mamunar Rashid)
Roll No. 1051501, Session: January 2010

Counter signed by

Supervisor

(Professor Dr. Mohammad Arif Hossain)
Department of Mathematics
Khulna University of Engineering & Technology
Khulna-9203, Bangladesh

Approval

We the Examination committee do here by recommend that the thesis prepared by Gazi Mamunar Rashid, Roll No. 1051501 to be accepted as the partial fulfillment of the requirement of the Master of Philosophy(M. Phil.) degree in Mathematics.

Committee Members:

1. Prof. Dr. M. Arif Hossain
   Supervisor
   Department of Mathematics
   Khulna University of Engineering & Technology
   Khulna-9203, Bangladesh.
   — Chairman — 27.12.12

2. Head
   Department of Mathematics
   Khulna University of Engineering & Technology
   Khulna-9203, Bangladesh.
   — Member — 29/12/12

3. Prof. Dr. Fouzia Rahman.
   Department of Mathematics
   Khulna University of Engineering & Technology
   Khulna-9203, Bangladesh
   — Member

4. Dr. M. M. Touhid Hossain.
   Department of Mathematics
   Khulna University of Engineering & Technology
   Khulna-9203, Bangladesh
   — Member

5. Prof. Dr. Md. Mahmud Alam
   Mathematics Discipline
   Khulna University
   Khulna-9208, Bangladesh
   — Member (External) — 27.12.12

Acknowledgement

I would like to express my deepest gratitude and appreciation to my Supervisor Dr. Mohammad Arif Hossain, professor, Department of Mathematics, Khulna University of Engineering & Technology, Khulna-9203, Bangladesh for his willingness to accept me as a M. Phil student and for his constant supervision, invaluable instructions and never-ending encouragement in preparing this thesis. I would also like to thank my supervisor for his earnest feelings and helps in matter concerning my academic affairs.

I take the opportunity to express my great indebtedness to Professor Dr. Md. Abul Kalam Azad, Head, Department of Mathematics, khulna University of Engineering & Technology, Khulna for his help in matter concerning academic affairs.

I would like to thank all other teachers of Department of Mathematics, khulna University of Engineering & Technology, Khulna for their necessary advice and cordial co-operation during the period of study. I would like to thank all other research students and all of my friends for their help in many aspects.

Finally, I would like to express that my profound debts to my parents and specially my wife Shamima Sultana who always inspired me to make the thesis are also unlimited.

The author

Abstract

In this thesis, the transient free convection in micropolar fluid with heat generation and constant heat flux is discussed. The governing equations are set. To solve them two different techniques namely, the finite difference method and Laplace transform method, has been adopted. Before use of the finite difference method the governing equations are made dimensionless. The solutions obtained are plotted and discussed. The values proportional to the coefficient of skin friction and Nusselt number are also tabulated and discussed. The Laplace transform method is also used to the set of equations which are linearized by dropping the convective terms. For inverse Laplace transform Mathematica is used. The solutions of the linearized form of the equations are also plotted and discussed.

Table of Content

List of Figures

List of Tables

Chapter 1

Introduction

The concept of micropolar fluids introduced by Eringen [1] deals with a class of fluids which exhibit certain microscopic effects arising from the local structure and micromotions of the fluid elements. These fluids contain dilute suspensions of rigid macromolecules with individual motions which support stress and body moments and are influenced by spin-inertia. Zakaria [2] pointed that the theory of micropolar fluid and its extension to thermo-micropolar fluids [3] may form suitable non-Newtonian fluid models which can be used to analyze the behavior of exotic lubricants [4,5], colloidal suspensions or polymeric fluids [6], liquid crystals [7,8] and animal blood [9]. Some theoretical studies [7–9] have been compared and favorably agree with experimental measurement. Furthermore, Kolpashchikov et al. [10] have devised a way to measure micropolar parameters experimentally. However, more experimental and theoretical work is still required in this area. A thorough review of the subject and application of micropolar fluid mechanics was provided by Arman et al. [11,12].Crane [13] considered a moving strip the velocity of which is proportional to the local distance. Free convection in the boundary layer flow of a micropolar fluid along a vertical wavy surface was investigated by Chiu and Chou [14]. Hassanien and Gorla [15] studied the heat transfer to a micropolar fluid from a non-isothermal stretching sheet with suction and blowing. Mixed convection boundary layer flow of a micropolar fluid on a horizontal plate was derived by Gorla [16]. The theory of micropolar fluids as introduced by Eringen [1] can be used to explain the flow of colloidal fluids, liquid crystals, animal blood, paints, polymers, etc. in which the classical Newtonian fluids theory is inadequate. Ramachandran et al. [17] studied laminar mixed convection in two-dimensional stagnation flows around heated surfaces by considering both cases of an arbitrary wall temperature and arbitrary surface heat flux variations. They found that a reversed flow developed in the buoyancy opposing flow region, and dual solutions are found to exist for a certain range of the buoyancy parameter. This work was then extended by Hassanien and Gorla [18] to micropolar fluids. They also considered both assisting and opposing flows, but the existence of dual solutions was not reported. Devi et al. [19] extended the problem posed by Ramachandran et al. [17] to the unsteady case, and they found that dual solutions exist for a certain range of the buoyancy parameter when the flow is opposing. Recently, Lok et al. [20,21] studied the similar

problem for steady and unsteady cases, for a vertical surface immersed in a micropolar fluid. As the previous investigations, the existence of dual solutions was reported in [20] only for the opposing flow regime. The flow through porous channels with expanding or contracting walls has become very important because of its applications in biophysical flows, e.g., pulsating diaphragms, filtration, blood flow, artificial dialysis, binary gas diffusion, and air and blood circulation in the respiratory system. Uchida and Aoki [22] first examined the viscous flow inside an impermeable tube with contracting cross sections. Ohki [23] investigated the unsteady flow in a porous semi-infinite tube, whose elastic wall had a varied length and a stable cross section. To simulate the laminar flow field in cylindrical solid rocket motors, Goto and Uchida [24] analyzed the laminar incompressible flow in a semi-infinite porous pipe, whose radius varied with time. Bujurke et al. [25] obtained a series solution to the unsteady flow in a contracting or expanding pipe. Majdalani et al. [26] obtained an exact similarity solution to the viscous flow with small wall contractions or expansions and weakly permeability. Dauenhauer and Majdalani [27] obtained a numerical solution and Majdalani and Zhou [28] got both numerical and asymptotical solutions for moderate to large Reynolds numbers.

Physically micropolar fluids represent fluids consisting of randomly oriented particles suspended in a viscous medium, where the deformation of fluid particles is ignored It has found its applications specially, in lubrication theory. Soundalgekar [29] obtained approximate solutions for the two dimensional flow of an incompressible, viscous fluid flow past an infinite porous vertical plate with constant suction velocity normal to the plate. It was found that the difference between the temperature of the plate and the free stream is significant to cause the free convection currents. Natural convection driven by thermal dispersion and internal heat generation plays important role in the overall heat transfer. Natural convection with internal heat generation finds application in fire and combustion modeling. Gorla and Tornabene [30] investigated the effects of thermal radiation on mixed convection flow over a vertical plate with non-uniform heat flux boundary condition. Raptis [31] studied numerically the case of a steady two dimensional flow of a micropolar fluid past a continuously moving plate with a constant velocity in the presence of thermal radiation. Kim [32] studied the unsteady free convection flow of a micropolar fluid through a porous medium bounded by an infinite vertical plate. Kim and Fedorov [33] studied the transient mixed radiative convection flow of a micropolar fluid past a moving, semi-infinite vertical porous plate. El-Amin [34] studied the combined

effect of internal heat generation and magnetic field on free convection and mass transfer flow in a micropolar fluid with constant suction. El-Hakiem [35] studied the natural convection in a micropolar fluid with thermal dispersion and internal heat generation.

1.1 Some Useful Dimensionless Parameters

Reynolds number (R_e)

The Reynold's number (R_e), the most important parameter of the dynamics of a viscous fluid, which represents the ratio of the inertia force to viscous force and is defined as

$$R_e = \frac{Inertia\ force}{Viscous\ force} = \frac{\rho U^2 L^2}{\mu UL} = \frac{UL}{\upsilon}$$

where U and L denotes the characteristic velocity and length respectively and $\upsilon = \frac{\mu}{\rho} is$ the kinematic viscosity (ρ and μ are the density and coefficient of viscosity of the fluid respectively). When the Reynolds number of the system is small, the viscous force is predominant and the effect of viscosity with be felt in the whole velocity field. When the Reynolds number is large the inertial force is predominant and the effects of viscosity is important only in a narrow region near the solid wall or other restricted region which is known as boundary layer. If the Reynolds numbers is enormously large, the flow becomes turbulent.

Prandtl number (P_r)

The Prandtl number is the ratio of kinematic viscosity to thermal diffusivity and may be written as follows

$$P_r = \frac{Kinematic\ vis\cos ity}{Thermal\ diffusivity} = \frac{\upsilon}{k/\rho C_p}$$

where C_p is the specific heat at the constant pressure and k is the thermal conductivity.

The value of $\frac{k}{\rho C_p}$ is the thermal diffusivity due to the heat conduction. The smaller value of that is, the narrower is the region which is affected by the heat conduction and it is known as the thermal boundary layer. The value of $\upsilon = \frac{\mu}{\rho}$ is the effect of viscosity of fluid. Thus the Prandtl number shows the relative importance of heat conduction and

viscosity of a fluid. For a gas the Prandtl number is of order of unity. Evidently, P_r varies from fluid to fluid, for air P_r = 0.71 (approx.), for water at 15.5 ^{0}C, P_r = 7.00 (approx.), for mercury P_r = 0.044 (approx.), but for high viscous fluid it may be very large, e.g. for glycerin P_r = 7250 (approx.).

Schmidt number (S_c)

Schmidt number is a dimensionless number defined as the ratio of momentum diffusivity (viscosity) and mass diffusivity and is used to characterize fluid flow in which there are simultaneous momentum and mass diffusion convection processes. It physically relates the relative thickness of the hydrodynamic layer and mass transfer boundary layer.

Schmidt number is the mass transfer equivalent of Prandtl number. For gasses, S_c and Pr have similar values (≈ 0.7) and this is used as the basis for simple heat and mass transfer analogies.

The ratio of the viscous diffusivity to the chemical molecular diffusivity and is defined as

$$S_c = \frac{Viscous\ diffusivity}{Chemical\ molecular\ diffusivity} = \frac{\upsilon}{D_m}$$

Grashof number (G_r)

It frequently arises in the study of situations involving natural convection. The volume expansion coefficient β is defined as $\beta = -\frac{1}{\rho}\left(\frac{\partial \rho}{\partial T}\right)_p$

The Grashof number G_r is defined as

$$G_r = \frac{\nu g * \beta(T_s - T_\alpha)}{U_0^{\ 3}}$$

and is a measure of the relative importance of the buoyancy forces and viscous forces.

Eckert number (E_c)

The Eckert number E_c is useful in determining the relative importance in a heat transfer situation of the kinetic energy of a flow. It is the ratio of the kinetic energy to the enthalpy(or the dynamic temperature to the temperature) driving force for heat transfer

$E_c = \frac{U^2}{c_p \Delta T}$, U is the fluid velocity outside the boundary layer, c_p is the specific heat at constant pressure and ΔT is the driving force for heat transfer (e.g. wall temperature minus free stream temperature).

Dufour number (D_u)

The Dufour number D_u is defined as

$D_u = \frac{D_m k_T (C_w - C_\infty)}{c_s c_p (T_w - T_\infty)}$, k_T Thermal diffusion ratio, D_m molecular diffusivity and c_s concentration susceptibility.

Soret number (S_r)

The Soret number S_r is defined as $S_r = \frac{D_m k_T (T_w - T_\infty)}{c_s T_m (C_w - C_\infty)}$, T_m mean temperature.

Nusselt number (N_u)

Nusselt number is defined as the ratio of convection heat transfer to fluid conduction heat transfer under the same conditions

$$N_u = \frac{h(T_w - T_\infty)}{k_f (T_w - T_\infty)/L} = \frac{hL}{k_f}$$

k_f thermal conductivity of the fluid, h convective heat transfer coefficient, L characteristic length.

It can be also put in the form $N_u = \frac{-1}{\Delta T}\left(\frac{\partial T}{\partial y}\right)_{y=0}$.

1.2 Heat and Mass Transfer

Combined heat and mass transfer problems are of importance in many processes and have therefore received a considerable amount of attention. In many mass transfer processes, heat transfer considerations arise owing to chemical reaction and are often due to the nature of the process. In processes such as drying, evaporation at the surface water body, energy transfer in a wet cooling tower and the flow in a desert cooler, heat and mass transfer occur simultaneously. In many of these processes, the interest lies in the

determination of the total energy transfer, although in processes such as drying, the interest lies mainly in the overall mass transfer for moisture removal. Natural convection processes involving the combined mechanisms are also encountered in many natural processes, such as evaporation, condensation and agricultural drying, in many industrial applications involving solutions and mixtures, in the absence of an externally induced flow, and in many chemical processing systems. In many processes such as the curing of plastics, cleaning and chemical processing of materials relevant to the manufacture of printed circuitry, manufacture of pulp-insulated cables etc., the combined buoyancy mechanisms arise and the total energy and material transfer resulting from the combined mechanisms, has to be determined.

The basic problem is governed by the combined buoyancy effects arising from the simultaneous diffusion of thermal energy and of chemical species. Therefore the continuity, momentum, energy and concentration equations are coupled through the buoyancy terms alone, if the other effects, such as the Soret and Dufour effects are neglected. This would again be valid for low species concentration levels. These additional effects have also been considered in several investigations, for example, the work of Caldwel [36], Groots and Mozur [37], Hurle and Jakeman [38] and Legros, et al. [39,40].

Somers [41] considered combined buoyancy mechanisms for flow adjacent to a wet isothermal vertical surface in an unsaturated environment. Uniform temperature and uniform species concentration at the surface were assumed and an integral analysis was carried out to obtain results which are expected to be valid for P_r and S_c values around 1.0 with one buoyancy effect being small compared with the other. Gill et al. [42] and Lowell and Adams [43] also considered this problem, including additional effects such as appreciable normal velocity at the surface and comparable species concentrations in the mixture. Similar solutions were investigated by Lowel and Adams [43] and by Adams and Lowell [44]. Light foot [45] and Saville and Churchill [46] considered some asymptotic solutions. Adams and McFadden [47] presented experimental measurements of heat and mass transfer parameters, with opposed buoyancy effects. Gebhart and Pera [48] studied laminar vertical natural convection flows resulting from the combined buoyancy mechanisms in terms of similarity solutions. Similar analyses have been carried out by Pera and Gebhart [49] for flow over horizontal surfaces.

Mollendrof and Gebhart [50] carried out a similar analysis for axisymetric flows. The governing equations were solved for the combined effects of thermal and mass diffusion in an axisymetric plume flow. Tenner and Gebhart [51], Hubbell and Gebhart [52] and Boura and Gebhart [53] have studied buoyant free boundary flows in a concentration-stratified medium. Agrawal et al. [54, 55] have studied the combined buoyancy effects on the thermal and mass diffusion on MHD natural convection flows, and it is observed that, for the fixed G_r and P_r, the value of X_t (dimensionless length parameter) decreases as the strength of the magnetic parameter increases. Georgantopoulos et al. [56] discussed the effects of free convective and mass transfer in a conducting liquid, when the fluid is subjected to a transverse magnetic field. Haldavnekar and Soundalgekar [57] studied the effects of mass transfer on free convective flow of an eclectically conducting viscous fluid past an infinite porous plate with constant suction and transversely applied magnetic field. An exact analysis was made by Soundalgekar et al. [58] of the effects of mass transfer and the free convection currents of the MHD Stokes (Rayleigh) problem for the flow of an electrically conducting incompressible viscous fluid past an impulsively started vertical plate under the action of a transversely applied magnetic field. They neglected the heat due to viscous and Joule dissipation and induced magnetic field.

During the course of discussion, the effects of heating $G_r < 0$ of the plate by free convection currents , and G_m (modified Grashof number), S_c and M on the velocity and the skin friction are studied. Nanousis and Goudas [59] have studied the effects to mass transfer on free convective problem in the Stokes problem for an infinite vertical limiting surface. Raptis and Kafoussias [60] presented the analysis of free convection and mass transfer of steady hydromagnetic flow of an electrically conducting viscous incompressible fluid through a porous medium, occupying a semi-infinite region of the space boundary by an infinite vertical and porous plate under the action of transverse magnetic field. Approximate solutions have been obtained for the velocity, temperature, concentration field and the rate of heat transfer. The effects of different parameters on the velocity field and the rate of heat transfer are discussed for the case of air (Prandtl number $P_r = .71$) and the water vapour (Schmidt number $S_c = .60$). Raptis and Tzivanidis [61] consider the effects of variable suction/injection on the unsteady two dimensional free convective flow with mass transfer of an eclectically conducting fluid past a vertical accelerated plate in the presence of transverse magnetic field. Solutions of the equations

governing the flow are obtained with the power series. An analysis of two dimensional steady free convective flow of a conducting fluid, in presence of a magnetic field and a foreign mass, past an infinite vertical porous and unmoving surface is carried out by Raptis [62], when the heat flux is constant at the limiting surface and the magnetic Reynolds number of the flow is not small. Assuming constant suction at the surface, approximate solutions of the coupled nonlinear equations are derived for the velocity field, the temperature field, the magnetic field and for their related quantities. Agrawal et al. [63] consider the steady free convection flow with mass transfer of an electrically conducting liquid along a plane wall with periodic suction.

1.3 Free and Forced Convection

In the studies related to heat transfer considerable effort has been directed towards the convective mode in which the relative motion of the fluid provides an additional mechanism for the transfer of energy and material, the later being a more important consideration in cases where mass transfer, due to a concentration difference, occurs. Convection is inevitably coupled with the conductive mechanisms, since, although the fluid motion modifies the transport process, the eventual transfer of energy from one fluid element to another in its neighborhood is through conduction. Also, at the surface the process is predominantly that of conduction because the relative fluid motion is brought to zero at the surface. A study of the convective heat transfer therefore involves the mechanisms of conduction and sometimes those of radiative processes as well, coupled with that fluid flow. These make the study of this mode of heat or mass transfer very complex, although its importance in technology and in nature can hardly be exaggerated. The heat transfer in convective mode is divided into two basic processes. If no externally induced flow is provided and flow arises naturally simply owing to the effect of a density difference, resulting from a temperature or concentration difference in a body force field, such as the gravitational field, the process is referred to the natural convection. On the other hand if the motion of the fluid is caused by an external agent such as the externally imposed flow of a fluid stream over a heated object, the process is termed as forced convection. In the forced convection, the fluid flow may be the result of, for instance, a fan, a blower, the wind or the motion of the heated object itself. Such problems are very frequently encountered in technology where the heat transfers to or from a body is often due to an imposed flow of a fluid at a different temperature from that of a body. On the other side, in the natural convection, the density difference gives rise to buoyancy effects,

owing to which the flow is generated. A heated body cooling in ambient air generates such a flow in the region surrounding it. Similarly the buoyant flow arising from heat rejection to the atmosphere, and to other ambient media, circulations arising in heated rooms, in the atmosphere, and in bodies of water, rise of buoyant flow to cause thermal stratification of the medium, as in temperature inversion and many other such heat transfer process in our natural environment, as well as in many technological applications, are included in the area of natural convection. The flow may also arise owing to concentration differences such as those caused by salinity differences in the sea and by composition differences in chemical processing unit, and these cause a natural convection mass transfer. Practically some time both processes, natural and forced convection are important and heat transfer is by mixed convection, in which neither mode is truly predominant. The main difference between the two really lies in the word external. A heated body lying in still air loses energy by natural convection. But it also generates a buoyant flow above it and body placed in that flow is subjected to an external flow and it becomes necessary to determine the natural, as well as the forced convection effects and the regime in which the heat transfer mechanisms lie. When MHD became a popular subject, in was natural that these flows be investigated with the additional ponder for different body force as well as the buoyancy force. At a first glance there seems to be no practical applications for these MHD solutions, for most heat exchangers utilize liquids, whose conductively is so small that prohibitively large magnetic fields are necessary to influence the flow. But some nuclear power plants employ heat exchangers with liquid metal coolants, so the application of moderate magnetic fields to change the convection pattern appears feasible. Another classical natural convection problem is the thermal instability that occurs in a liquid heated from below. This subject is of natural interest to geophysicists and astrophysicists, although some applications might arise in boiling heat transfer. The basic concepts involve in employing the boundary layer approximation to natural convection flows are very similar to those in forced flows. The main difference lies in the fact that the pressure in the region beyond the boundary layer is hydrostatic instead of being imposed by an external flow, and that the velocity out side the layer is zero. However the basic treatment and analysis remain the same. The book by Schlichting [64] is an excellent collection of the boundary layer analysis. There are several methods for the solution of the boundary layer equations namely the similarity variable method, the perturbation method, analytical method etc. and their details are available in the books by Rosenberg [65] Patanker and Spalding [66] and Spalding [67].

1.4 MHD Micropolar Fluid

The concept of micropolar fluid deals with a class of fluids that exhibit microscopic effects arising from the local structure and micromotions of the fluid elements. These fluids contain dilute suspension of rigid macromolecules with individual motions that support stress and body moments and are influenced by spin inertia. Micropolar fluids are those which contain micro-constituents that can undergo rotation, the presence of which can affect the hydrodynamics of the flow so that in can be distinctly non-Newtonian. It has many practical applications, for example analyzing the behavior of exotic lubricants, the flow of colloidal suspensions or polymeric fluids, liquid crystals, additive suspensions, human and animal blood, turbulent shear flow and so forth.

The theory of micropolar fluids was first proposed by Eringen [1]. In this theory the local effects arising from the microstructure and the intrinsic motion of the fluid elements are taken into account. Physically, the micropolar fluid can consist of a suspension of small, rigid cylindrical elements such as large dumbbell-shaped molecules. The theory of micropolar fluids is generating a very much increased interest and many classical flows are being re-examined to determine the effects of the fluid microstructure. Peddision and McNitt [68] applied the micropolar boundary layer theory to the problems of steady stagnation point flow and steady flow over a semi-infinite flat plate. Eringen [3] developed the theory of thermomicropolar fluids by extending the theory of micropolar fluids. Gorla [69] investigated the steady boundary layer flow of a micropolar fluid at a two dimensional stagnation point on a moving wall and claimed that the micropolar fluid model is capable of predicting results which exhibit turbulent flow characteristics. Although it is difficult to see how a steady laminar boundary layer flow could 'appear' to be turbulent. Takhar and Soundalgekar [70] have studied the effects of suction and injection on the flow of a micropolar fluid past a continuously moving semi-infinite porous plate. Hossain and Ahmed [71] have studied the common effect of forced and free convection with uniform heat flux in the presence of a strong magnetic field. In their study, the effect of both viscous and Joule heating were neglected. Mohammadein and Gorla [72] analyzed the effects of magnetic field on the laminar boundary layer mixed convection flow of a micropolar fluid over a horizontal plate. However the work by Rees and Bassom [73] on the Blassius boundary layer flow over a flat plate suggests that much more information about the solution of boundary layer flows of a micropolar fluid can be obtained.

Rees [74] have studied free convection boundary layer flow of a micropolar fluid from a vertical flat plate. In this paper he showed the qualitative behaviour which was found in his previous work. This qualitative result was different from that given in his previous work, where Blasius boundary layer flow of a micropolar fluid was found to reduce to a self-similar form when s=0.5, where s is a constant. In this work he has sought to analyze in detail the micropolar analogue of the classical vertical free convection boundary-layer flow. The presence of micropolar effects served to cause the boundary layer (i) to become non-similar and (ii) to form a well defined two-layer structure at a large distance from the leading edge. Finally it is of interest to query why two-layer asymptotic structure was not found in the mixed convection analysis of Gorla [69]. In that paper the authors showed correctly that forced convection effects dominate near the leading edge, but that free convection effects dominates further downstream. The natural convection flow of micropolar fluids in a porous medium was studied by Mohammadein and Gorla [72]. They obtained the effects of Joule heating on the magnetohydrodynamic free convection of a micropolar fluid.

El-Hakiem [35] has studied Joule heating effects on magnetohydrodynamic free convection flow of a micropolar fluid. Numerical solutions are obtained for the flow and temperature fields for several values of the material properties of the micropolar fluid and the magnetic field strength parameter. El-Amin [75] has studied magnetohydrodynamic free convection and mass transfer flow in micropolar fluid with constant suction. Approximate solutions of the coupled nonlinear governing equations are obtained for different values of the microrotation parameter.

Rahman and Sattar [76] have studied about magnetodynamic convective flow of a micropolar fluid past a continuously moving vertical porous plate in the presence of heat generation/absorption. In this works they have extended the work of El- Arabawy [77] to a magnetohydrodynamic flow taking into account the effect of free convection and microrotation inertia term which has been neglected by El-Arabawy [77]. They have also considered the heat generation/absorption effects to a porous plate with constant suction. In this work, the effect of the internal heat generation/ absorption on a steady two-dimensional convective flow of a viscous incompressible micropolar fluid past a vertical porous plate has been investigated using Finite difference method iteration technique.

Chapter 2

The Basic Governing Equations

In this chapter those equations governs the flow of micropolar fluids in presence of magnetic field or not will be put forward.

The generalized Continuity equation, Momentum equation, Angular Momentum equation, Energy equation and Concentration equation together with the Ohm's law and Maxwell's equations from the basis of studying Magneto Fluid Dynamics (MFD). These equations are as follows:

The continuity equation for a viscous compressible electrically conducting fluid in vector form is

$$\frac{\partial \rho}{\partial t} + \nabla.(\rho \mathbf{q}) = 0 \tag{2.1}$$

For incompressible fluid, the equation (2.1) becomes

$$\nabla.\mathbf{q} = 0 \tag{2.2}$$

In three dimensional Cartesian coordinate system the equation (2.1) becomes

$$\frac{\partial u}{\partial x} + \frac{\partial v}{\partial y} + \frac{\partial w}{\partial z} = 0 \tag{2.3}$$

The momentum equation for a viscous compressible fluid in vector form is

$$\frac{d\mathbf{q}}{dt} = \mathbf{F} - \frac{1}{\rho}\nabla P + \frac{\upsilon}{3}\nabla(\nabla.\mathbf{q}) + \upsilon\nabla^2\mathbf{q} \tag{2.4}$$

For incompressible fluid, the equation (2.4) becomes

$$\frac{d\mathbf{q}}{dt} = \mathbf{F} - \frac{1}{\rho}\nabla P + \upsilon\nabla^2\mathbf{q} \tag{2.5}$$

When the fluid moves through a porous medium, the equation (2.5) becomes

$$\frac{d\mathbf{q}}{dt} = \mathbf{F} - \frac{1}{\rho}\nabla P + \upsilon\nabla^2\mathbf{q} - \frac{\upsilon}{K'}\mathbf{q} \tag{2.6}$$

When electrically conducting fluid moves through a magnetic field of intensity $\mathbf{H}$ ($\mathbf{B} = \mu_e\mathbf{H}$, where $\mathbf{B}$ is the magnetic field.), the equation (2.6) becomes as a magnetohydrodynamic (MHD) equation in the following form

$$\frac{d\mathbf{q}}{dt} = \mathbf{F} - \frac{1}{\rho}\nabla P + \upsilon\nabla^2\mathbf{q} + \frac{1}{\rho}\mathbf{J}\wedge\mathbf{B} - \frac{\upsilon}{K'}\mathbf{q} \tag{2.7}$$

where $\mathbf{J} \wedge \mathbf{B}$ is the force on the fluid per unit volume produced by the interaction of the electric and magnetic field (called Lorentz force).

Due to the presence of micro particles having microrotation the viscosity effect on the momentum equation will be changed and the fluid velocity will also be influenced by microrotation. As a result the momentum equation for a viscous incompressible electrically conducting micropolar fluid is

$$\frac{d\mathbf{q}}{dt} = \mathbf{F} - \frac{1}{\rho}\nabla P + (\upsilon + \frac{\kappa}{\rho})\nabla^2\mathbf{q} + \frac{\kappa}{\rho}(\nabla \wedge \mathbf{G}) + \frac{1}{\rho}\mathbf{J} \wedge \mathbf{B} - \frac{\upsilon}{K'}\mathbf{q} \tag{2.8}$$

The equation (2.8) can be written in the following form

$$\frac{\partial \mathbf{q}}{\partial t} + (\mathbf{q}.\nabla)\mathbf{q} = \mathbf{F} - \frac{1}{\rho}\nabla P + (\upsilon + \frac{\kappa}{\rho})\nabla^2\mathbf{q} + \frac{\kappa}{\rho}(\nabla \wedge \mathbf{G}) + \frac{1}{\rho}\mathbf{J} \wedge \mathbf{B} - \frac{\upsilon}{K'}\mathbf{q} \tag{2.9}$$

where we have used $\frac{d\mathbf{q}}{dt} = \frac{\partial \mathbf{q}}{\partial t} + (\mathbf{q}.\nabla)\mathbf{q}$

The angular momentum equation for a viscous incompressible electrically conducting micropolar fluid is

$$\frac{d\mathbf{G}}{dt} = \frac{\gamma}{\rho j}\nabla^2\mathbf{G} + \frac{\kappa}{\rho j}(\nabla \wedge \mathbf{q}) - \frac{2\kappa}{\rho j}\mathbf{G} \tag{2.10}$$

The equation (2.10) can be written in the following form

$$\frac{\partial \mathbf{G}}{\partial t} + (\mathbf{G}.\nabla)\mathbf{G} = \frac{\gamma}{\rho j}\nabla^2\mathbf{G} + \frac{\kappa}{\rho j}(\nabla \wedge \mathbf{q}) - \frac{2\kappa}{\rho j}\mathbf{G} \tag{2.11}$$

where again $\frac{d\mathbf{G}}{dt} = \frac{\partial \mathbf{G}}{\partial t} + (\mathbf{G}.\nabla)\mathbf{G}$ is used

The Energy equation for a viscous incompressible micropolar fluid with heat generation and constant heat flux can be put in the following form

$$\frac{\partial T}{\partial t} + (\mathbf{q}.\nabla)T = \frac{k'}{\rho c_p}\nabla^2 T + Q(T - T_\infty) \tag{2.12}$$

The generalized Ohm's law is of the form

$$\mathbf{J} = \sigma'(\mathbf{E} + \mathbf{q} \wedge \mathbf{B}) - \frac{\sigma'}{en_e}(\mathbf{J} \wedge \mathbf{B}) + \frac{\sigma'}{en_e}\nabla P_{\mathbf{e}} \tag{2.13}$$

The Maxwell's equations are

$$\nabla \wedge \mathbf{H} = \mathbf{J} \tag{2.14}$$

$$\nabla \wedge \mathbf{E} = -\frac{\partial \mathbf{B}}{\partial t} \tag{2.15}$$

$$\nabla.\mathbf{B} = 0 \tag{2.16}$$

where ρ is the density of the fluid, **q** is the fluid velocity, u, v and w are the velocity component in the x, y and z direction respectively, **F** is the body force per unit volume, P is the fluid pressure and υ is the kinematic viscosity, K' is the permeability of the porous medium, **J** is the current density vector , **B** is the magnetic field vector, k is the thermal conductivity, **G** is the microrotation, γ is the spin gradient viscosity, j is the microinertia per unit mass, T is the fluid temperature, k_T is thermal diffusion ratio, C_p is the specific heat at constant pressure, σ' is the electrical conductivity, **E** is the electric field intensity, C_s is the concentration susceptibility, n_e is the number of electron, P_e is the pressure of the electron. Also φ denotes the dissipation function involving the viscous stress and it represents the rate at which energy is being dissipated per unit volume through the action of viscosity. In fact the energy is dissipated in a viscous fluid in motion on account of internal friction and for incompressible fluid, where

$$\varphi = (\mu + \kappa)\left[\left\{\left(\frac{\partial u}{\partial x}\right)^2 + \left(\frac{\partial v}{\partial y}\right)^2 + \left(\frac{\partial w}{\partial z}\right)^2\right\} + \left(\frac{\partial v}{\partial x} + \frac{\partial u}{\partial y}\right)^2 + \left(\frac{\partial w}{\partial y} + \frac{\partial v}{\partial z}\right)^2 + \left(\frac{\partial u}{\partial z} + \frac{\partial w}{\partial x}\right)^2\right] \quad (2.17)$$

which is always positive, since all the terms are quadratic, where μ is the coefficient of viscosity.

The generalized Ohm's law in the absence of electric field and neglecting the half-current is of the form

$$\mathbf{J} = \sigma'(\mathbf{q} \wedge \mathbf{B}) \quad (2.18)$$

The magnetic field is $\mathbf{B} = (B_x, B_y, B_z)$ (2.19)

where (B_x, B_y, B_z) be the components of magnetic field.

$$\text{Then } \mathbf{q} \wedge \mathbf{B} = \begin{vmatrix} \mathbf{i} & \mathbf{j} & \mathbf{k} \\ u & v & w \\ B_x & B_y & B_z \end{vmatrix} = (vB_z - wB_y)\mathbf{i} + (wB_x - uB_z)\mathbf{j} + (uB_y - vB_x)\mathbf{k} \quad (2.20)$$

Therefore the equation (2.18) becomes

$$\mathbf{J} = \sigma'(vB_z - wB_y)\mathbf{i} + \sigma'(wB_x - uB_z)\mathbf{j} + \sigma'(uB_y - vB_x)\mathbf{k} \quad (2.21)$$

$$\mathbf{J} \wedge \mathbf{B} = \begin{bmatrix} \mathbf{i} & \mathbf{j} & \mathbf{k} \\ \sigma'(vB_z - wB_y) & \sigma'(wB_x - uB_z) & \sigma'(uB_y - vB_x) \\ B_x & B_y & B_z \end{bmatrix}$$

$$= \sigma'\{(wB_xB_z - uB_z^2) - (uB_y^2 - vB_xB_y)\}\mathbf{i} + \sigma'\{(uB_xB_y - vB_x^2) - (vB_z^2 - wB_yB_z)\}\mathbf{j}$$

$$+ \sigma'\{(vB_yB_z - wB_y^2) - (wB_x^2 - uB_xB_z)\}\mathbf{k}$$

$$= (\sigma' wB_xB_z - \sigma' uB_z^2 - \sigma' uB_y^2 + \sigma' vB_xB_y)\mathbf{i} \quad + (\sigma' uB_xB_y - \sigma' vB_x^2 - \sigma' vB_z^2 + \sigma' wB_yB_z)\mathbf{j}$$

$$+ (\sigma' vB_yB_z - \sigma' wB_y^2 - \sigma' wB_x^2 + \sigma' uB_xB_z)\mathbf{k} \tag{2.22}$$

Let $\mathbf{F} = (F_x, F_y, F_z)$ (2.23)

where (F_x, F_y, F_z) be the components of body force.

The microrotation is

$\mathbf{G} = (0,0,N)$ (2.24)

where $(0,0,N)$ be the components of microrotation and the component N is the angular velocity acting in z-direction (the rotation of N is in the x-y plane).

Then, $\nabla \wedge \mathbf{G} = \begin{vmatrix} \mathbf{i} & \mathbf{j} & \mathbf{k} \\ \frac{\partial}{\partial x} & \frac{\partial}{\partial y} & \frac{\partial}{\partial z} \\ 0 & 0 & N \end{vmatrix} = \mathbf{i}\frac{\partial N}{\partial y} + \mathbf{j}\frac{\partial N}{\partial x}$ (2.25)

$$\nabla \wedge \mathbf{q} = \begin{vmatrix} \mathbf{i} & \mathbf{j} & \mathbf{k} \\ \frac{\partial}{\partial x} & \frac{\partial}{\partial y} & \frac{\partial}{\partial z} \\ u & v & w \end{vmatrix} = (\frac{\partial w}{\partial y} - \frac{\partial v}{\partial z})\mathbf{i} + (\frac{\partial u}{\partial z} - \frac{\partial w}{\partial x})\mathbf{j} + (\frac{\partial v}{\partial x} - \frac{\partial u}{\partial y})\mathbf{k} \tag{2.26}$$

Again from (2.21) we have

$$\mathbf{J}^2 = \sigma'^2(vB_z - wB_y)^2 + \sigma'^2(wB_x - uB_z)^2 + \sigma'^2(uB_y - vB_x)^2 \tag{2.27}$$

In three dimensional Cartesian coordinate system the momentum equation (2.9) with the help of the equations (2.22), (2.23) and (2.25) becomes

$$\frac{\partial u}{\partial t} + u\frac{\partial u}{\partial x} + v\frac{\partial u}{\partial y} + w\frac{\partial u}{\partial z} = F_x - \frac{1}{\rho}\frac{\partial P}{\partial x} + (\upsilon + \frac{\kappa}{\rho})\left(\frac{\partial^2 u}{\partial x^2} + \frac{\partial^2 u}{\partial y^2} + \frac{\partial^2 u}{\partial z^2}\right) + \frac{\kappa}{\rho}\frac{\partial N}{\partial y}$$
$$+ \frac{\sigma'}{\rho}\{(wB_xB_z - uB_z^2) - (uB_y^2 - vB_xB_y)\} - \frac{\upsilon}{k'}w \tag{2.28}$$

$$\frac{\partial v}{\partial t} + u\frac{\partial v}{\partial x} + v\frac{\partial v}{\partial y} + w\frac{\partial v}{\partial z} = F_y - \frac{1}{\rho}\frac{\partial P}{\partial y} + (\upsilon + \frac{\kappa}{\rho})\left(\frac{\partial^2 v}{\partial x^2} + \frac{\partial^2 v}{\partial y^2} + \frac{\partial^2 v}{\partial z^2}\right) - \frac{\kappa}{\rho}\frac{\partial N}{\partial x}$$
$$+ \frac{\sigma'}{\rho}\{(uB_xB_y - vB_x^2) - (vB_z^2 - wB_yB_z)\} - \frac{\upsilon}{k'}v \tag{2.29}$$

$$\frac{\partial w}{\partial t}+u\frac{\partial w}{\partial x}+v\frac{\partial w}{\partial y}+w\frac{\partial w}{\partial z}=F_z-\frac{1}{\rho}\frac{\partial P}{\partial z}+(\upsilon+\frac{\kappa}{\rho})\left(\frac{\partial^2 w}{\partial x^2}+\frac{\partial^2 w}{\partial y^2}+\frac{\partial^2 w}{\partial z^2}\right)$$
$$+\frac{\sigma'}{\rho}\{(vB_yB_z-wB_y^2)-(wB_x^2-uB_xB_z)\}-\frac{\upsilon}{k'}w \qquad (2.30)$$

In three dimensional Cartesian coordinate system the angular momentum equation (2.11) with the help of the equations (2.24) and (2.26) becomes

$$\frac{\partial N}{\partial t}+u\frac{\partial N}{\partial x}+v\frac{\partial N}{\partial y}+w\frac{\partial N}{\partial z}=\frac{\gamma}{\rho j}\left(\frac{\partial^2 N}{\partial x^2}+\frac{\partial^2 N}{\partial y^2}+\frac{\partial^2 N}{\partial z^2}\right)+\frac{\kappa}{\rho j}(\frac{\partial v}{\partial x}-\frac{\partial u}{\partial y})-2\frac{\kappa}{\rho j}N \qquad (2.31)$$

In three dimensional Cartesian coordinate system the energy equation (2.12) becomes

$$\frac{\partial T}{\partial t}+u\frac{\partial T}{\partial x}+v\frac{\partial T}{\partial y}+w\frac{\partial T}{\partial z}=\frac{K'}{\rho C_P}\left(\frac{\partial^2 T}{\partial x^2}+\frac{\partial^2 T}{\partial y^2}+\frac{\partial^2 T}{\partial z^2}\right)+Q(T-T_\infty) \qquad (2.32)$$

Thus in three dimensional Cartesian coordinate system the continuity equation, the momentum equation, the angular momentum equation and the energy equation become

The Continuity equation

$$\frac{\partial u}{\partial x}+\frac{\partial v}{\partial y}+\frac{\partial w}{\partial z}=0 \qquad (2.33)$$

The Momentum Equations

$$\frac{\partial u}{\partial t}+u\frac{\partial u}{\partial x}+v\frac{\partial u}{\partial y}+w\frac{\partial u}{\partial z}=F_x-\frac{1}{\rho}\frac{\partial P}{\partial x}+(\upsilon+\frac{\kappa}{\rho})\left(\frac{\partial^2 u}{\partial x^2}+\frac{\partial^2 u}{\partial y^2}+\frac{\partial^2 u}{\partial z^2}\right)+\frac{\kappa}{\rho}\frac{\partial N}{\partial y}$$
$$+\frac{\sigma'}{\rho}\{(wB_xB_z-uB_z^2)-(uB_y^2-vB_xB_y)\}-\frac{\upsilon}{k'}w \qquad (2.34)$$

$$\frac{\partial v}{\partial t}+u\frac{\partial v}{\partial x}+v\frac{\partial v}{\partial y}+w\frac{\partial v}{\partial z}=F_y-\frac{1}{\rho}\frac{\partial P}{\partial y}+(\upsilon+\frac{\kappa}{\rho})\left(\frac{\partial^2 v}{\partial x^2}+\frac{\partial^2 v}{\partial y^2}+\frac{\partial^2 v}{\partial z^2}\right)-\frac{\kappa}{\rho}\frac{\partial N}{\partial x}$$
$$+\frac{\sigma'}{\rho}\{(uB_xB_y-vB_x^2)-(vB_z^2-wB_yB_z)\}-\frac{\upsilon}{k'}v \qquad (2.35)$$

$$\frac{\partial w}{\partial t}+u\frac{\partial w}{\partial x}+v\frac{\partial w}{\partial y}+w\frac{\partial w}{\partial z}=F_z-\frac{1}{\rho}\frac{\partial P}{\partial z}+(\upsilon+\frac{\kappa}{\rho})\left(\frac{\partial^2 w}{\partial x^2}+\frac{\partial^2 w}{\partial y^2}+\frac{\partial^2 w}{\partial z^2}\right)$$
$$+\frac{\sigma'}{\rho}\{(vB_yB_z-wB_y^2)-(wB_x^2-uB_xB_z)\}-\frac{\upsilon}{k'}w \qquad (2.36)$$

The Angular momentum equation

$$\frac{\partial N}{\partial t}+u\frac{\partial N}{\partial x}+v\frac{\partial N}{\partial y}+w\frac{\partial N}{\partial z}=\frac{\gamma}{\rho j}\left(\frac{\partial^2 N}{\partial x^2}+\frac{\partial^2 N}{\partial y^2}+\frac{\partial^2 N}{\partial z^2}\right)+\frac{\kappa}{\rho j}(\frac{\partial v}{\partial x}-\frac{\partial u}{\partial y})-2\frac{\kappa}{\rho j}N \qquad (2.37)$$

The Energy equation

$$\frac{\partial T}{\partial t}+u\frac{\partial T}{\partial x}+v\frac{\partial T}{\partial y}+w\frac{\partial T}{\partial z}=\frac{K'}{\rho C_P}\left(\frac{\partial^2 T}{\partial x^2}+\frac{\partial^2 T}{\partial y^2}+\frac{\partial^2 T}{\partial z^2}\right)+Q(T-T_\infty) \qquad (2.38)$$

Chapter 3

The Calculation Technique

Many physical phenomena in applied science and engineering when formulated into mathematical models fall into a category of system known as non-linear coupled partial differential equations. Most of these problems can be formulated as second order partial differential equations. A system of non-linear coupled partial differential equations with the boundary conditions is very difficult to solve analytically. For obtaining the solution of such problem numerical methods are adopted. The governing equations contain a system of partial differential equations that are transformed by usual transformation into a non-dimensional system of non-linear coupled partial differential equations with initial and boundary conditions. The Finite Difference Method may be adopted for solving the non-linear coupled partial differential equations numerically.

When a partial differential equation contain both time and space derivatives sometimes a technique is adopted to transfer that to an Ordinary Differential Equation (O.D.E.) containing only space derivatives, as they are comparatively easy to handle. Laplace transform provides the opportunity to do that. When this method is adopted three steps are required to obtain the solution of the partial differential equation.

1) Taking Laplace transform of the equation(s) along with the initial and boundary conditions (It will provide ODE with additional parameter that will come from the kernel of the transform).
2) Obtaining particular solution of the ODE in terms of the position and the parameter.
3) Use of Inverse Laplace Transform to get back the time variable in the obtained particular solution.

In this research work the physical system considered has provided nonlinear coupled partial differential equations, in terms of time and space derivatives. Hence **Finite Difference Method** is adopted to solve those nonlinear partial differential equations numerically. Attempt has also been made to solve coupled partial differential equations analytically (to solve analytically the nonlinear terms present in the equations will not be considered). To do that **Laplace Transform Method** is adopted. It may be mentioned that convolution theorem has an important role in case of obtaining **Inverse Laplace Transform**. The integrals arising through convolution theorem are quite tedious and to

integrate them Mathematica® is used. In the following subsections finite difference method, Laplace tramsform and inverse Laplace transform will be discussed.

3.1 Finite difference method:

In order to solve the governing partial differential equations by finite difference method, let us consider a two-dimensional region. It is covered by a rectangular grid formed by two sets of lines drawn parallel to the coordinate axes with grid spacing Δx and Δy in x and y directions respectively.

The numerical values of the dependent variables are obtained at the points of intersection of the parallel lines, called mesh points, lattice points or nodal points. These values are obtained by discretizing the governing partial differential equations over the region of interest to derive approximately equivalent algebraic equations. The discretization consists of replacing each derivative of the partial differential equation at a mesh point by a finite difference approximation in terms of the values of the dependent variable at the mesh point and at the immediate neighboring mesh points and boundary points. In doing so, a set of algebraic equations arise.

Let the temperature T at a representative point be a function of two spatial coordinate x, y and time t. We adopt the following notation. Let the subscripts i and j represent x and y coordinates respectively and superscript n represents time. Let the mesh spacing in x and y directions are denoted by Δx and Δy, also the time step by Δt. Thus T(x,y,t) can be represented by $T(i\Delta x, j\Delta y, n\Delta t) = T_{i,j}^{n}$

With this notation, let the function T and its derivatives are continuous. Then from Taylor's series expansions, the finite difference approximations to derivatives can be obtained. For example, the Taylor's series expansion of $T_{i+1,j}$ about the grid point (i, j) gives

$$T_{i+1,j} = T_{i,j} + [\Delta x \frac{\partial T}{\partial x} + \frac{(\Delta x)^2}{2!}\frac{\partial^2 T}{\partial x^2} + \frac{(\Delta x)^2}{3!}\frac{\partial^3 T}{\partial x^3} + \frac{(\Delta x)^4}{4!}\frac{\partial^4 T}{\partial x^4} + \textit{higher order terms}]_{i,j} \quad (3.1.1)$$

or, $\left[\frac{\partial T}{\partial x}\right]_{i,j} = \frac{T_{i+1,j} - T_{i,j}}{\Delta x} + [O(\Delta x)]$ is the forward difference approximation to the derivative

$\frac{\partial T}{\partial x}$ with the truncation error of order Δx. Similarly

$$T_{i-1,j} = T_{i,j} - [\Delta x \frac{\partial T}{\partial x} - \frac{(\Delta x)^2}{2!}\frac{\partial^2 T}{\partial x^2} + \frac{(\Delta x)^2}{3!}\frac{\partial^3 T}{\partial x^3} - \frac{(\Delta x)^4}{4!}\frac{\partial^4 T}{\partial x^4} + \textit{higher order terms}]_{i,j} \quad (3.1.2)$$

or, $\left(\frac{\partial T}{\partial x}\right)_{i,j} = \frac{T_{i,j} - T_{i-1,j}}{\Delta x} + [O(\Delta x)]$ is the backward difference approximation to the derivative $\frac{\partial T}{\partial x}$ with the truncation error of order Δx and both are first order accurate.

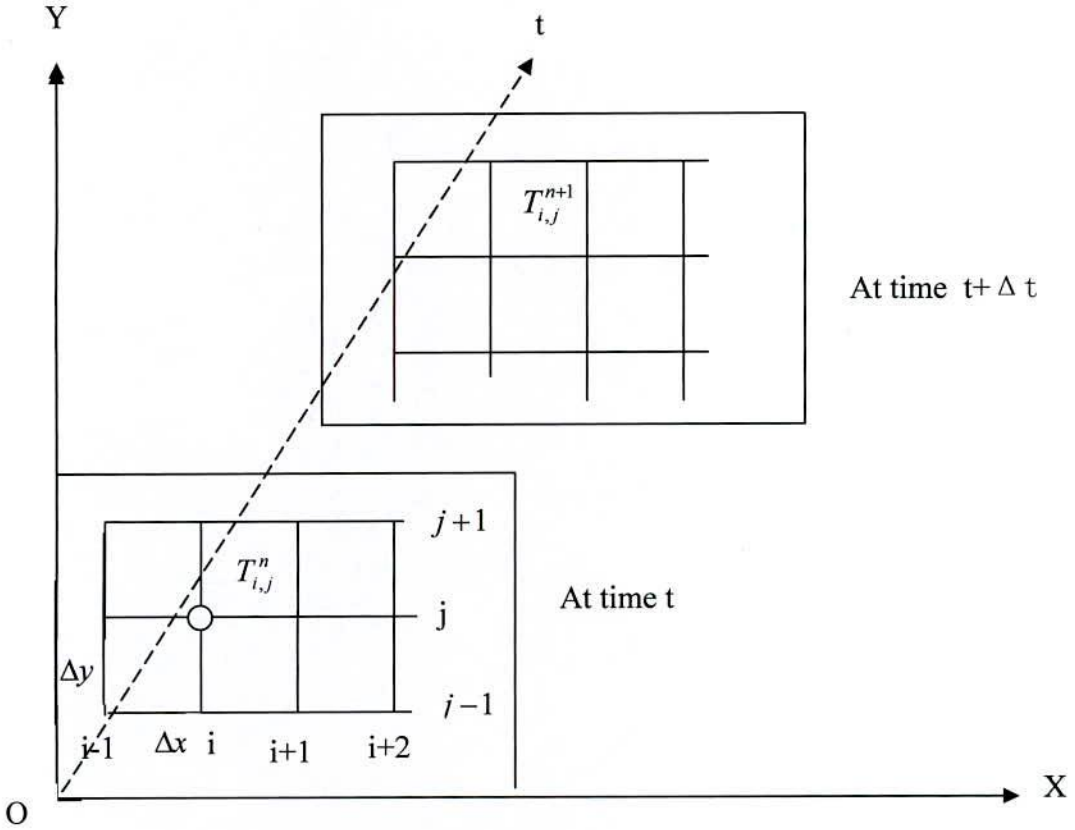

Fig. 3.1: Space time distribution

Subtracting equation (3.1.2) from equation (3.1.1), we obtain

$$\left(\frac{\partial T}{\partial x}\right)_{i,j} = \frac{T_{i+1,j} - T_{i-1,j}}{2\Delta x} + [O(\Delta x)^2]$$

This is a central difference approximation to the derivative $\frac{\partial T}{\partial x}$ with the truncation error of order $(\Delta x)^2$, which is second order accurate.

The central difference approximation to a second order partial derivative $\frac{\partial^2 T}{\partial x^2}$ can be similarly obtained by adding the equations (3.1.1) and (3.1.2).

Thus $\left(\frac{\partial^2 T}{\partial x^2}\right)_{i,j} = \frac{T_{i+1,j} - 2T_{i,j} + T_{i-1,j}}{\Delta x^2} + [O(\Delta x)^2]$

Similar expressions can be written for y derivatives.

$$\left(\frac{\partial^2 T}{\partial y^2}\right)_{i,j} = \frac{T_{i,j+1} - 2T_{i,j} + T_{i,j-1}}{\Delta y^2} + [O(\Delta y)^2]$$ which is also second order accurate.

For time it can be similarly written

$$\left(\frac{\partial T}{\partial t}\right)_{i,j} = \frac{T_{i,j}^{n+1} - T_{i,j}^{n}}{\Delta t} + [O(\Delta t)]$$ which is 1st order accurate.

The expressions for mixed derivatives can be obtained by differentiating with respect to each variable in turn. Thus for example,

$$\left(\frac{\partial^2 T}{\partial x \partial y}\right)_{i,j} = \frac{\partial}{\partial x}\left(\frac{\partial T}{\partial y}\right)_{i,j} = \frac{\left(\frac{\partial T}{\partial y}\right)_{i+1,j} - \left(\frac{\partial T}{\partial y}\right)_{i-1,j}}{2\Delta x} = \frac{\frac{(T_{i+1,j+1} - T_{i+1,j-1})}{2\Delta y} - \frac{(T_{i-1,j+1} - T_{i-1,j-1})}{2\Delta y}}{2\Delta x}$$

Therefore,

$$\left(\frac{\partial^2 T}{\partial x \partial y}\right)_{i,j} = \frac{T_{i+1,j+1} - T_{i+1,j-1} - T_{i-1,j+1} + T_{i-1,j-1}}{4\partial x \partial y}$$

Proceeding in a similar manner, the central difference approximation to the third derivative is found to be

$$\left(\frac{\partial^3 T}{\partial x^3}\right)_{i,j} = \frac{T_{i+2,j} - 2T_{i+1,j} + 2T_{i-1,j} - T_{i-2,j}}{2\Delta x^3}$$

Similar approximations can be obtained even to higher order derivatives.

3.2 Laplace Transform.

Let F(t) be an arbitrary function of the real variable t that has only a finite number of maxima and minima and discontinuities and whose value is zero for negative values of t.

$$\text{If} \quad g(s) = \int_0^\infty e^{-st} F(t)dt \qquad \text{Re } s \geq c \geq 0 \tag{3.2.1}$$

then

$$F(t) = \frac{1}{2\pi j}\int_{c-j\infty}^{c+j\infty} g(s)e^{st}ds \text{, where } j^2 = -1 \tag{3.2.2}$$

provided

$$\int_0^\infty e^{-ct} F(t)dt \quad \text{converges absolutely.} \tag{3.2.3}$$

This is also known as Fourier-Mellin theorem.

It is generally used that

$$g(s)=\mathrm{L}\{F(t)\} \tag{3.2.4}$$

To denote the functional relation between $g(s)$ and $F(t)$ expressed in (3.2.1) it is said that $g(s)$ is the **direct Laplace transform** of $F(t)$. The relation (3.2.2) is expressed conveniently by the notation

$$F(t) = L^{-1}\{g(s)\} \tag{3.2.5}$$

It is then said that $F(t)$ is the **inverse Laplace transform** of $g(s)$.

3.3 Inverse Laplace Transform.

The problem of computing the inverse transforms of a function $g(s)$ by the use of the equation

$$F(t) = \frac{1}{2\pi j}\int_{c-j\infty}^{c+j\infty} g(s)e^{st}ds \tag{3.3.1}$$

will now be considered.

The line integral for $F(t)$ is usually evaluated by transforming it into a closed contour and applying the calculus of residues.

Let the closed contour Γ consists of the straight line parallel to the axis of imaginaries and at a distance c to the right of it and the large semicircle s_0 whose centre is at (c, 0).

Then

$$\oint_{\Gamma} e^{st}g(s)ds = \int_{c-jR}^{c+jR} e^{st}g(s)ds + \int_{s_0} e^{st}g(s)ds \tag{3.3.2}$$

where c is chosen great enough so that all the singularities of the integral lie to the left of the straight line along which the integral from $c-j\infty$ to $c+j\infty$ is taken.

The evaluation of the contour integral along the contour Γ is greatly facilitated by the use of Jordan's lemma, which in this case may be stated in the following form:

Let $\varphi(s)$ be an integrable function of the complex variable s such that

$$\lim_{|s|\to\infty}|\varphi(s)| = 0 \tag{3.3.3}$$

Then

$$\lim_{R\to\infty}\left|\int_{s_0} e^{st}\varphi(s)ds\right| = 0 \qquad t>0 \text{ and Re } s \le 0 \tag{3.3.4}$$

It usually happens in practice that the function

$$\phi(s) = g(s) \tag{3.3.5}$$

have such properties that Jordan's lemma is applicable. In such a case the integral around the large semicircle in (3.2.2) vanishes as $R \to \infty$, and provides

$$F(t) = \frac{1}{2\pi j}\int_{c-j\infty}^{c+j\infty} g(s)e^{st}ds = \lim_{R\to\infty}\frac{1}{2\pi j}\oint e^{st}g(s)ds \tag{3.3.6}$$

Now, by Cauchy's residue theorem, it follows that

$$\oint e^{st}g(s)ds = 2\pi j\sum residue\ of\ e^{st}g(s) \text{ inside } \Gamma \tag{3.3.7}$$

Hence by (3.3.6)

$$F(t) = \sum residue\ of\ e^{st} g(s)\ \text{inside}\ \Gamma \tag{3.3.8}$$

when R is large enough to include all singularities.

If the function $e^{st} g(s)$ is not single-valued within the contour Γ and possesses branch point within Γ, it may be made single-valued by introducing suitable cuts.

For the computation of an inverse transform, consider the determination of the inverse transform of

$$g(s) = \frac{1}{s^2 + a^2} = L\{F(t)\} \tag{3.3.9}$$

This function clearly satisfies the condition imposed by Jordan's lemma.

Hence $F(t)$ is given by (3.2.8) in the form

$$F(t) = \sum res \frac{e^{st}}{s^2 + a^2} \tag{3.3.10}$$

The poles of $e^{st}/(s^2 + a^2)$ are at $s = \pm ja$ (3.3.11)

For the above case the residue of the simple pole at $s=ja$ is

$$res_{s=ja} \frac{e^{st}}{s^2 + a^2} = \frac{e^{jat}}{2ja} \tag{3.3.12}$$

Similarly

$$res_{s=-ja} \frac{e^{st}}{s^2 + a^2} = \frac{-e^{-jat}}{2ja} \tag{3.3.13}$$

Hence

$$F(t) = \frac{1}{a} \frac{e^{jst} - e^{-jst}}{2j} = \frac{\sin at}{a} \tag{3.3.14}$$

Again consider

$$L^{-1}\{g(s)\} = \frac{\omega}{(s+a)^2 + \omega^2} = F(t) \tag{3.3.15}$$

This function also satisfies the condition of Jordan's lemma. To get $F(t)$ one must compute the sum of the residues of

$$\varphi(s) = \frac{e^{st}\omega}{(s+a)^2 + \omega^2} \tag{3.3.16}$$

The poles of this function are at $s = -a \pm j\omega$ (3.3.17)

The sum of the residues at these poles is

$$\frac{e^{-at}e^{j\omega t}}{2j\omega} - \frac{e^{-at}e^{-j\omega t}}{2j\omega} = e^{-at}\sin\omega t = F(t) \tag{3.3.18}$$

It may be thus concluded that once the function $g(s)$ is known, its inverse may be readily evaluated, provided $g(s)$ satisfies the conditions of Jordan's lemma, by means of the residue theorem. Summarizing the results of the theory of residues as applied to (3.2.8) it may stated that if $g(s)$ has a simple pole at $s = s_0$ then

$$\operatorname*{res}_{s=s_0} e^{st} = \lim_{s\to s_0}(s - s_0)g(s)e^{st} \tag{3.3.19}$$

Or if $g(s)$ has a pole of order n at $s = s_0$, then

$$\operatorname*{res}_{s=s_0} g(s)e^{st} = \lim_{s\to s_0}[1/(n-1)!](d^{n-1}/ds^{n-1})(s - s_0)^n g(s)e^{st} \tag{3.3.20}$$

Thus these formulas may be used to evaluate the residues of $g(s)e^{st}$ at all of its poles and through the application of (3.2.8) the inverse is found.

Convolution theorem

This theorem is known in the literature as the Faltung or convolution theorem. In the older literature of the operational calculus it is sometimes referred to as the superposition theorem.

Let

$$L^{-1}\{g_1(s)\} = F_1(t) \tag{3.3.21}$$

$$L^{-1}\{g_2(s)\} = F_2(t) \tag{3.3.22}$$

then according to convolution theorem

$$L^{-1}\{g_1 g_2\} = \int_0^t F_1(y)F_2(t-y)dy = \int_0^t F_2(y)F_1(t-y)dy \tag{3.3.23}$$

To prove this, consider

$$L^{-1}\{g_1(s)g_2(s)\} = F_3(t) \tag{3.3.24}$$

Then, by the Fourier-Mellin formula,

$$F_3(t) = \frac{1}{2\pi j}\int_{c-j\infty}^{c+j\infty} g_1(s)g_2(s)e^{st}ds \tag{3.3.25}$$

However, by hypothesis,

$$g_2(s) = \int_0^\infty e^{-sy}F_2(y)dy \tag{3.3.26}$$

Therefore

$$F_3(t) = \frac{1}{2\pi j}\int_0^{\infty} F_2(y)dy \int_{c-j\infty}^{c+j\infty} g_1(s)e^{s(t-y)}ds \tag{3.3.27}$$

if no question is asked for reversing the order of integration.

However

$$\frac{1}{2\pi j}\int_{c-j\infty}^{c+j\infty} g_1(s)e^{s(t-y)}ds = F_1(t-y) \tag{3.3.28}$$

Hence

$$F_3(t) = \int_0^{\infty} F_2(y)F_1(t-y)dy \tag{3.3.29}$$

Now, by hypothesis, $F_1(t) = 0$ if t is less than 0.

$$F_1(t-y) = 0 \text{ for } y > t \tag{3.3.30}$$

Consequently the infinite limit of integration may be replaced by the limit t. Therefore (3.3.29) can be written in the form

$$F_3(t) = \int_0^{t} F_2(y)F_1(t-y)dy \tag{3.3.31}$$

and by symmetry,

$$F_3(t) = \int_0^{t} F_1(y)F_2(t-y)dy \tag{3.3.32}$$

Chapter 4

Numerical Solution of the Transient Free Convection in Micropolar Fluid with Heat Generation and Constant Heat Flux.

4.1 Introduction.

In this chapter the governing equations of the system will be solved numerically. To do that the equations will be transferred to their non-dimensional form. The non-dimensional equations will then be discretized to obtain their finite difference counterpart. As stability is a very important issue for finite difference method to converge, that will also be discussed.

4.2 Non-Dimensionalization of the governing equations

Let us consider the free convection of a micropolar fluid along the vertical plate. The temperature of the plate is held at constant value of T_s and the heat flux is considered as constant, the thermal dispersion effect is also included. We have considered x-axis along the plate in the vertical direction and y-axis perpendicular to the plate. The governing equations with the Boussinesq approximation can be put in the following form

1) Mass equation: $\frac{\partial u}{\partial x}+\frac{\partial v}{\partial y}=0$

2) Momentum equation: $\frac{\partial u}{\partial t}+u\frac{\partial u}{\partial x}+v\frac{\partial v}{\partial y}=(\nu+\frac{k}{\rho})\frac{\partial^2 u}{\partial y^2}+g^*\beta(T-T_\infty)+\frac{k}{\rho}\frac{\partial N}{\partial y}$

3) Angular momentum equation: $\frac{\partial N}{\partial t}+u\frac{\partial N}{\partial x}+v\frac{\partial N}{\partial y}=\frac{\gamma}{\rho j}\frac{\partial^2 N}{\partial y^2}-\frac{k}{\rho j}(2N+\frac{\partial u}{\partial y})$

4) Energy equation: $\frac{\partial T}{\partial t}+u\frac{\partial T}{\partial x}+v\frac{\partial T}{\partial y}=\frac{k'}{\rho c_p}\frac{\partial^2 T}{\partial y^2}+Q(T-T_\infty)$

With the boundary conditions: $u(x,0,t)=0,\ N(x,0,t)=0,\ T(x,0,t)=T_s$

$$u(x,\infty,t)=0,\ N(x,\infty,t)=0,\ T(x,\infty,t)=T_\alpha,$$

Here u and v are velocity components associated with x and y directions measured along and normal to the vertical plate respectively, ν the kinematic coefficient of viscosity, k the vortex viscosity, ρ the density of the fluid, g^* the acceleration due to gravity, β the coefficient of thermal expansion, T the temperature of the fluid in the boundary layer, T_α the free steam temperature, N the angular velocity, γ the spin gradient viscosity, j the microinertia per unit mass, k' the thermal conductivity, c_p specific heat at constant pressure and Q the heat generation.

The variables are made dimensionless with the following substitution.

$$u^* = \frac{u}{U_0}, \qquad v^* = \frac{v}{U_0}, \qquad x^* = \frac{U_0}{\nu}x\ , \quad y^* = \frac{U_0}{\nu}y\ , \qquad t^* = \frac{U_0^2}{\nu}t\ ,$$

$$N^* = \frac{\nu}{U_0^2}N \qquad j^* = \frac{U_0^2}{\nu^2}j\ , \qquad \theta = \frac{(T-T_\infty)}{(T_s-T_\infty)}$$

Along with them the following dimensionless quantities are introduced.

Prandtl Number, $P_r = \dfrac{\upsilon}{k/\rho C_p} = \dfrac{\upsilon\rho c_p}{k}$, Grashof number, $Gr = \dfrac{\nu g^*\beta(T_s-T_\infty)}{U_0^3}$

$\lambda = \dfrac{\gamma}{\rho\nu j}$, $\Delta = \dfrac{k}{\rho\nu}$ (Dimensionless material parameter)

Momentum equation: $\dfrac{\partial u}{\partial t} + u\dfrac{\partial u}{\partial x} + v\dfrac{\partial u}{\partial y} = (\nu + \dfrac{k}{\rho})\dfrac{\partial^2 u}{\partial y^2} + g^*\beta(T-T_\infty) + \dfrac{k}{\rho}\dfrac{\partial N}{\partial y}$

or, $\dfrac{\partial(U_0u^*)}{\partial(\nu t^*/U_0^2)} + U_0u^*\dfrac{\partial(U_0u^*)}{\partial(\nu x^*/U_0)} + U_0v^*\dfrac{\partial(U_0u^*)}{\partial(\nu y^*/U_0)} =$

$$(\nu + \frac{k}{\rho})\frac{\partial}{\partial(\nu y^*/U_0)}\cdot\frac{\partial(U_0u^*)}{\partial(\nu y^*/U_0)} + g^*\beta(T-T_\infty) + \frac{k}{\rho}\frac{\partial(N^*U_0^2/\nu)}{\partial(\nu y^*/U_0)}$$

or, $\dfrac{U_0^3}{\nu}\dfrac{\partial u^*}{\partial t^*} + \dfrac{U_0^3}{\nu}u^*\dfrac{\partial u^*}{\partial x^*} + \dfrac{U_0^3}{\nu}v^*\dfrac{\partial u^*}{\partial y^*} = (\nu + \dfrac{k}{\rho})\dfrac{U_0^3}{\nu^2}\dfrac{\partial^2 u^*}{\partial y^{*2}}$

$$+ g^*\beta(T-T_\infty) + \frac{k}{\rho}\cdot\frac{U_0^3}{\nu^2}\frac{\partial N^*}{\partial y^*}$$

or,

$$\frac{\partial u^*}{\partial t^*} + u^*\frac{\partial u^*}{\partial x^*} + v^*\frac{\partial u^*}{\partial y^*} = (\nu + \frac{k}{\rho})\frac{1}{\nu}\frac{\partial^2 u^*}{\partial y^{*2}} + \frac{\nu}{U_0^3}g^*\beta(T-T_\infty) + \frac{k}{\rho\nu}\cdot\frac{\partial N^*}{\partial y^*}$$

or,

$$\frac{\partial u^*}{\partial t^*} + u^*\frac{\partial u^*}{\partial x^*} + v^*\frac{\partial u^*}{\partial y^*} = (1 + \frac{k}{\rho\nu})\frac{\partial^2 u^*}{\partial y^{*2}} + \frac{\nu}{U_0^3}g^*\beta\frac{(T-T_\infty)(T_s-T_\infty)}{(T_s-T_\infty)} + \frac{k}{\rho\nu}\cdot\frac{\partial N^*}{\partial y^*}$$

or, $\dfrac{\partial u^*}{\partial t^*} + u^*\dfrac{\partial u^*}{\partial x^*} + v^*\dfrac{\partial u^*}{\partial y^*} = (1+\Delta)\dfrac{\partial^2 u^*}{\partial y^{*2}} + G_r\theta + \Delta\dfrac{\partial N^*}{\partial y^*}$

After dropping the asterisks, we have

$$\frac{\partial u}{\partial t} + u\frac{\partial u}{\partial x} + v\frac{\partial u}{\partial y} = (1+\Delta)\frac{\partial^2 u}{\partial y^2} + \Delta\frac{\partial N}{\partial y} + G_r\theta \qquad (4.1)$$

Angular momentum equation: $\frac{\partial N}{\partial t}+u\frac{\partial N}{\partial x}+v\frac{\partial N}{\partial y}=\frac{\gamma}{\rho j}\frac{\partial^2 N}{\partial y^2}-\frac{k}{\rho j}(2N+\frac{\partial u}{\partial y})$

or,

$$\frac{\partial(N^*U_0^2/\nu)}{\partial(\nu t^*/U_0^2)}+U_0u^*\frac{\partial(N^*U_0^2/\nu)}{\partial(\nu x_*/U_0)}+U_0v^*\frac{\partial(N^*U_0^2/\nu)}{\partial(\nu y^*/U_0)}=$$

$$\frac{\gamma}{\rho j}\frac{\partial}{\partial(\nu y^*/U_0)}\cdot\frac{\partial(N^*U_0^2/\nu)}{\partial(\nu y^*/U_0)}-\frac{k}{\rho j}\{\frac{2N^*U_0^2}{\nu}+\frac{\partial(U_0u^*)}{\partial(\nu y^*/U_0)}\}$$

or, $\frac{U_0^4}{\nu^2}\frac{\partial N^*}{\partial t^*}+\frac{U_0^4}{\nu^2}u^*\frac{\partial N^*}{\partial x^*}+\frac{U_0^4}{\nu^2}v^*\frac{\partial N^*}{\partial y^*}=\frac{\gamma}{\rho j}\frac{U_0^4}{\nu^3}\frac{\partial^2 N^*}{\partial y^{*2}}-\frac{k}{\rho j}\frac{U_0^2}{\nu}(2N^*+\frac{\partial u^*}{\partial y^*})$

or, $\frac{\partial N^*}{\partial t^*}+u^*\frac{\partial N^*}{\partial x^*}+v^*\frac{\partial N^*}{\partial y^*}=\frac{\gamma}{\rho\nu j}\frac{\partial^2 N^*}{\partial y^{*2}}-\frac{k\nu}{U_0^2\rho j}(2N^*+\frac{\partial u^*}{\partial y^*})$

or, $\frac{\partial N^*}{\partial t^*}+u^*\frac{\partial N^*}{\partial x^*}+v^*\frac{\partial N^*}{\partial y^*}=\frac{\gamma}{\rho\nu j}\frac{\partial^2 N^*}{\partial y^{*2}}-\frac{k}{\rho\nu}\cdot\frac{\nu^2}{U_0^2 j}(2N^*+\frac{\partial u^*}{\partial y^*})$

or, $\frac{\partial N^*}{\partial t^*}+u^*\frac{\partial N^*}{\partial x^*}+v^*\frac{\partial N^*}{\partial y^*}=\lambda\frac{\partial^2 N^*}{\partial y^{*2}}-\frac{\Delta}{j^*}(2N^*+\frac{\partial u^*}{\partial y^*})$

After dropping the asterisks, we have

$$\frac{\partial N}{\partial t}+u\frac{\partial N}{\partial x}+v\frac{\delta N}{\partial y}=\lambda\frac{\partial^2 N}{\partial y^2}-\frac{\Delta}{j}(2N+\frac{\partial u}{\partial y}) \qquad (4.2)$$

Energy equation: $\frac{\partial T}{\partial t}+u\frac{\partial T}{\partial x}+v\frac{\partial T}{\partial y}=\frac{k}{\rho c_p}\frac{\partial^2 T}{\partial y^2}+Q(T-T_\infty)$

We have, $\theta=\frac{(T-T_\infty)}{(T_s-T_\infty)}$

or, $T=(T_s-T_\infty)\theta+T_\infty$

Putting this value at the above energy equation, we get

$$\frac{\partial\{(T_s-T_\infty)\theta+T_\infty\}}{\partial(\nu t^*/U_0^2)}+U_0u^*\frac{\partial\{(T_s-T_\infty)\theta+T_\infty\}}{\partial(\nu x^*/U_0)}+U_0v^*\frac{\partial\{(T_s-T_\infty)\theta+T_\infty\}|}{\partial(\nu y^*/U_0)}=$$

$$\frac{k}{\rho c_p}\frac{\partial}{\partial(\nu y^*/U_0)}\cdot\frac{\partial\{(T_s-T_\infty)\theta+T_\infty\}}{\partial(\nu y^*/U_0)}+Q(T-T_\infty)$$

or,

$$\frac{U_0^2}{\nu}(T_s-T_\infty)\frac{\partial\theta}{\partial t^*}+\frac{U_0^2}{\nu}u^*(T_s-T_\infty)\frac{\partial\theta}{\partial x^*}+\frac{U_0^2}{\nu}v^*(T_s-T_\infty)\frac{\partial\theta}{\partial y^*}=\frac{k}{\rho c_p}\cdot\frac{U_0^2}{\nu^2}(T_s-T_\infty)\frac{\partial^2\theta}{\partial y^{*2}}+Q(T-T_\infty)$$

or, $\frac{\partial\theta}{\partial t^*}+u^*\frac{\partial\theta}{\partial x^*}+v^*\frac{\partial\theta}{\partial y^*}=\frac{k}{\nu\rho c_p}\frac{\partial^2\theta}{\partial y^{*2}}+\frac{\nu}{U_0^2}Q\frac{(T-T_\infty)}{(T_s-T_\infty)}$

or, $\frac{\partial\theta}{\partial t^*}+u^*\frac{\partial\theta}{\partial x^*}+v^*\frac{\partial\theta}{\partial y^*}=\frac{1}{P_r}\frac{\partial^2\theta}{\partial y^{*2}}+\frac{\nu}{U_0^2}Q.\theta$

or, $\frac{\partial\theta}{\partial t^*}+u^*\frac{\partial\theta}{\partial x^*}+v^*\frac{\partial\theta}{\partial y^*}=\frac{1}{P_r}\frac{\partial^2\theta}{\partial y^{*2}}+\alpha\theta$

where, $\alpha=\frac{\nu}{U_0^{\,2}}Q$

After dropping the asterisks, we have

$$\frac{\partial\theta}{\partial t}+u\frac{\partial\theta}{\partial x}+v\frac{\partial\theta}{\partial y}=\frac{1}{P_r}\frac{\partial^2\theta}{\partial y^2}+\alpha\theta \tag{4.3}$$

The transferred boundary conditions are:

$$u(x,0,t)=0,\ \ N(x,0,t)=0,\ \ \theta(x,0,t)=1$$
$$u(x,\infty,t)=0,\ \ N(x,\infty,t)=0,\ \ \theta(x,\infty,t)=0,$$

4.3 Discretization

For simplicity an explicit method will be used. Let u', N', θ' denote the values u, N and θ at the end of a time step. Then the appropriate finite difference equations corresponding to equations (4.1), (4.2), and (4.3) are

$$\frac{u'_{ij}-u_{ij}}{\delta\tau}+u_{ij}\frac{u_{ij}-u_{i-1j}}{\delta X}+v_{ij}\frac{u_{ij+1}-u_{ij}}{\delta Y}=(1+\Delta)\frac{u_{ij+1}-2u_{ij}+u_{ij-1}}{(\delta Y)^2}+\Delta\frac{N_{ij+1}-N_{ij}}{\delta Y}+G_r\theta \tag{4.4}$$

$$\frac{N'_{ij}-N_{ij}}{\delta\tau}+u_{ij}\frac{N_{ij}-N_{i-1j}}{\delta X}+v_{ij}\frac{N_{ij+1}-N_{ij}}{\delta Y}=\lambda\frac{N_{ij+1}-2N_{ij}+N_{ij-1}}{(\delta Y)^2}-\frac{\Delta}{j}(2N_{ij}+\frac{u_{ij+1}-u_{ij}}{\delta Y}) \tag{4.5}$$

$$\frac{\theta'_{ij}-\theta_{ij}}{\delta\tau}+u_{ij}\frac{\theta_{ij}-\theta_{i-1j}}{\delta X}+v_{ij}\frac{\theta_{ij+1}-\theta_{ij}}{\delta Y}=\frac{1}{P_r}\frac{\theta_{ij+1}-2\theta_{ij}+\theta_{ij-1}}{(\delta Y)^2}+\alpha\theta_{ij} \tag{4.6}$$

during any time step. The coefficients u_{ij}, v_{ij} appearing in (4.4), (4.5) and (4.6) are generally considered as constant. Then at the end of any time step $\delta\tau$, the new temperature θ', the new angular momentum N' and the new velocity components u' at all interior grid points may be obtained by successive applications of (4.6), (4.5) and (4.4) respectively. This process is repeated in time and provided the time step is sufficiently small u, N, θ should eventually converge to values which approximate the steady state solution of equations (4.1), (4.2) and (4.3).

4.4 Stability Analysis

Since the explicit procedure will to be used, we wish to know the largest time-step consistent with stability. The stability analysis for simultaneous partial differential equations is outlined below.

The general terms of the Fourier expansion for u, N, and θ at a time arbitrarily called t=0 are all $e^{i\alpha X}e^{i\beta Y}$ apart from a constant (here $i=\sqrt{-1}$). At a time τ later, these terms will become

$$u=\psi(\tau)e^{i\alpha X}e^{i\beta Y},\ \mathrm{N}=\zeta(\tau)e^{i\alpha X}e^{i\beta Y},\ \theta=\xi(\tau)\ e^{i\alpha X}e^{i\beta Y}$$

Substituting these values in (4.4), (4.5) and (4.6) regarding the coefficients U and V as constant over any one-time step, and denoting values after time-step by ψ', ζ' and ξ' gives

$$\frac{\psi'(\tau)e^{i\alpha X}e^{i\beta Y}-\psi(\tau)e^{i\alpha X}e^{i\beta Y}}{\delta\tau}+\mathrm{U}\frac{\psi(\tau)e^{i\alpha X}e^{i\beta Y}-\psi(\tau)e^{i\alpha(X-\delta X)}e^{i\beta Y}}{\delta X}$$

$$+\mathrm{V}\frac{\psi(\tau)e^{i\propto X}e^{i\beta(Y+\delta Y)}-\psi(\tau)e^{i\propto X}e^{i\beta Y}}{\delta Y}=$$

$$(1+\Delta)\frac{\psi(\tau)e^{i\propto X}e^{i\beta(Y+\delta Y)}-2\psi(\tau)e^{i\propto X}e^{i\beta Y}+\psi(\tau)e^{i\propto X}e^{i\beta(Y+\delta Y)}}{(\delta Y)^2}$$

$$+\Delta\frac{\zeta(\tau)e^{i\propto X}e^{i\beta(Y+\delta Y)}-\zeta(\tau)e^{i\propto X}e^{i\beta Y}}{\delta Y}+G_r\xi(\tau)e^{i\propto X}e^{i\propto Y}$$

$$\text{or, }\frac{\psi'-\psi}{\delta\tau}+\mathrm{U}\frac{\psi(1-e^{-i\propto\delta X})}{\delta X}+\mathrm{V}\frac{\psi(e^{i\beta\delta Y}-1)}{\delta Y}=(1+\Delta)\frac{\psi(e^{i\beta\delta Y}-2+e^{-i\beta\delta Y})}{(\delta Y)^2}$$

$$+\Delta\frac{\zeta(e^{i\beta\delta Y}-1)}{\delta Y}+G_r\xi$$

$$\text{or, }\frac{\psi'-\psi}{\delta\tau}+\mathrm{U}\frac{\psi(1-e^{-i\propto\delta X})}{\delta X}+\mathrm{V}\frac{\psi(e^{i\beta\delta Y}-1)}{\delta Y}=2\ (1+\Delta)\frac{\psi(\cos\beta\delta Y-1\ )}{(\delta Y)^2}$$

$$+\Delta\frac{\zeta(e^{i\beta\delta Y}-1)}{\delta Y}+G_r\xi$$

or,

$$\psi'=[1-\{\frac{U}{\delta X}(1-e^{-i\propto\delta X})+\frac{V}{\delta Y}(e^{i\beta\delta Y}-1)+\frac{2(1+\Delta)}{(\delta Y)^2}(1-\cos\beta\delta Y)\}\delta\tau]\psi+\Delta\frac{\delta\tau}{\delta Y}(e^{i\beta\delta Y}-1)\zeta+G_r\delta\tau\xi$$

$$\text{or, }\psi'=A\psi+B\zeta+c\xi \qquad (4.7)$$

where, $A=1-\{\frac{U}{\delta X}(1-e^{-i\propto\delta X})+\frac{V}{\delta Y}(e^{i\beta\delta Y}-1)+\frac{2(1+\Delta)}{(\delta Y)^2}(1-\cos\beta\delta Y)\}\delta\tau$

$B=\Delta\frac{\delta\tau}{\delta Y}(e^{i\beta\delta Y}-1)$ and $C=G_r\delta\tau\xi$.

From equation (4.5) we have

$$\frac{\zeta'(\tau)e^{i\propto X}e^{i\beta Y}-\zeta(\tau)e^{i\propto X}e^{i\beta Y}}{\delta\tau}+\mathrm{U}\frac{\zeta(\tau)e^{i\propto X}e^{i\beta Y}-\zeta(\tau)e^{i\propto(X-\delta X)}e^{i\beta Y}}{\delta X}$$

$$+\mathrm{V}\frac{\zeta(\tau)e^{i\propto X}e^{i\beta(Y+\delta Y)}-\zeta(\tau)e^{i\propto X}e^{i\beta Y}}{\delta Y}=$$

$$\lambda\frac{\zeta(\tau)e^{i\propto X}e^{i\beta(Y+\delta Y)}-2\zeta(\tau)e^{i\propto X}e^{i\beta Y}+\zeta(\tau)e^{i\propto X}e^{i\beta(Y+\delta Y)}}{(\delta Y)^2}$$

$$-\frac{\Delta}{j}\frac{\zeta(\tau)e^{i\propto X}e^{i\beta(Y+\delta Y)}-\zeta(\tau)e^{i\propto X}e^{i\beta Y}}{\delta Y}-\frac{2\Delta}{j}\zeta(\tau)e^{i\propto X}e^{i\propto Y}$$

$$\text{or, }\frac{\zeta'-\zeta}{\delta\tau}+\mathrm{U}\frac{\zeta(1-e^{-i\propto\delta X})}{\delta X}+\mathrm{V}\frac{\zeta(e^{i\beta\delta Y}-1)}{\delta Y}=\lambda\frac{\zeta(e^{i\beta\delta Y}-2+e^{-i\beta\delta Y})}{(\delta Y)^2}$$

$$-\frac{\Delta}{j}\frac{\psi(e^{i\beta\delta Y}-1)}{\delta Y}-\frac{2\Delta}{j}\zeta$$

or,

$$\zeta'=[1-\{\frac{U}{\delta X}(1-e^{-i\propto\delta X})+\frac{V}{\delta Y}(e^{i\beta\delta Y}-1)+\frac{2\lambda}{(\delta Y)^2}(1-\cos\beta\delta Y)+\frac{2\Delta}{j}\}\delta\tau]\zeta+\frac{\Delta}{j}\frac{1}{\delta Y}(1-e^{i\beta\delta Y})\psi$$

$$\text{or, }\zeta'=D\psi+E\zeta \tag{4.8}$$

$$\text{where, }\quad D=\frac{\Delta}{j}\frac{1}{\delta Y}(1-e^{i\beta\delta Y})$$

$$\text{and }\quad E=1-\{\frac{U}{\delta X}(1-e^{-i\propto\delta X})+\frac{V}{\delta Y}(e^{i\beta\delta Y}-1)+\frac{2\lambda}{(\delta Y)^2}(1-\cos\beta\delta Y)+\frac{2\Delta}{j}\}\delta\tau$$

Again from equation (4.6) we get

$$\frac{\xi'(\tau)e^{i\propto X}e^{i\beta Y}-\xi(\tau)e^{i\propto X}e^{i\beta Y}}{\delta\tau}+\mathrm{U}\frac{\xi(\tau)e^{i\propto X}e^{i\beta Y}-\xi(\tau)e^{i\propto(X-\delta X)}e^{i\beta Y}}{\delta X}$$

$$+\mathrm{V}\frac{\xi(\tau)e^{i\propto X}e^{i\beta(Y+\delta Y)}-\xi(\tau)e^{i\propto X}e^{i\beta Y}}{\delta Y}$$

$$=\frac{1}{P_r}\frac{\xi(\tau)e^{i\propto X}e^{i\beta(Y+\delta Y)}-2\xi(\tau)e^{i\propto X}e^{i\beta Y}+\xi(\tau)e^{i\propto X}e^{i\beta(Y+\delta Y)}}{(\delta Y)^2}+H\xi(\tau)e^{i\propto X}e^{i\propto Y}$$

(in the previous equation H is used in place of α, the heat source parameter)

$$\text{or, }\frac{\xi'-\xi}{\delta\tau}+U\frac{\xi(1-e^{-i\alpha\delta X})}{\delta x}+V\frac{\xi(e^{i\beta\delta Y}-1)}{\delta Y}=\frac{1}{P_r}\frac{\xi(e^{i\beta\delta Y}-2+e^{-i\beta\delta Y})}{(\delta Y)^2}+H\xi$$

$$\text{or, }\frac{\xi'-\xi}{\delta\tau}+U\frac{\xi(1-e^{-i\propto\delta X})}{\delta x}+V\frac{\xi(e^{i\beta\delta Y}-1)}{\delta Y}=\frac{2}{P_r}\frac{\xi(\cos\beta\delta Y-1)}{(\delta Y)^2}+H\xi$$

or, $\xi' = [1 - \{\frac{U}{\delta X}(1 - e^{-i\alpha\delta X}) + \frac{V}{\delta Y}(e^{i\beta\delta Y} - 1) + \frac{1}{P_r}.\frac{2}{(\delta Y)^2}(1 - \cos\beta\delta Y) - H\}\delta\tau]\xi$

or, $\xi' = F\xi$ (4.9)

where, $F = 1 - \{\frac{U}{\delta X}(1 - e^{-i\alpha\delta X}) + \frac{V}{\delta Y}(e^{i\beta\delta Y} - 1) + \frac{1}{P_r}.\frac{2}{(\delta Y)^2}(1 - \cos\beta\delta Y) - H\}\delta\tau$

Equations (4.7), (4.8) and (4.9) are then expressed in matrix form

$$\begin{bmatrix} \psi' \\ \zeta' \\ \xi' \end{bmatrix} = \begin{bmatrix} A & B & C \\ D & E & 0 \\ 0 & 0 & F \end{bmatrix} \begin{bmatrix} \psi \\ \zeta \\ \xi \end{bmatrix}$$

That is $\boldsymbol{\eta}' = s\boldsymbol{\eta}$

where $\boldsymbol{\eta}$ is the column vector whose elements are ψ, ζ and ξ.

For stability each eigen value λ_1 λ_2 and λ_3 of the amplification matrix s must not exceed unity in modulus.

The eigen value equation will be $|I\lambda - s| = 0$

or, $(\lambda - F)(\lambda - A)(\lambda - E) - BD = 0$

But as $\delta\tau$ is very small and $(\delta\tau)^2$ is too small and is thus negligible. So we can take

$(\lambda - A)(\lambda - E)(\lambda - F) = 0$

$\therefore\ \lambda_1 = A,\ \lambda_2 = E$ and $\lambda_3 = F$.

Hence the stability conditions will be

$|A| \le 1$, $|E| \le 1$ and $|F| \le 1$ for all α and β.

It is assumed that U is everywhere non-negative and that V is everywhere non-positive. That is to be expected, since the heated fluid rises in the positive X direction and fluid is drawn in from the positive Y direction to take its place.

Let

$$a = \frac{U\delta\tau}{\delta X},\quad b = \frac{|V|\delta\tau}{\delta Y} \text{ and } c = \frac{\delta\tau}{(\delta Y)^2}$$

Hence, $A = 1 - \{a(1 - e^{-i\alpha\delta X}) + b(e^{i\beta\delta Y} - 1) + 2c(1 + \Delta)(1 - \cos\beta\delta Y)\}$

or, $A = 1 - \{a + b + 2c(1 + \Delta)\} + ae^{-i\alpha\delta X} - be^{i\beta\delta Y} + 2c(1 + \Delta)\cos\beta\delta Y$

Let $2c(1 + \Delta) = L$ then

$A = 1 - (a + b + L) + ae^{-i\alpha\delta X} + be^{i\beta\delta Y} + L\cos\beta\delta Y$

The coefficients a, b and c are all real and nonnegative. By representing A on an Argand diagram, we can demonstrate that the maximum modulus of A occurs when $\alpha\delta X = m\pi$ and $\beta\delta Y = n\pi$, where m and n are integer, and hence occurs when A is real. For $\delta\tau$ sufficiently large the value of $|A|$ is greatest when both m and n are odd integers. In which case

A=1-(a+b+L)-a-b-L

or, A=1-2(a+b+L)

i.e. A=1-2{a+b+2c(1+Δ)} (Putting the value of L)

which becomes increasingly more and more negative with the increase in $\delta\tau$. To satisfy $|A| \le 1$, the most negative allowable value is $A = -1$. Hence the stability condition is that

$2\{a+b+2c\,(1+\Delta)\} \le 2$

That is $\frac{U\delta\tau}{\delta X} + \frac{|V|\delta\tau}{\delta Y} + 2(1+\Delta)\frac{\delta\tau}{(\delta Y)^2} \le 1$ (4.10)

Again for the stability condition $|E| \le 1$

$$E = 1 - \{\frac{U}{\delta X}(1 - e^{-i\alpha\delta X}) + \frac{V}{\delta Y}(e^{i\beta\delta Y} - 1) + \frac{2\lambda}{(\delta Y)^2}(1 - \cos\beta\delta Y) + \frac{2\Delta}{j}\}\delta\tau$$

or, $$E = 1 - \{\frac{U\delta\tau}{\delta X}(1 - e^{-i\alpha\delta X}) + \frac{V\delta\tau}{\delta Y}(e^{i\beta\delta Y} - 1) + \frac{2\lambda\delta\tau}{(\delta Y)^2}(1 - \cos\beta\delta Y) + \frac{2\Delta\delta\tau}{j}\}$$

For all α and β defining $a = \frac{U\delta\tau}{\delta X}$, $b = \frac{|V|\delta\tau}{\delta Y}$, $c = \frac{\delta\tau}{(\delta Y)^2}$ and $d = \frac{\delta\tau}{j}$, we have

$$= 1 - \{a(1 - e^{-i\alpha\delta X}) + b(e^{i\beta\delta Y} - 1) + 2\lambda c(1 - \cos\beta\delta Y) + 2\Delta d\}$$

$$= 1 - (a + b + 2\lambda c + 2\Delta d) + ae^{-i\alpha\delta X} - be^{i\beta\delta Y} + 2\lambda\cos\beta\delta Y$$

The coefficients a, b, c and d are all real and non-negative. By representing E on an Argand diagram, we can demonstrate that the maximum modulus of E occurs when $\alpha\delta X = m\pi$ and $\beta\delta Y = n\pi$, where m and n are integer, and hence occurs when E is real. For $\delta\tau$ sufficiently large the value of $|E|$ is greatest when both m and n are odd integers. In which case $E = 1 - 2(a + b + 2\lambda c + 2\Delta d) - a - b - 2\lambda c$

or, $E = 1 - 2(a + b + 2\lambda c + \Delta d)$

which becomes increasingly more and more negative with the increase in $\delta\tau$. To satisfy $|E| \le 1$, the most negative allowable value is $E = -1$. Hence the stability condition is that

$2(a + b + 2\lambda c + \Delta d) \le 2$

That is $\frac{U\delta\tau}{\delta X}+\frac{|V|\delta\tau}{\delta Y}+2\lambda\frac{\delta\tau}{(\delta Y)^2}+\Delta\frac{\delta\tau}{j}\le 1$ (4.11)

Likewise, the third condition $|F|\le 1$ will require that

$$\frac{U\delta\tau}{\delta X}+\frac{|V|\delta\tau}{\delta Y}+\frac{1}{\Pr}\frac{2\delta\tau}{(\delta Y)^2}+(\frac{-H\delta\tau}{2})\le 1 \quad (4.12)$$

In the present problem, with chosen value of Pr, we need only be concerned with satisfying (4.12) since (4.10) and (4.11) follows automatically. The co-efficient U and $|V|$, although treated as constants over any one-step, will vary from one time-step to the next in a manner which cannot be predicted a priori. That is, the maximum permissible time step consistent with stability is itself variable, but its value can always be checked, during computation if necessary.

4.5 Skin –friction coefficient

One of the quantities of chief physical interest is the skin friction coefficient. The equation defining the wall shear stress is

$$\tau_w=(\mu+k)\left(\frac{\partial u}{\partial y}\right)_{y=0}+kN(y)_{y=0}$$

Hence the skin-friction coefficient is given by

$$c_f=\frac{2\tau}{\rho U_0^2}=\frac{2(\mu+k)}{\rho U_0^2}\left(\frac{\partial u}{\partial y}\right)_{y=0}=\frac{2}{U_0^2}[\nu+\Delta\nu]\left(\frac{\partial u}{\partial y}\right)_{y=0}$$

$$=\frac{2}{U_0^2}[1+\Delta]\nu\left(\frac{\partial u}{\partial y}\right)_{y=0}$$

Thus we can say that the skin friction coefficient c_f is proportional to $\frac{1}{U_0^2}[1+\Delta]\nu\left(\frac{\partial u}{\partial y}\right)_{y=0}$

4.6 Results and Discussion

In this thesis, the effect of transient free convection on micropolar fluid with heat generation and constant heat flux has been investigated using the finite difference method technique. To study the physical situation of this problem, we have computed the numerical values of the velocity, temperature and angular momentum within the boundary layer and also the coefficients proportional to the skin friction coefficient and Nusselt number is calculated. It is seen that the solution will be affected by the parameters, namely heat source parameter α, micro inertia per unit mass j, dimensionless material parameter Δ, the Grashof number Gr, dimensionless material parameter λ and the

Prandtl number Pr. The values 0.2, 0.5, 0.71, 0.73, 1, 2, 5, 7.01 are considered for Pr (0.2, o.5, 0.71, 0.73 for air and 1, 2, 5, 7.01 for water). The values of other parameters are however chosen arbitrarily.

Figures (4.1)-(4.3) show the velocity, temperature and angular momentum profiles for different values of heat source parameter α respectively. From figure (4.1) it is observed that with the increase of α the velocity is increasing rapidly. But the spreading of velocity squeezes with the increase in α and within a short distance the velocity is becoming zero. Figure (4.2) is expressing that with the increase in α the temperature is increasing rapidly. But the spreading of temperature squeezes with the increase of α and within a short distance the temperature is becoming zero, as in the case of velocity. In Figure (4.3), with the increase in α, the negative value of angular momentum increases. Also the magnitude of positive value of the angular momentum increases with the increase of α. When α is large the negative zone of the angular momentum is small in comparison to the small α. For large value of α the angular momentum oscillates more from negative to positive.

Figures (4.4)-(4.6) are showing the velocity, temperature and angular momentum profiles for different values of micro inertia per unit mass, J respectively. In figure (4.4), there is a very small change of velocity due to increase the value of J. The velocity spreads very small with the increase of J and within a short distance the velocity is becoming zero. In figure (4.5), there is again a small increase of temperature with the increase of J. In figure (4.6), with the increase of J the negative value of angular momentum decreases. Also the magnitude of positive value of the angular momentum increases with the increases of J. When J is large the negative zone of the angular momentum is large in comparison to the small J.

Figures (4.7)-(4.9) are representing respectively the velocity, temperature and angular momentum profiles for different values of dimensionless material parameter Δ. In figure (4.7) here with the increase of Δ the velocity is decreasing. But the spreading of velocity is more for higher values of Δ though the velocity is becoming zero at the same distance from the plate. In figure (4.8), the temperature increases very slowly with the increase of Δ and like velocity becoming zero at the same distance. In Figure (4.9), with the

increase of Δ, the negative value of angular momentum increases. Also the magnitude of positive value of the angular momentum increases with the increase of Δ. When Δ is large the negative zone of the angular momentum is small in comparison to the small Δ. For large value of Δ the angular momentum oscillates more from negative to positive.

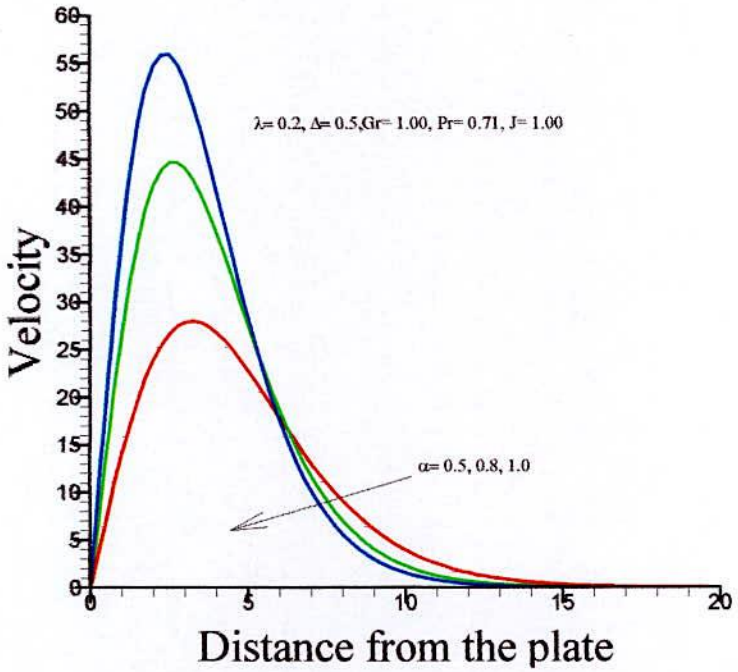

Fig. 4.1: Velocity profiles for different values of heat source parameter, α

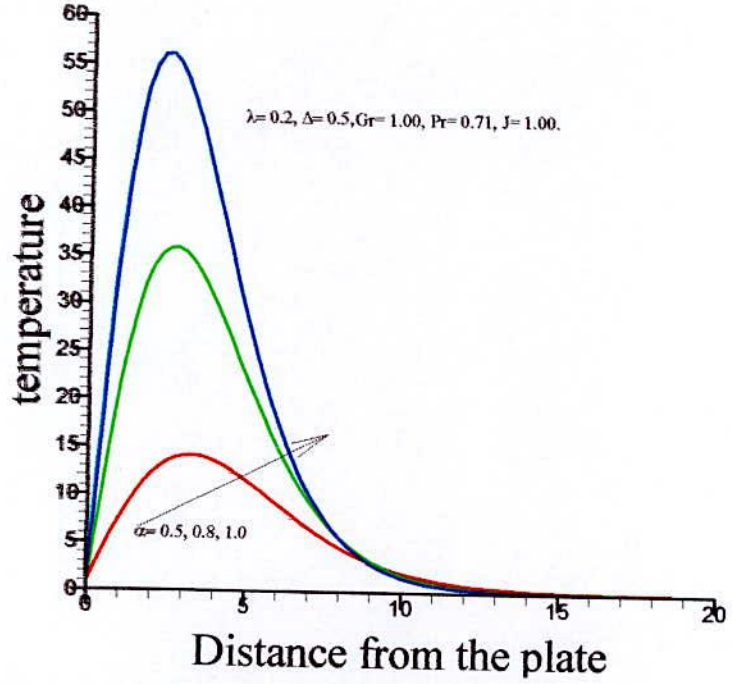

Fig. 4.2: Temperature profiles for different values of heat source parameter, α

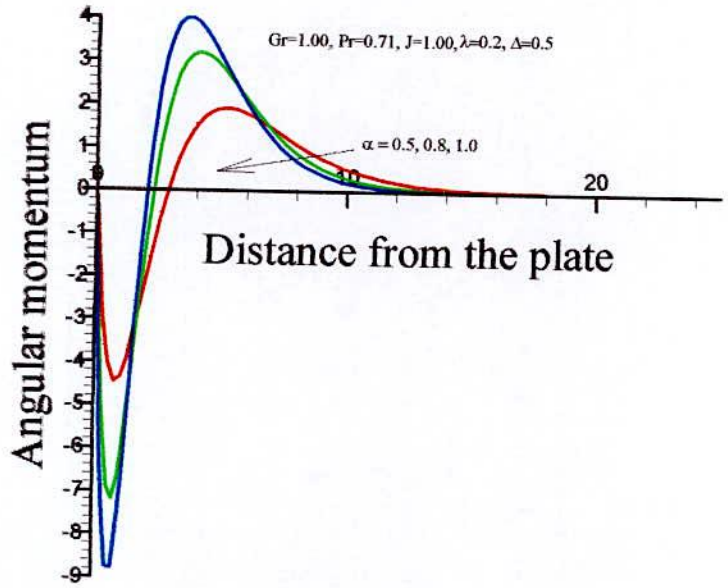

Fig 4.3: Angular Momentum profiles for different values of heat source parameter, α

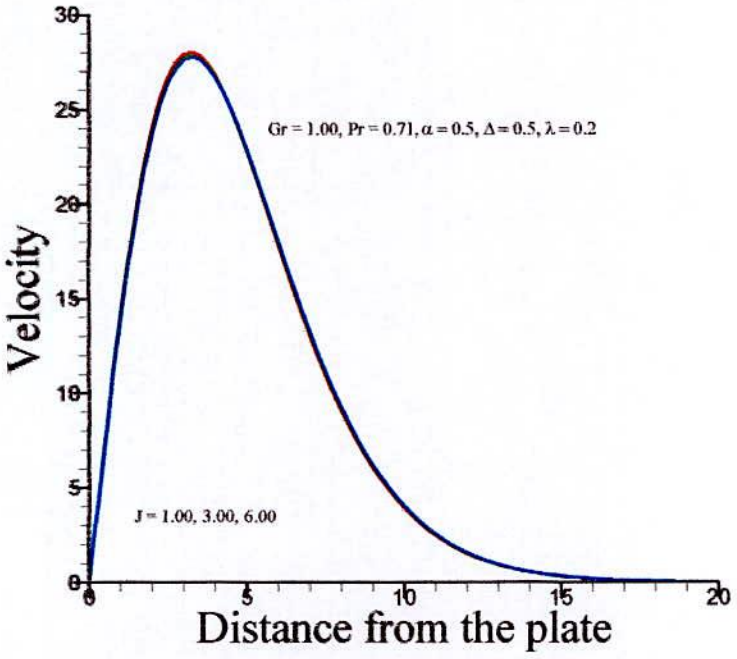

Fig 4.4: Velocity profiles for different values of micro inertia per unit mass, J

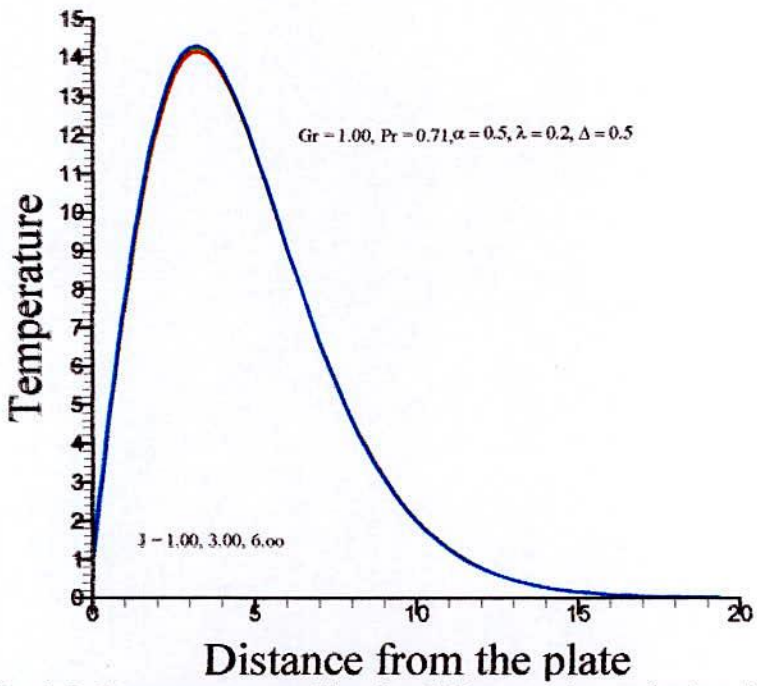

Fig. 4.5: Temperature profiles for different values of micro inertia per unit mass, J

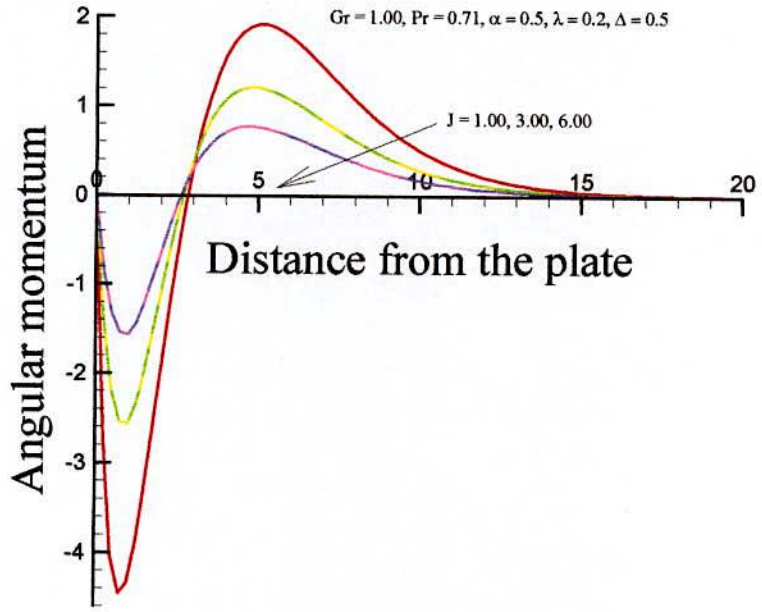

Fig. 4.6: Angular momentum profiles for different values of micro inertia per unit mass, J

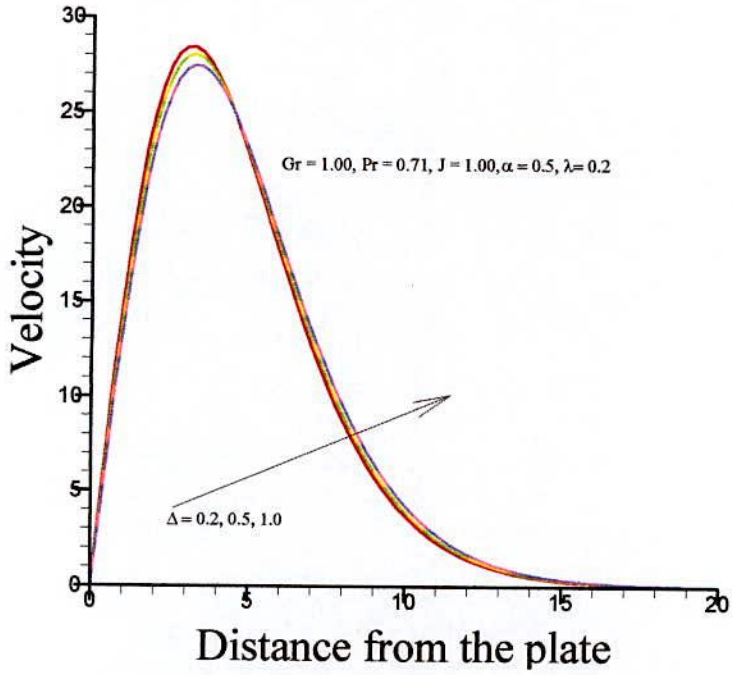

Fig. 4.7: Velocity profiles for different values of dimensionless parameter, Δ

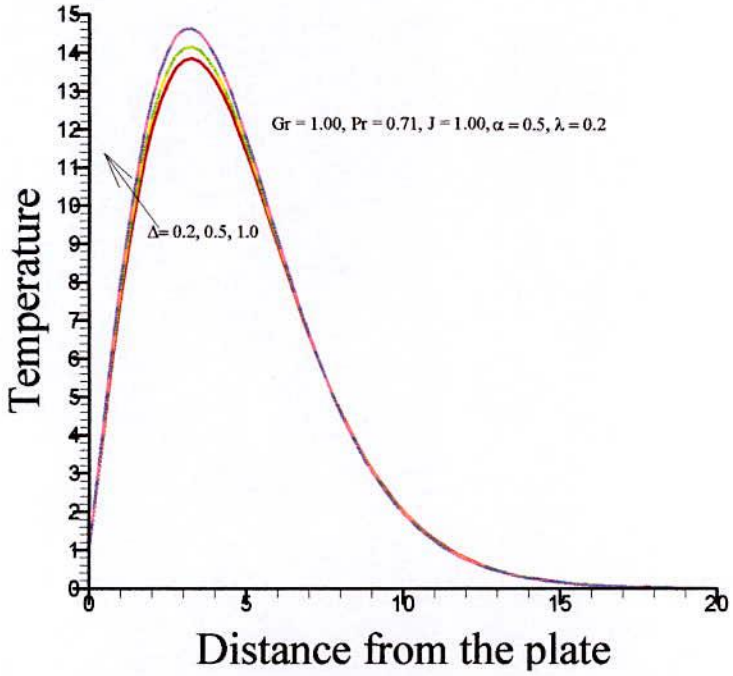

Fig. 4.8: Temperature profiles for different values of dimensionless parameter, Δ

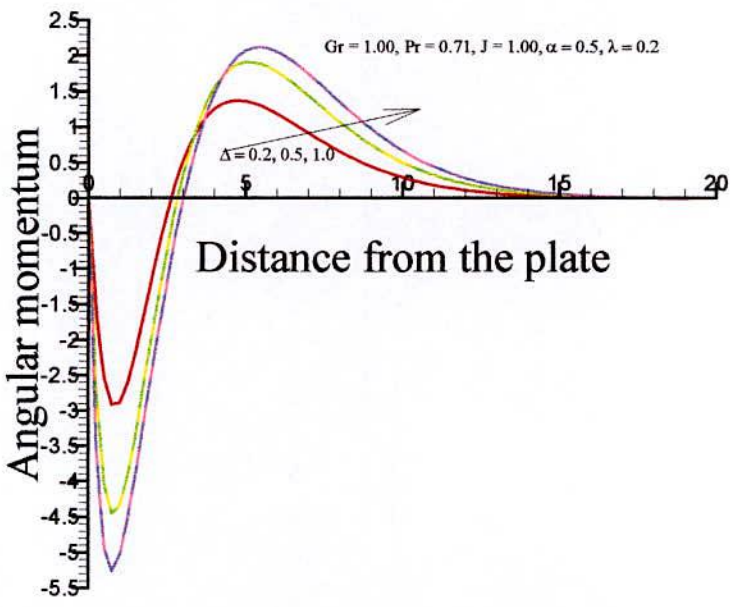

Fig. 4.9: Angular momentum profiles for different values of dimensionless parameter, Δ

For different values of Grashof Number Gr, The Profiles for velocily, Temperature and angular momentum are presented in Fig (4.10)-(4.12). In fig (4.10), we observed that with the increase in Gr maximum of the velocity increases whereas the spreading of velocity decreases.

From fig (4.11), it is found that the temperature decreases with the increase in Gr. Also the temperature is becoming zero far away from the plate for lower values of Gr. The angular momentum fluctuation from negative to positive increases with the increase in Gr and for lower values of Gr though the magnitude of angular momentum are less but its spreading is more.

Fig(4.13)-(4.15) represents the velocity, Temperature and angular momentum profiles respectively for different values of material parameter λ . It is seen from fig (4.13) and (4.14) that the material parameter λ has very little impact on velocity and temperature . Infact the Curves for different values of λ are not clearly distinguishable. But with the increase in λ the magnitude of angular momentum decreases.

The profiles for velocity, temperature and angular momentum for different values of Prandtl number Pr are shown respectively in fig.(4.16) - (4.18). The velocity is not only decreasing with the increase in Pr but also it is becoming zero within a short distance from the wall. The temperature profile squeezes with the increase in Pr but the pick value of the temperature rises sharply. Incase of angular momentum from fig. (4.18), it is seen that the negative value of angular momentum near the wall has no appreciable change with the increase in Pr. But positive values of angular momentum increases with Pr. Though with the increase in Pr. the effective zone of angular momentum decreases with the increase in Pr.

Fig.(4.19) – (4.21) representing the velocity, temperature and angular momentum profiles for different values of time t respectively. From fig.(4.19) and (4.20) it is seen that both the velocity and temperature are primarily increasing with the increase in time but after sometime they decreases a little and remain almost same for different times. The angular momentum has the same time effect as that of temperature and velocity i. e. primary increase then decrease then remaining close with the increasing time.

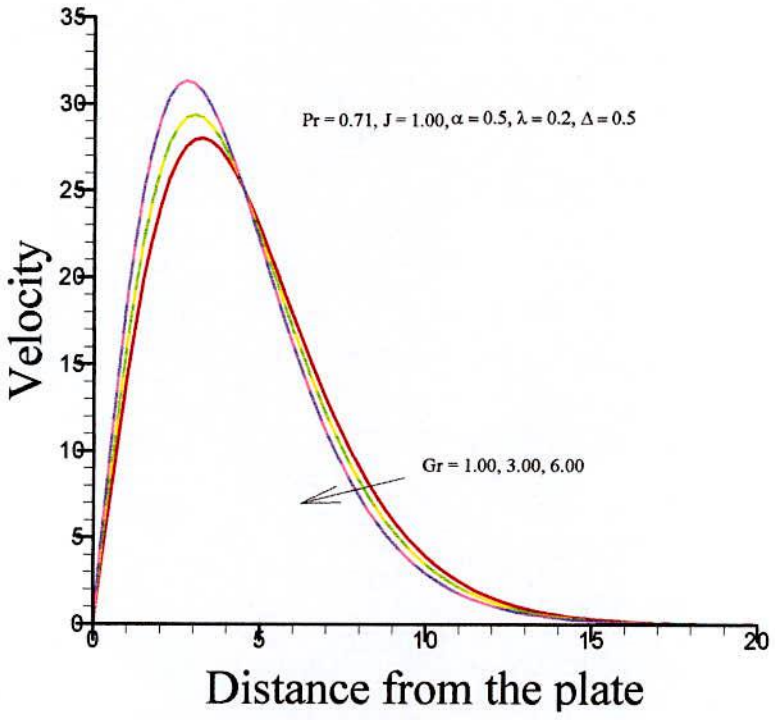

Fig. 4.10: Velocity profiles for different values of the Grashof number, Gr

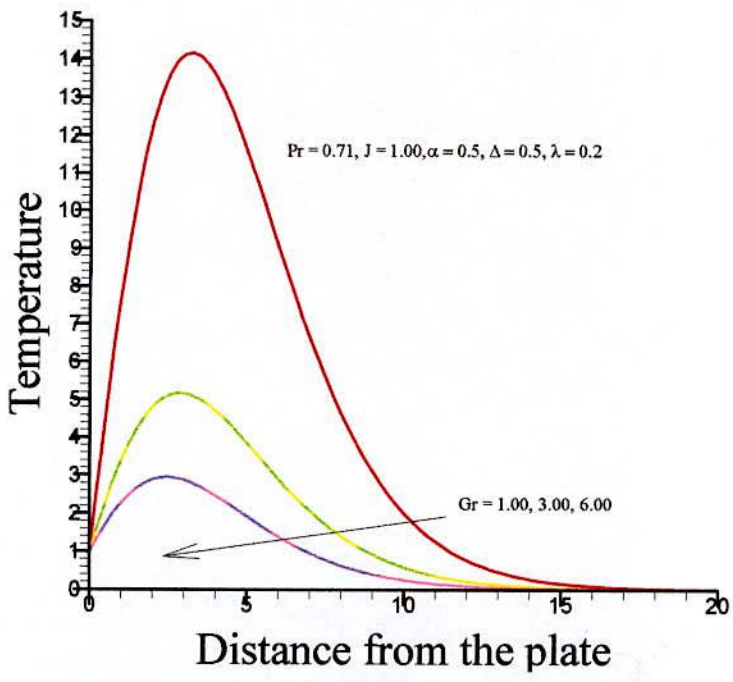

Fig. 4.11: Temperature profiles for different values of the Grashof number, Gr

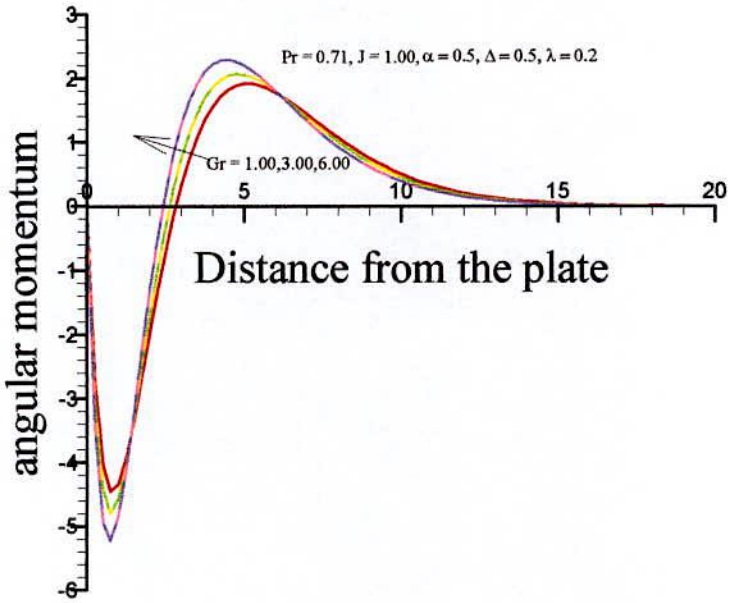

Fig. 4.12: Angular momentum profiles for different values of the Grashof number, Gr

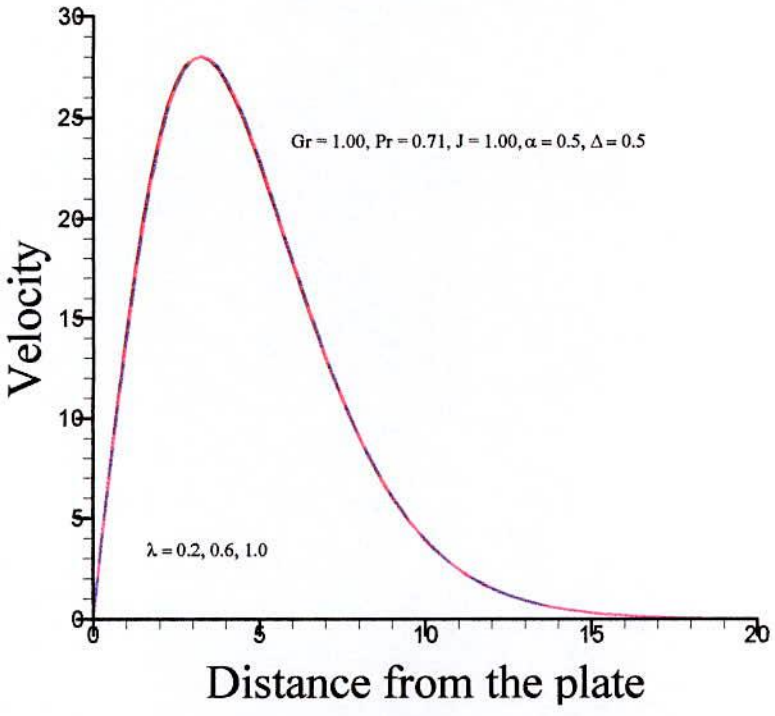

Fig. 4.13: Velocity profiles for different values of dimensionless material parameter, λ

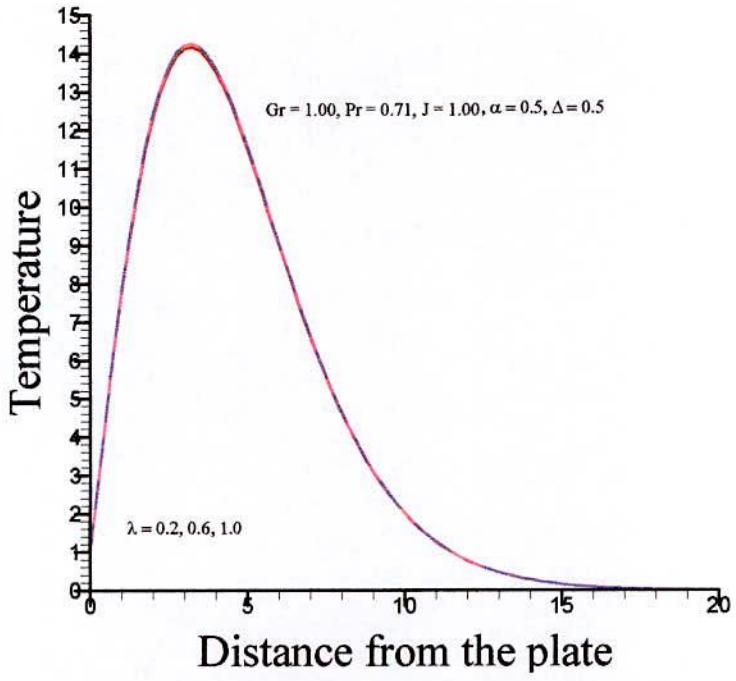

Fig. 4.14: Temperature profiles for different values of dimensionless material parameter, λ

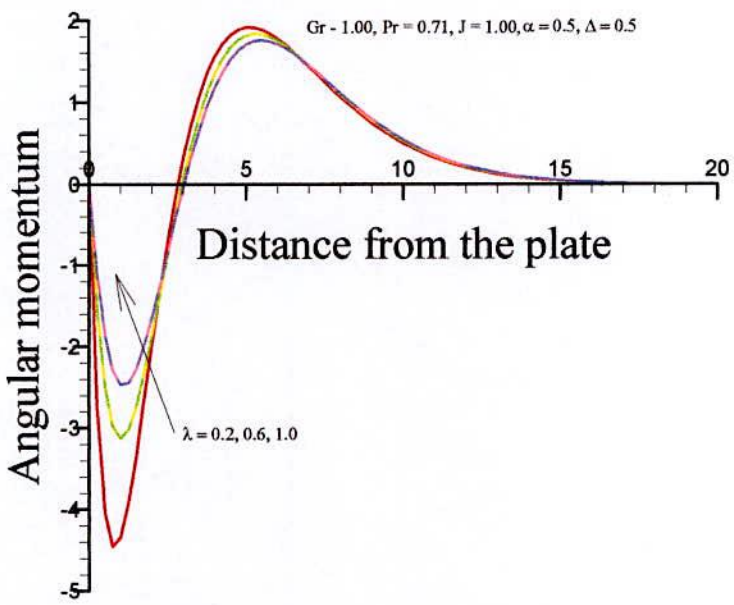

Fig. 4.15: Angular momentum profiles for different values of dimensionless material parameter, λ

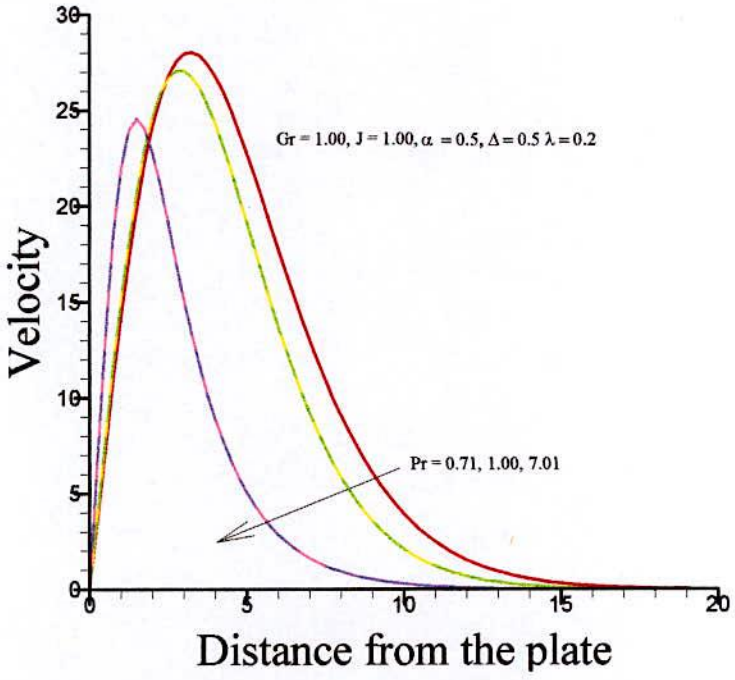

Fig. 4.16: Velocity profiles for different values of the Prandtl number, Pr

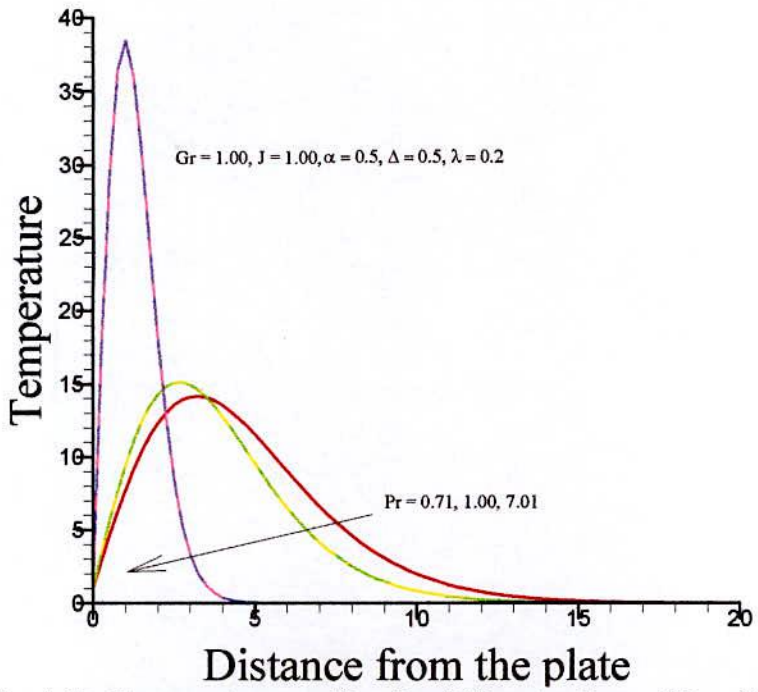

Fig. 4.17: Temperature profiles for different values of Prandtl number, Pr

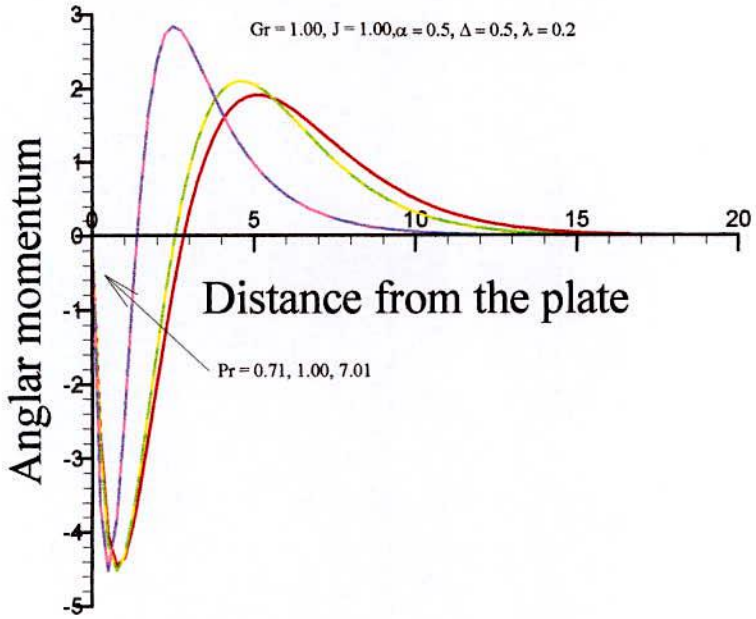

Fig. 4.18: Angular momentum profiles for different values of Prandtl number, Pr

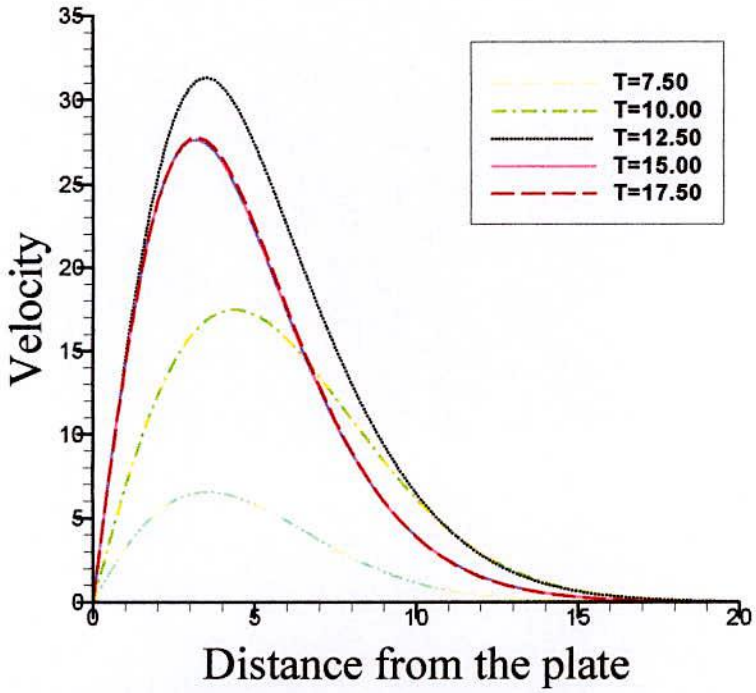

Fig. 4.19: Velocity profiles for different values of time, T

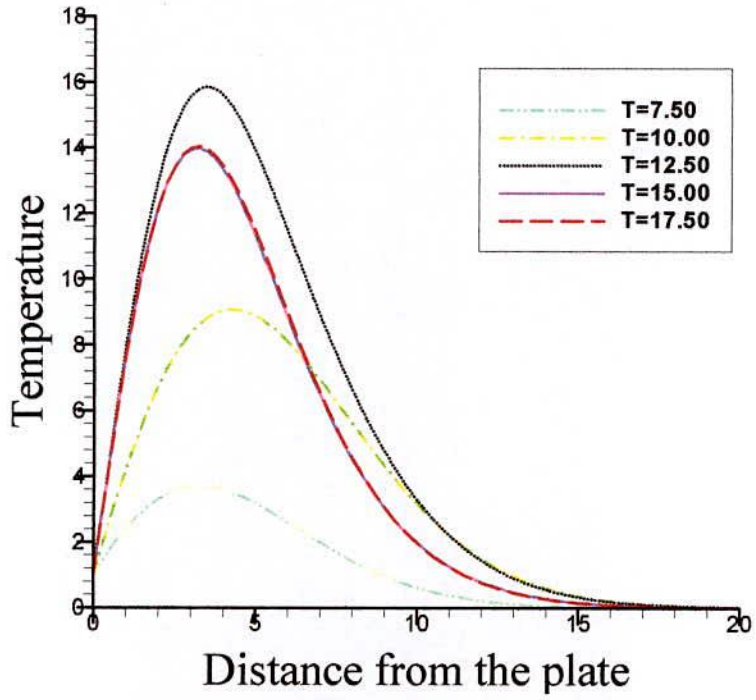

Fig. 4.20: Temperature profiles for different values of time, T

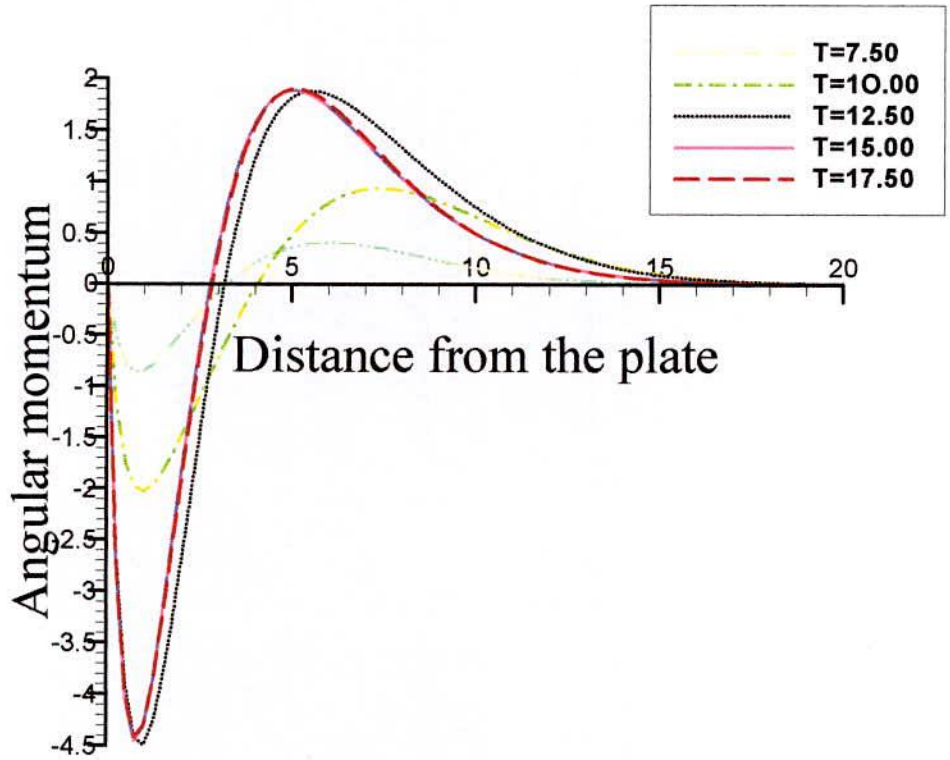

Fig. 4.21: Angular momentum profiles for different values of time, T

In the following the effect of different parameters on the coefficient of skin friction and Nusselt number are discussed which are tabulated in table (4.1) – (4.6). The values shown there are proportional to the coefficient of skin friction and Nusselt number.

In Table (4.1), the values proportional to the coefficient of skin friction and Nusselt numbers for different values of α is tabulated with fixed values of the other parameters. From the table it is observed that with the increase in α the value proportional to the skin friction increases, whereas in the case of Nusselt number the situation is reversed. Also the rate of decrease in Nusselt number is far more than the rate of increase.

In table (4.2), the same is tabulated as table (4.1), but different values of micro inertia J with the other parameters are kept fixed. From the table it is observed that the coefficient proportional to the skin friction increases primarily (from 1 to 4) then decreases. In both cases the rate of change is very small. Whereas the case of Nusselt number the rate of decreases is monotonous, although slow. Thus it may be considered that the microinertia has a very little impact on the coefficient of skin friction and Nusselt numbers.

The effect of dimensionless material parameter, Δ on the coefficient of skin friction and Nusselt numbers cab be observed from table (4.3). In the table only the dimensionless material parameter Δ has been varying , keeping other parameters as fixed. It is observed that both the tabulated values are decreasing with the increase in Δ .and the rate of decrease has no significant difference.

Table 4.1: Numerical values proportional to skin friction coefficient C_f and Nusselt number Nu for different values of α , taking $Gr = 1.00, \Pr = 0.71, J = 1.00, \lambda = 0.2, \Delta = 0.5$ as fixed

α	Values proportional to C_f	Values proportional to Nu
0.5	9.822492	-4.726112
0.8	18.620130	-14.733240
1.0	25.665870	-25.549920
1.5	46.543100	-69.980420
2.0	71.292650	-143.382300
2.5	99.310490	-250.198700

Table 4.2: Numerical values proportional to skin friction coefficient C_f and Nusselt number Nu for different values of J, taking $Gr = 1.00, \Pr = 0.71, \alpha = 0.5, \lambda = 0.2, \Delta = 0.5$ as fixed.

J	Values proportional to C_f	Values proportional to Nu
1.00	9.822492	-4.726112
2.00	9.792691	-4.752003
3.00	9.788363	-4.766579
4.00	9.788019	-4.775903
5.00	9.788466	-4.782364
6.00	9.789032	-4.787105

Table 4.3: Numerical values proportional to skin friction coefficient, C_f and Nusselt number Nu for different values of Δ, taking $Gr = 1.00, \Pr = 0.71, J = 1.00, \alpha = 0.5, \lambda = 0.2,$ as fixed.

Δ	Values proportional to C_f	Values proportional to Nu
0.2	10.540360	-4.584459
0.5	9.822492	-4.726112
1.0	9.070086	-4.933964
1.5	8.594524	-5.130653
2.0	8.256192	-5.323051
2.5	7.996166	-5.513247

In table (4.4) the values proportional to the skin-friction coefficient and the Nusselt number are tabulated against the Grashhof number Gr. It is seen that both of them increases with the increase in Gr. For skin friction the rate of increase is almost same , but in the case of Nusselt number the rate slows down for higher values of Gr.

Table (4.5) shows the values proportional to the skin-friction coefficient and the Nusselt number against the dimensionless material parameter λ. It has the same effect on them as that of J. Also the rate of change here is similar to that in J.

Finally the effect of Prandtl number, Pr on the coefficient of skin friction and Nusselt numbers are presented in table (4.6). Here again, as usual, the other parameters are kept as constant. It is seen that with the increase in Pr the value proportional to skin friction increases, whereas the Nusselt number decreases.

Table 4.4: Numerical values proportional to skin friction coefficient C_f and Nusselt number Nu for different values of Gr , taking $\Pr = 0.71, J = 1.00, \alpha = 0.5, \lambda = 0.2 \Delta = 0.5$ as fixed.

Gr	Values proportional to C_f	Values proportional to Nu
1.00	9.822492	-4.726112
2.00	11.018580	-2.537850
3.00	12.156370	-1.796058
4.00	13.238690	-1.416348
5.00	14.273790	-1.182411
6.00	15.268690	-1.022038

Table 4.5: Numerical values proportional to skin friction coefficient C_f and Nusselt number Nu for different values of λ , taking $Gr = 1.00 \Pr = 0.71, J = 1.00, \alpha = 0.5, \Delta = 0.5$ as fixed.

λ	Values proportional to C_f	Values proportional to Nu
0.2	9.822492	-4.726112
0.4	9.748273	-4.742879
0.5	9.735003	-4.748732
0.6	9.727735	-4.753602
0.8	9.722200	-4.761340
1.0	9.722288	-4.767288

Table 4.6: Numerical values proportional to skin friction coefficient C_f and Nusselt number Nu for different values of Pr, taking $Gr = 1.00, J = 1.00, \alpha = 0.5, \lambda = 0.2 \Delta = 0.5$ as fixed.

Pr	Values proportional to C_f	Values proportional to Nu
0.20	7.927539	-2.109994
0.71	9.822492	-4.726112
0.73	9.869625	-4.819553
1.00	10.446450	-6.076511
5.00	16.005450	-27.739200
7.01	18.124500	-40.557210

Chapter 5

Analytical solution of the Transient Free Convection in Micropolar Fluid with Heat Generation and Constant Heat Flux.

5.1 Introduction.

In this chapter the governing equations of the system will be solved analytically. To do that the non-dimensional forms of the governing equations obtained in the previous chapter will be considered. The non-dimensional equations are also non linear as their dimensional counterparts. To solve them they are made linear by dropping the non linear convective terms. For the solution purpose Laplace transform is to be used to transfer the partial differential equations to ordinary differential equations, as the time variable or derivatives with respect to time will not be there. After the introduction of Laplace transform the equations will contain additional parameter coming from the kernel of the transform. The ordinary differential equations will be solved including the additional parameter and then the inverse Laplace transform will be used to get back the solution that will also include time.

5.2. Manipulation of the governing equations

The non-dimensional equations of the system with the non-linear convective terms (that are developed in chapter 4) are

$$\frac{\partial u}{\partial t}+u\frac{\partial u}{\partial x}+v\frac{\partial u}{\partial y}=(1+\Delta)\frac{\partial^2 u}{\partial y^2}+\Delta\frac{\partial N}{\partial y}+G_r\theta \tag{5.2.1}$$

$$\frac{\partial N}{\partial t}+u\frac{\partial N}{\partial x}+v\frac{\delta N}{\partial y}=\lambda\frac{\partial^2 N}{\partial y^2}-\frac{\Delta}{j}(2N+\frac{\partial u}{\partial y}) \tag{5.2.2}$$

$$\frac{\partial \theta}{\partial t}+u\frac{\partial \theta}{\partial x}+v\frac{\partial \theta}{\partial y}=\frac{1}{P_r}\frac{\partial^2 \theta}{\partial y^2}+\alpha\theta \tag{5.2.3}$$

The transformed boundary conditions are:

$$u(x,0,t)=0,\ N(x,0,t)=0,\ \theta(x,0,t)=1$$

$$u(x,\infty,t)=0,\ N(x,\infty,t)=0,\ \theta(x,\infty,t)=0, \tag{5.2.4}$$

To solve the above equations analytically the non-linear convective terms will not be considered and thus the equations will be linearized. Also as the non-dimensional velocity component u, angular momentum N and temperature θ have no derivative in terms of x, the vertical distance, so it may be considered that u=u(y,t), N=N(y,t) and $\theta=\theta(y,t)$.

Hence equations (5.2.1)-(5.2.3) can be written as

$$\frac{\partial u}{\partial t} = (1+\Delta)\frac{\partial^2 u}{\partial y^2} + \Delta\frac{\partial N}{\partial y} + G_r\theta \tag{5.2.5}$$

$$\frac{\partial N}{\partial t} = \lambda\frac{\partial^2 N}{\partial y^2} - \frac{\Delta}{j}(2N + \frac{\partial u}{\partial y}) \tag{5.2.6}$$

$$\frac{\partial \theta}{\partial t} = \frac{1}{P_r}\frac{\partial^2 \theta}{\partial y^2} + \alpha\theta \tag{5.2.7}$$

The transferred boundary conditions will be:

$$u(0,t) = 0, \mathrm{N}(\varepsilon, \mathrm{t})=\mathrm{E},\ \theta(0,t) = 1$$

$$u(\infty,t) = 0,\ N(\infty,t) = 0,\ \theta(\infty,t) = 0, \tag{5.2.8}$$

where it has been assumed that near the plate the angular momentum is not zero and ε is a very small number.

5.3 Analytical solution.

As mentioned earlier to solve the equations (5.2.5) - (5.2.7) with the boundary conditions (5.2.8) Laplace transform will be used. Laplace transform will transform the partial differential equations into ordinary differential equations and they will be solved usually. In the following subsection the use of Laplace transform and the solution of the ordinary differential equation will be discussed.

5.3.1 Laplace transform and ordinary differential equation

Taking the Laplace transform on the equations (5.2.5)-(5.2.8) on considering L{u}=V, L{N}=φ, L{θ}=ψ the following relations will be obtained:

$$sV - u(y,0) = (1+\Delta)\frac{d^2V}{dy^2} + \Delta\frac{d\varphi}{dy} + G_r\psi \tag{5.3.1}$$

$$s\varphi - N(y,0) = \lambda\frac{d^2\varphi}{dy^2} - \frac{\Delta}{j}(2\varphi + \frac{dV}{dy}) \tag{5.3.2}$$

$$s\psi - \theta(y,0) = \frac{1}{\mathrm{Pr}}\frac{d^2\psi}{dy^2} + \alpha\psi \tag{5.3.3}$$

with transferred boundary conditions:

$$V(0,s)=0,\ \varphi(\varepsilon,s)=\frac{E}{s},\ \psi(0,s)=\frac{1}{s},$$

$$V(\infty,s)=0,\ \varphi(\infty,s)=0,\ \psi(\infty,s)=0$$

As initially there was no flow so u(y,0)=0, N(y,0)=0, θ(y,0)=0. As a result (5.3.1), (5.3.2) and (5.3.3) become

$$sV=(1+\Delta)\frac{d^2V}{dy^2}+\Delta\frac{d\varphi}{dy}+G_r\psi \tag{5.3.4}$$

$$s\varphi=\lambda\frac{d^2\varphi}{dy^2}-\frac{\Delta}{j}(2\varphi+\frac{dV}{dy}) \tag{5.3.5}$$

$$s\psi=\frac{1}{\Pr}\frac{d^2\psi}{dy^2}+\alpha\psi \tag{5.3.6}$$

Equation (5.3.6) can be written as

$$\frac{1}{\Pr}\frac{d^2\psi}{dy^2}-(s-\alpha)\psi=0$$

whose solution is

$$\psi=Ae^{ky}+Be^{-ky}\ ,\quad k^2=\Pr(s-\alpha) \tag{5.3.7}$$

The boundary condition requires that A to be zero and $B=\frac{1}{s}$.

Thus the solution of (5.3.6) is $\psi=\frac{1}{s}e^{-y\sqrt{\Pr(s-\infty)}}$ (5.3.8)

To obtain the solution of equation (5.3.5) it is assumed that the microinertia per unit mass, in its non dimensional form, is quite large so that the second term on the right of equation (5.3.5) can be considered as zero and thus the equation will be of the form

$$s\varphi=\lambda\frac{d^2\varphi}{dy^2} \tag{5.3.9}$$

whose solution is $\varphi=C_1e^{ry}+C_2e^{-ry}$,where $r^2=\frac{s}{\lambda}$. The boundary conditions suggest that C_1 be zero and C_2 be E/s.

Thus the solution of (5.3.9) is $\varphi=\frac{E}{s}e^{-\sqrt{\frac{s}{\lambda}}y}$ (5.3.10)

$$\therefore \quad \frac{d\varphi}{dy} = -E\sqrt{\frac{1}{\lambda s}}e^{-\sqrt{\frac{s}{\lambda}}y}$$

With the solutions already obtained, equation (5.3.4) will become

$$\frac{d^2V}{dy^2} - (\frac{s}{1+\Delta})V = (\frac{\Delta}{1+\Delta})E\sqrt{\frac{1}{\lambda s}}e^{\frac{y}{\sqrt{\lambda}}(-\sqrt{s})} - \frac{Gr}{1+\Delta}\frac{1}{s}e^{-y\sqrt{\Pr(s-\alpha)}}$$

whose complementary function be

$$V = Te^{wy} + He^{-wy} \quad \text{where } w^2 = \frac{s}{1+\Delta}$$

Boundary condition requires T to be Zero.

$$\therefore V = He^{\frac{y}{\sqrt{1+\Delta}}(-\sqrt{s})}$$

and the particular integral be

$$\frac{E\Delta\sqrt{\lambda}}{(1+\Delta-\lambda)}\left[\frac{e^{(\frac{y}{\sqrt{\lambda}})(-\sqrt{s})}}{\sqrt{s^3}}\right] - \left[\frac{Gr}{\{(1+\Delta)\Pr-1\}s^2 - \Pr\alpha(1+\Delta)s}\left[e^{-y\sqrt{\Pr(s-\alpha)}}\right]\right]$$

So the general solution is

$$V = He^{\frac{y}{\sqrt{1+\Delta}}(-\sqrt{s})} + \frac{E\Delta\sqrt{\lambda}}{(1+\Delta-\lambda)}\left[\frac{e^{(\frac{y}{\sqrt{\lambda}})(-\sqrt{s})}}{\sqrt{s^3}}\right] - \left[\frac{Gr}{\{(1+\Delta)\Pr-1\}s^2 - \Pr\alpha(1+\Delta)s}\left[e^{-y\sqrt{\Pr(s-\alpha)}}\right]\right]$$

Applying boundary condition V(0,s)=0 the following will be obtained,

$$0 = H + \frac{E\Delta\sqrt{\lambda}}{(1+\Delta-\lambda)}\frac{1}{\sqrt{s^3}} - \frac{Gr}{\{(1+\Delta)\Pr\}s^2 - \Pr\alpha(1+\Delta)s}$$

$$\text{i.e. } H = -\frac{E\Delta\sqrt{\lambda}}{(1+\Delta-\lambda)}\frac{1}{\sqrt{s^3}} + \frac{Gr}{\{(1+\Delta)\Pr\}s^2 - \Pr\alpha(1+\Delta)s}$$

Hence

$$V = \left[\frac{Gr}{\{(1+\Delta)\Pr-1\}s^2 - \Pr\alpha(1+\Delta)s} - \frac{E\Delta\sqrt{\lambda}}{(1+\Delta-\lambda)\sqrt{s^3}}\right]e^{\frac{y}{\sqrt{1+\Delta}}(-\sqrt{s})}$$

$$+ \frac{E\Delta\sqrt{\lambda}}{1+\Delta-\lambda}\left\{\frac{e^{\frac{y}{\sqrt{\lambda}}(-\sqrt{s})}}{\sqrt{s^3}}\right\} - \frac{Gr}{\{(1+\Delta)\Pr-1\}s^2 - \Pr\alpha(1+\Delta)s}\left\{e^{-y\sqrt{\Pr(s-\alpha)}}\right\}$$

$$V = Gr\left[\frac{e^{\frac{y}{\sqrt{1+\Delta}}(-\sqrt{s})}}{\{(1+\Delta)\Pr-1\}s^2 - \Pr\alpha(1+\Delta)s} - \frac{e^{-y\sqrt{\Pr(s-\alpha)}}}{\{(1+\Delta)\Pr-1\}s^2 - \Pr\alpha(1+\Delta)s}\right]$$

or,

$$+\frac{E\Delta\sqrt{\lambda}}{1+\Delta-\lambda}\left[\frac{e^{\frac{Y}{\sqrt{\lambda}}(-\sqrt{s})}}{\sqrt{s^3}} - \frac{e^{\frac{y}{\sqrt{1+\Delta}}(-\sqrt{s})}}{\sqrt{s^3}}\right] \qquad (5.3.11)$$

The solutions so far obtained have no terms containing t. To get the solutions including the time t can be obtained by taking the inverse Laplace transform to the equations (5.3.8), (5.3.10) and (5.3.11). In the following subsection how the inverse Laplace transform can be obtained will be discussed.

5.3.2 Inverse Laplace transform

The non dimensional temperature can be obtained by taking inverse Laplace transform on ψ in equation (5.3.8), i.e.

$$\theta = L^{-1}\{\psi\} = L^{-1}\left\{\frac{1}{s}e^{-y\sqrt{\Pr(s-\alpha)}}\right\}$$

Now,

$$L^{-1}\left\{\frac{1}{s}\right\} = 1 \text{ .and } L^{-1}\left\{e^{-\sqrt{s}}\right\} = \frac{1}{2\pi t^{\frac{3}{2}}}e^{\frac{-1}{4t}}$$

So using change of scale property and 1st shifting property it can be written as

$$L^{-1}\{e^{-y\sqrt{\Pr(s-\alpha)}}\} = \frac{y\sqrt{\Pr}}{2\sqrt{\pi}t^{\frac{3}{2}}}e^{\alpha t - \frac{y^2\Pr}{4t}}$$

Hence by convolution theorem

$$L^{-1}\{\frac{e^{-y\sqrt{\Pr}(s-\alpha)^{1/2}}}{s}\} = \int_0 \frac{y\sqrt{\Pr}}{2\sqrt{\pi}u^{\frac{3}{2}}}e^{\alpha u - \frac{y^2\Pr}{4u}}du = \frac{2}{\sqrt{\pi}}\int_{\frac{y}{2}\sqrt{\frac{\Pr}{t}}}^{\infty} e^{\frac{\alpha y^2\Pr}{4z^2} - z^2}dz$$

The result of last integral can be obtained from Mathematica® and is

$$\theta = \frac{1}{4}e^{-\sqrt{-y^2\alpha\Pr}\sqrt{\pi}}\left(Erfc\left[\frac{\sqrt{\frac{\Pr}{t}}(y^2\Pr - 2t\sqrt{-y^2\alpha\Pr})}{2y\Pr}\right] + e^{2\sqrt{-y^2\alpha\Pr}}Erfc\left[\frac{\sqrt{\frac{\Pr}{t}}(y^2\Pr - 2t\sqrt{-y^2\alpha\Pr})}{2y\Pr}\right]\right) \qquad (5.3.12)$$

The non dimensional angular momentum, N can be obtained by taking inverse Laplace transform on the equation (5.3.10). Thus

$$N = L^{-1}\{\varphi\} = L^{-1}\{\frac{E}{s}e^{-y\sqrt{(\frac{s}{\lambda})}}\}$$

As has been done earlier $L^{-1}\left\{\frac{E}{s}e^{-\sqrt{\frac{s}{\lambda}}(y)}\right\} = \int_0^t \frac{Ey}{2\sqrt{\pi\lambda}}\frac{1}{u^{\frac{3}{2}}}e^{-\frac{y^2}{4\lambda u}}du = \frac{2E}{\sqrt{\pi}}\int_{\frac{y}{2\sqrt{\lambda t}}}^{\infty} e^{-z^2}dz$

$$\therefore N = E^*\left(1 - \frac{\sqrt{t}\sqrt{\lambda}Erf\left[\frac{y}{2\sqrt{t}\sqrt{\lambda}}\right]}{\sqrt{t\lambda}}\right) \tag{5.3.13}$$

Again the result of the integration is obtained through Mathematica®.

To obtain the non dimensional velocity u the inverse Laplace transform of (5.3.11) is to be taken. Thus

$$u = L^{-1}\{V\} = L^{-1}\left\{Gr\left[\frac{e^{(\frac{y}{\sqrt{1+\Delta}})(-\sqrt{s})}}{\{(1+\Delta)\Pr-1\}s^2 - \Pr\alpha(1+\Delta)s} - \frac{e^{-y\sqrt{\Pr(s-\alpha)}}}{\{(1+\Delta)\Pr-1\}s^2 - \Pr\alpha(1+\Delta)s}\right]\right.$$
$$\left. + \frac{E\Delta\sqrt{\lambda}}{1+\Delta-\lambda}\left[\frac{e^{(\frac{y}{\sqrt{\lambda}})(-\sqrt{s})}}{\sqrt{s^3}} - \frac{e^{(\frac{y}{\sqrt{1+\Delta}})(-\sqrt{s})}}{\sqrt{s^3}}\right]\right\}$$

$$= L^{-1}\left\{\frac{Gr}{\Pr\alpha(1+\Delta)}\left[\left\{\frac{1}{s - \frac{\Pr\alpha(1+\Delta)}{\Pr(1+\Delta)-1}} - \frac{1}{s}\right\}\left(e^{(\frac{y}{\sqrt{1+\Delta}})(-\sqrt{s})} - e^{-y\sqrt{\Pr(s-\alpha)}}\right)\right]\right.$$
$$\left. + \frac{E\Delta\sqrt{\lambda}}{1+\Delta-\lambda}\left[\frac{e^{(\frac{y}{\sqrt{\lambda}})(-\sqrt{s})}}{\sqrt{s^3}} - \frac{e^{(\frac{y}{\sqrt{1+\Delta}})(-\sqrt{s})}}{\sqrt{s^3}}\right]\right\}$$

To calculate the above one will require the following results:

$$L^{-1}\{\frac{1}{\sqrt{s^3}}\} = \frac{2\sqrt{t}}{\sqrt{\pi}}, \qquad L^{-1}\{e^{-y\sqrt{\Pr(s-\alpha)}}\} = \frac{y\sqrt{\Pr}}{2\sqrt{\pi}t^{\frac{3}{2}}}e^{\alpha t - \frac{y^2\Pr}{4t}}$$

$$L^{-1}\{e^{(\frac{y}{\sqrt{1+\Delta}})(-\sqrt{s})}\} = \frac{y}{2\sqrt{\pi(1+\Delta)}}\frac{1}{t^{\frac{3}{2}}}e^{-\frac{y^2}{4t(1+\Delta)}}, \qquad L^{-1}\{e^{(y/\sqrt{\lambda})(-\sqrt{s})}\} = \frac{y}{2\sqrt{\pi\lambda}}\frac{1}{t^{\frac{3}{2}}}e^{\frac{-y^2}{4\lambda t}}$$

and $$L^{-1}\left\{\frac{1}{\{(1+\Delta)\Pr-1\}s^2-\Pr\alpha(1+\Delta)s}\right\}=\frac{1}{\Pr\alpha(1+\Delta)}\left\{e^{\frac{\Pr\alpha(1+\Delta)}{\Pr(1+\Delta)-1}t}-1\right\}.$$

If one consider

$$F_1(t)=L^{-1}\{f_1(s)\}=L^{-1}\left\{e^{(\frac{y}{\sqrt{1+\Delta}})(-\sqrt{s})}\right\} \text{ and}$$

$$G_1(t)=L^{-1}\{g_1(s)\}=L^{-1}\left\{\frac{1}{\{(1+\Delta)\Pr-1\}s^2-\Pr\alpha(1+\Delta)s}\right\}$$

then by convolution theorem one will obtain

$$L^{-1}\{f_1(s)*g_1(s)\}=\int_0^t F_1(u)G_1(u-t)du$$

$$=\frac{y}{2\sqrt{\pi(1+\Delta)}\Pr\alpha(1+\Delta)}\left[e^{\frac{\Pr\alpha(1+\Delta)}{\Pr(1+\Delta)-1}t}\int_0^t\frac{1}{u^{\frac{3}{2}}}e^{-\frac{\Pr\alpha(1+\Delta)}{\Pr(1+\Delta)-1}u-\frac{y^2}{4u(1+\Delta)}}du-\int_0^t\frac{1}{u^{\frac{3}{2}}}e^{-\frac{y^2}{4u(1+\Delta)}}du\right]$$

$$=\frac{y}{2\sqrt{\pi(1+\Delta)}\Pr\alpha(1+\Delta)}\frac{4\sqrt{1+\Delta}}{y}\left[e^{\frac{\Pr\alpha(1+\Delta)}{\Pr(1+\Delta)-1}t}\int_{\frac{y}{2\sqrt{(1+\Delta)t}}}^{\infty}e^{-\frac{\Pr\alpha y^2}{\{\Pr(1+\Delta)-1\}4z^2}-z^2}dz-\int_{\frac{y}{2\sqrt{(1+\Delta)t}}}^{\infty}e^{-z^2}dz\right]$$

$$=\frac{2}{\sqrt{\pi}\Pr\alpha(1+\Delta)}\left[e^{\frac{\Pr\alpha(1+\Delta)}{\Pr(1+\Delta)-1}t}I_1-I_2\right]$$

where, $I_1=\int_{\frac{y}{2\sqrt{(1+\Delta)t}}}^{\infty}e^{-\frac{\Pr\alpha y^2}{\{\Pr(1+\Delta)-1\}4z^2}-z^2}dz$ and $I_2=\int_{\frac{y}{2\sqrt{(1+\Delta)t}}}^{\infty}e^{-z^2}dz$

Similarly on considering

$$L^{-1}\{f_2(s)\}=F_2(t)=L^{-1}\{e^{-y\sqrt{\Pr(s-\alpha)}}\} \text{ and}$$

$$L^{-1}\{g_2(s)\}=G_2(t)=L^{-1}\left\{\frac{1}{\{(1+\Delta)\Pr-1\}s^2-\Pr\alpha(1+\Delta)s}\right\}$$

by convolution theorem

$$L^{-1}\{f_2(s)*g_2(s)\}=\int_0^t F_2(u)G_2(t-u)du$$

$$=\frac{y}{2\sqrt{\pi\Pr}\alpha(1+\Delta)}\left[e^{\frac{\Pr\alpha(1+\Delta)}{\Pr(1+\Delta)-1}t}\int_0^t\frac{1}{u^{\frac{3}{2}}}e^{-\frac{\alpha}{\Pr(1+\Delta)-1}u-\frac{y^2\Pr}{4u}}du-\int_0^t\frac{1}{u^{\frac{3}{2}}}e^{\alpha u-\frac{y^2\Pr}{4u}}du\right]$$

$$= \frac{y}{2\sqrt{\pi\,\mathrm{Pr}\alpha(1+\Delta)}} \frac{4}{y\sqrt{\mathrm{Pr}}} \left[e^{\frac{\mathrm{Pr}\alpha(1+\Delta)}{\mathrm{Pr}(1+\Delta)-1}t} \int_{\frac{y}{2}\sqrt{\frac{\mathrm{Pr}}{t}}}^{\infty} e^{-\frac{\mathrm{Pr}\alpha y^2}{\{\mathrm{Pr}(1+\Delta)-1\}4z^2}-z^2} dz - \int_{\frac{y}{2}\sqrt{\frac{\mathrm{Pr}}{t}}}^{\infty} e^{\frac{\alpha\,\mathrm{Pr}\,y^2}{4z^2}-z^2} dz \right]$$

$$= \frac{2}{\sqrt{\pi}\,\mathrm{Pr}\alpha(1+\Delta)} \left[e^{\frac{\mathrm{Pr}\alpha(1+\Delta)}{\mathrm{Pr}(1+\Delta)-1}t} I_3 - I_4 \right]$$

where, $I_3 = \int_{\frac{y}{2}\sqrt{\frac{\mathrm{Pr}}{t}}}^{\infty} e^{-\frac{\mathrm{Pr}\alpha y^2}{\{\mathrm{Pr}(1+\Delta)-1\}4z^2}-z^2} dz$ and $I_4 = \int_{\frac{y}{2}\sqrt{\frac{\mathrm{Pr}}{t}}}^{\infty} e^{\frac{\alpha\,\mathrm{Pr}\,y^2}{4z^2}-z^2} dz$

Again considering

$L^{-1}\{f_3(s)\} = F_3(t) = L^{-1}\{\frac{1}{\sqrt{s^3}}\}$ and

$L^{-1}\{g_3(s)\} = G_3(t) = L^{-1}\{e^{(\frac{y}{\sqrt{\lambda}})(-\sqrt{s})}\}$

by convolution theorem

$$L^{-1}\{f_3(s) * g_3(s)\} = \int_0^t F_3\ (t-u)G_3(u)du = \frac{y}{\pi\sqrt{\lambda}} \left[\int_0^t \sqrt{t-u}\, \frac{1}{u^{\frac{3}{2}}} e^{-\frac{y^2}{4\lambda u}} du \right] = \frac{y}{\pi\sqrt{\lambda}} I_5$$

where $I_5 = \int_0^t \sqrt{t-u}\, \frac{1}{u^{\frac{3}{2}}} e^{-\frac{y^2}{4\lambda u}} du$

Lastly considering

$L^{-1}\{f_4(s)\} = F_4(t) = L^{-1}\{\frac{1}{\sqrt{s^3}}\}$ and $L^{-1}\{g_4(s)\} = G_4(t) = L^{-1}\{e^{(\frac{y}{\sqrt{1+\Delta}})(-\sqrt{s})}\}$

by convolution theorem

$$L^{-1}\{f_4(s) * g_4(s)\} = \int_0^t F_4(t-u)G_4(t)du = \frac{y}{\pi\sqrt{1+\Delta}} \left[\int_0^t \sqrt{t-u}\, \frac{1}{u^{\frac{3}{2}}} e^{-\frac{y^2}{4u(1+\Delta)}} du \right] = \frac{y}{\pi\sqrt{1+\Delta}} I_6$$

where $I_6 = \int_0^t \sqrt{t-u}\, \frac{1}{u^{\frac{3}{2}}} e^{-\frac{y^2}{4u(1+\Delta)}} du$

The results of the integrals I_1 to I_6 is obtained from Mathematica® and are as follows:

$$I_1 = \frac{\sqrt{\pi}}{4} e^{-\sqrt{\frac{y^2\alpha\,\mathrm{Pr}}{-1+\alpha(1+\Delta)\,\mathrm{Pr}}}} \left(\begin{array}{l} 1 + e^{2\sqrt{\frac{y^2\alpha\,\mathrm{Pr}}{-1+\alpha(1+\Delta)\,\mathrm{Pr}}}} - Erf\left[\dfrac{y^2 - 2t(1+\Delta)\sqrt{\dfrac{y^2\alpha\,\mathrm{Pr}}{-1+\alpha(1+\Delta)\,\mathrm{Pr}}}}{2y\sqrt{t(1+\Delta)}} \right] \\ \quad - e^{2\sqrt{\frac{y^2\alpha\,\mathrm{Pr}}{-1+\alpha(1+\Delta)\,\mathrm{Pr}}}} Erf\left[\dfrac{y^2 + 2t(1+\Delta)\sqrt{\dfrac{y^2\alpha\,\mathrm{Pr}}{-1+\alpha(1+\Delta)\,\mathrm{Pr}}}}{2y\sqrt{t(1+\Delta)}} \right] \end{array} \right)$$

$$I_2 = \frac{\sqrt{\pi}}{2} Erfc\left[\frac{y}{2\sqrt{t(1+\Delta)}} \right]$$

$$I_3 = \frac{\sqrt{\pi}}{4} e^{-\sqrt{\frac{y^2\alpha\,\mathrm{Pr}}{-1+\alpha(1+\Delta)\,\mathrm{Pr}}}} \left(\begin{array}{l} Erfc\left[\dfrac{\sqrt{\frac{\mathrm{Pr}}{t}}(y^2\,\mathrm{Pr} - 2t\sqrt{\dfrac{y^2\alpha\,\mathrm{Pr}}{-1+\alpha(1+\Delta)\,\mathrm{Pr}}})}{2y\,\mathrm{Pr}} \right] \\ \quad + e^{2\sqrt{\frac{y^2\alpha\,\mathrm{Pr}}{-1+\alpha(1+\Delta)\,\mathrm{Pr}}}} Erfc\left[\dfrac{\sqrt{\frac{\mathrm{Pr}}{t}}(y^2\,\mathrm{Pr} + 2t\sqrt{\dfrac{y^2\alpha\,\mathrm{Pr}}{-1+\alpha(1+\Delta)\,\mathrm{Pr}}})}{2y\,\mathrm{Pr}} \right] \end{array} \right)$$

$$I_4 = \frac{\sqrt{\pi}}{4} e^{-\sqrt{-y^2\alpha\,\mathrm{Pr}}} \left(Erfc\left[\frac{\sqrt{\frac{\mathrm{Pr}}{t}}(y^2\,\mathrm{Pr} - 2t\sqrt{-y^2\alpha\,\mathrm{Pr}})}{2y\,\mathrm{Pr}} \right] + e^{2\sqrt{-y^2\alpha\,\mathrm{Pr}}} Erfc\left[\frac{\sqrt{\frac{\mathrm{Pr}}{t}}(y^2\,\mathrm{Pr} + 2t\sqrt{-y^2\alpha\,\mathrm{Pr}})}{2y\,\mathrm{Pr}} \right] \right)$$

$$I_5 = -\pi + 2e^{-\frac{y^2}{4t\lambda}} \sqrt{\pi} \sqrt{\frac{\lambda t}{y^2}} + \pi\, Erf\left[\frac{1}{2\sqrt{\frac{t\lambda}{y^2}}} \right]$$

and

$$I_6 = -\pi + 2e^{-\frac{y^2}{4t(1+\Delta)}} \sqrt{\pi} \sqrt{\frac{t(1+\Delta)}{y^2}} + \pi\, Erf\left[\frac{1}{2\sqrt{\frac{t(1+\Delta)}{y^2}}} \right]$$

Thus the value of u is

$$u = \frac{2Gre^{\frac{\Pr\alpha(1+\Delta)}{\Pr(1+\Delta)-1}t}}{\sqrt{\pi}\,\Pr\alpha(1+\Delta)}[I_1 - I_3] + \frac{2Gr}{\sqrt{\pi}\,\Pr\alpha(1+\Delta)}[I_4 - I_2] + \frac{E\Delta y}{\pi(1+\Delta-\lambda)}(I_5) - \frac{E\Delta y\sqrt{\lambda}}{\pi(1+\Delta-\lambda)\sqrt{1+\Delta}}(I_6) \tag{5.3.14}$$

5.4. Result and discussion

The obtained velocity, temperature and angular momentum profiles are shown graphically in fig.(5.1)-(5.13), for different values of heat source parameter α, dimensionless material parameter Δ, the Grashof number Gr, dimensionless material parameter λ, the Prandtl number Pr, time t and constant E. The values 0.71, 0.73, 1.00 are considered for Pr, the values of other parameters are however chosen arbitrarily.

In Fig.(5.1)-(5.3) the velocity profiles for different values for α, Δ and t are shown respectively. In these figures it is common that with the increase in the parameters the velocity also increases. The rates of increases in different parameters are different. For fixed t, with the increases in α or Δ though the velocity is increasing but where it is again becoming zero is not changing that much. But with the change in t, velocity is not only increasing but also it is spreading i.e. it is becoming zero again far away from the plate.

The velocity profiles for different values of E, λ and Gr are shown in figures (5.4)-(5.6) respectively. These figures show that the velocity has no appreciably change due to the change in the value of E, λ and Gr.

In fig.(5.7), the velocity profiles for different values of Pr are shown. It is seen that the velocity increases with the increase in Pr. The velocity is again not spreading with the increase in Pr.

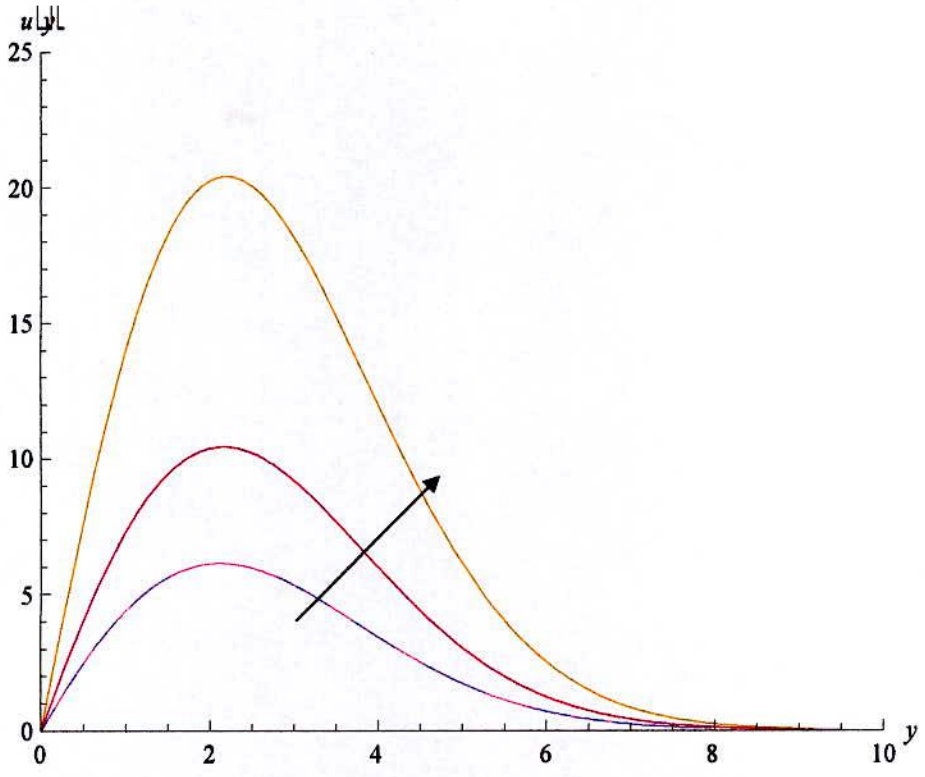

Fig.5.1 Velocity profiles for different values of α (0.1, 0.2, 0.3) with $Gr = 2.00, \Pr = 1.00, E = 0.1, t = 2, \lambda = 0.4, \Delta = 0.5$.

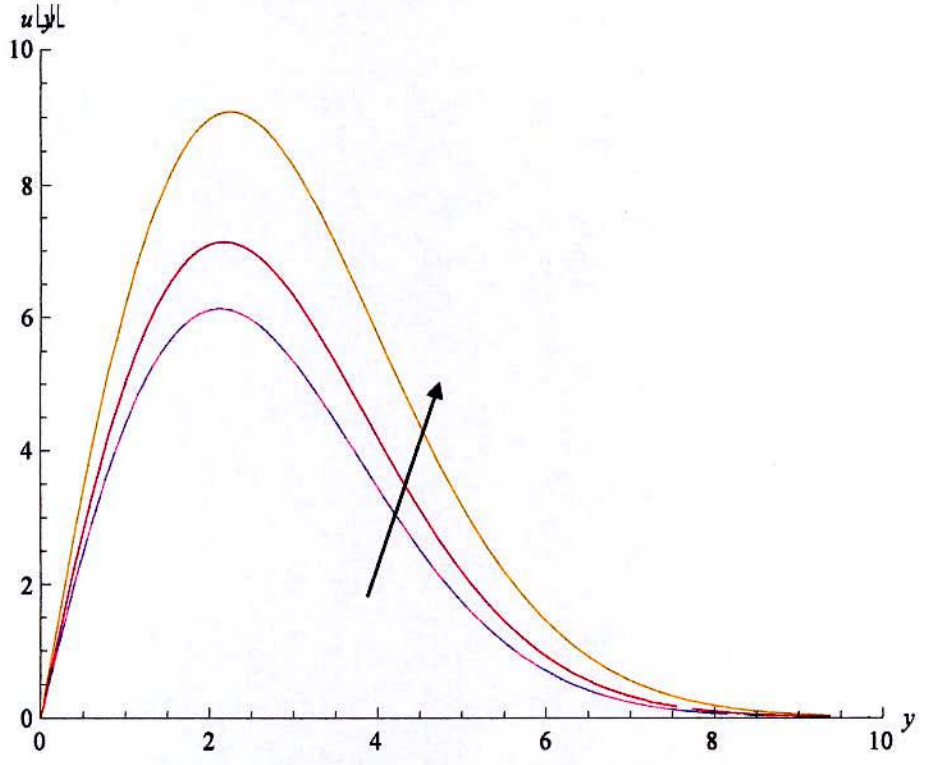

Fig.5.2 Velocity profiles for different values of Δ (0.5, 0.6, 0.8) with $Gr = 2.00, \Pr = 1.00, E = 0.1, t = 2, \lambda = 0.4, \alpha = 0.1$.

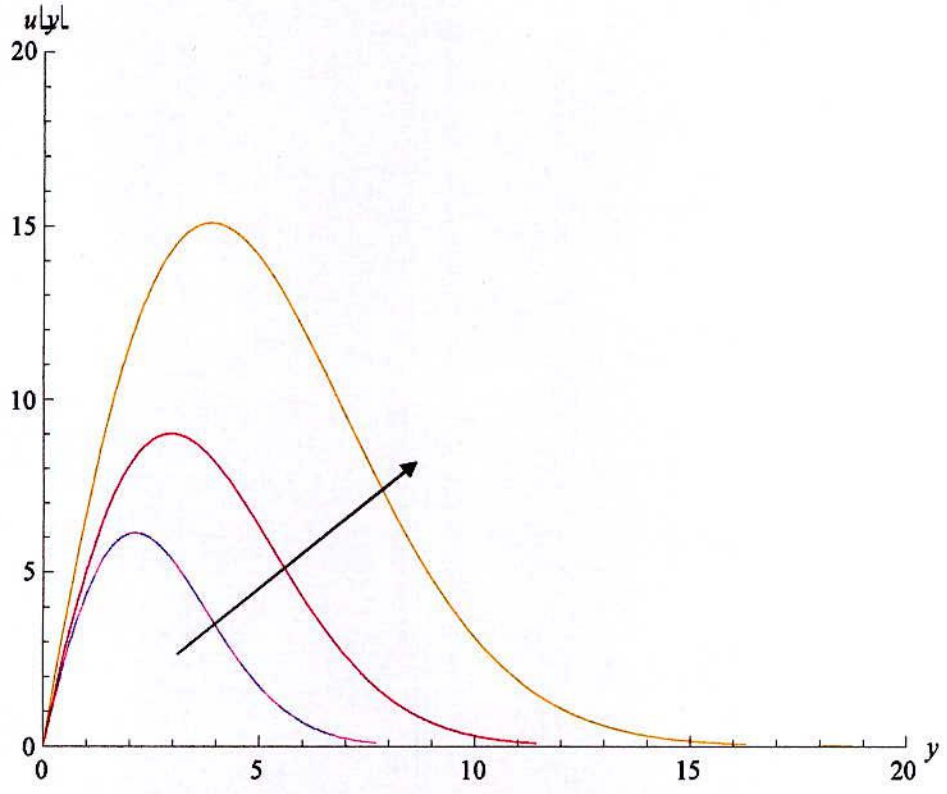

Fig.5.3 Velocity profiles for different values of t (2, 4, 7) with $Gr = 2.00, \Pr = 1.00, E = 0.1, \lambda = 0.4, \Delta = 0.5, \alpha = 0.1$.

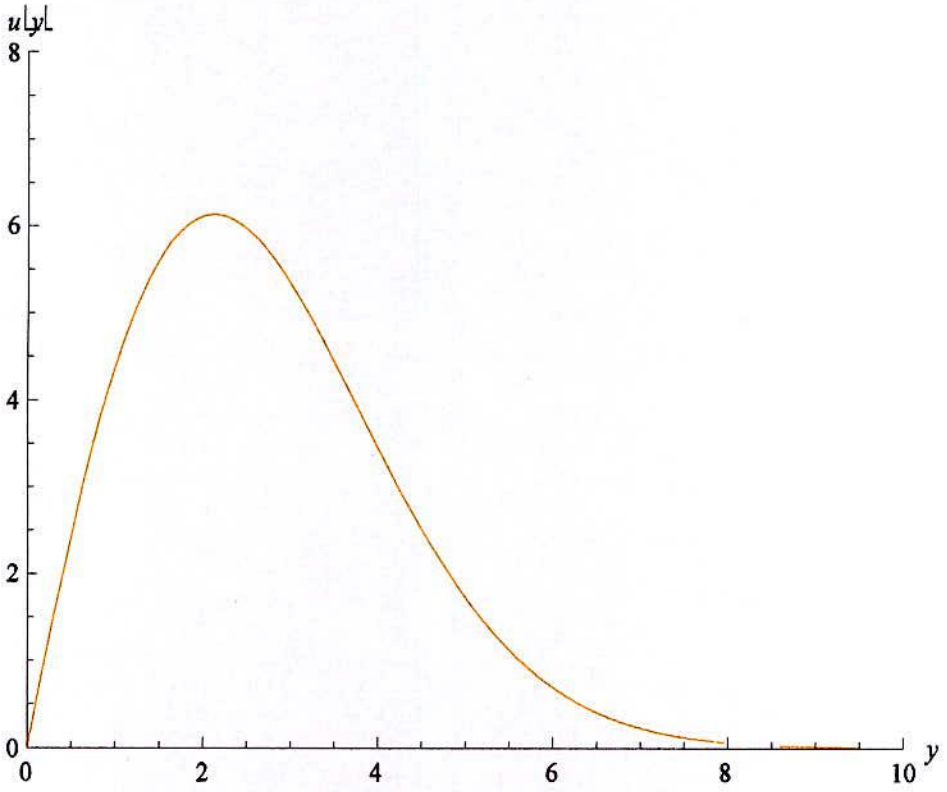

Fig.5.4 Velocity profiles for different values of E (.1, .2, .4) with $Gr = 2.00, \Pr = 1.00, t = 2, \lambda = 0.4, \Delta = 0.5, \alpha = 0.1$.

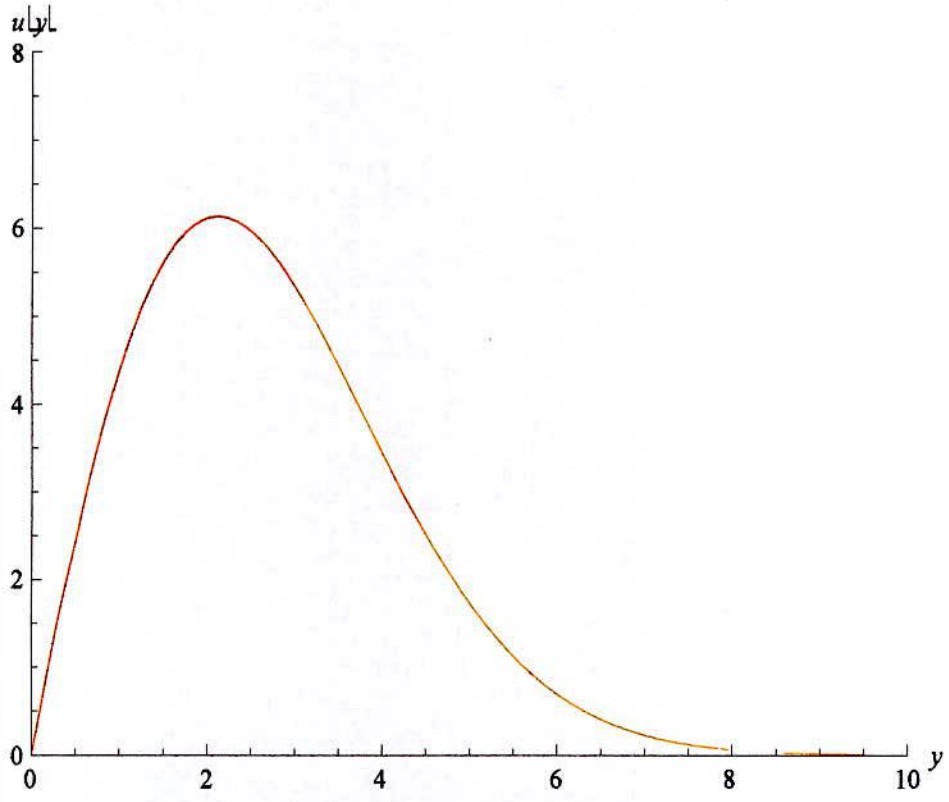

Fig.5.5 Velocity profiles for different values of λ (0.4, .6, .9), with $Gr = 2.00, \Pr = 1.00, E = 0.1, t = 2, \alpha = 0.1, \Delta = 0.5$.

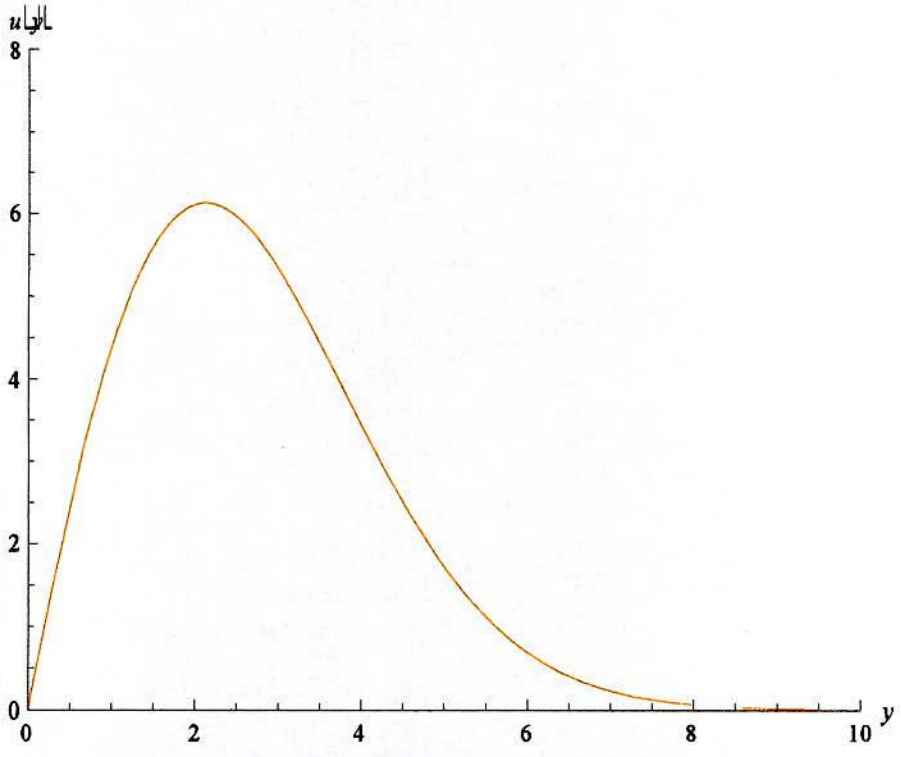

Fig.5.6 Velocity profiles for different values of Gr (2, 3, 5) with $\Pr = 1.00, E = 0.1, t = 2, \lambda = 0.4, \Delta = 0.5, \alpha = 0.1$.

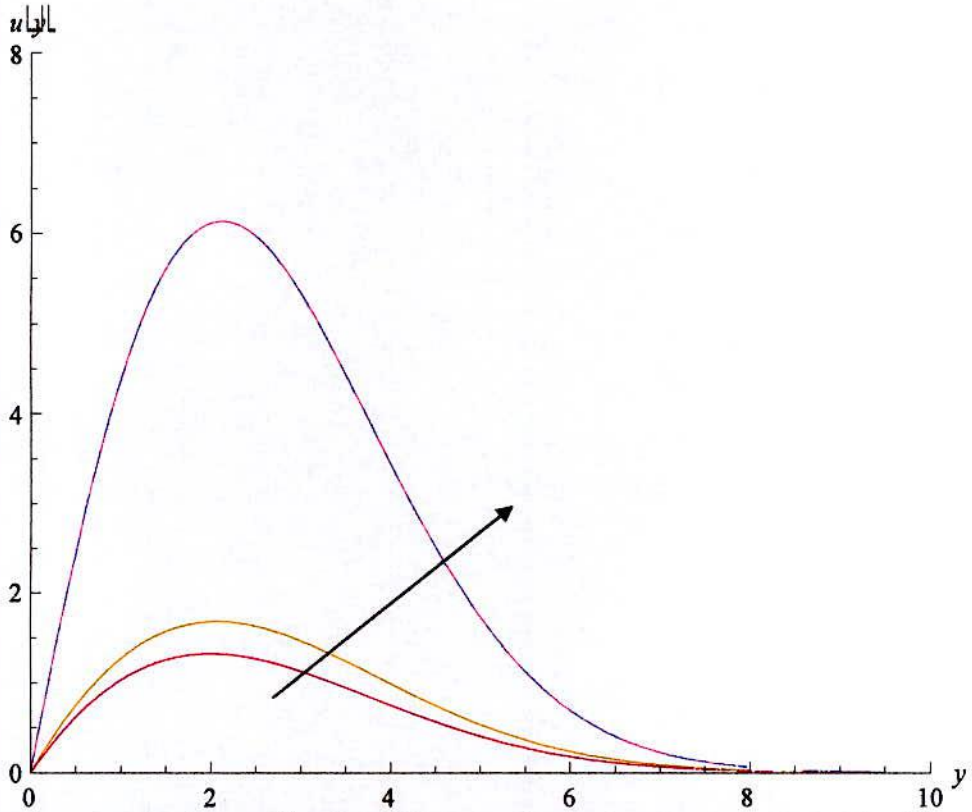

Fig.5.7 Velocity profiles for different values of Pr (0.71, 0.73, 1.00) with $Gr = 2.00, E = 0.1, t = 2, \lambda = 0.4, \Delta = 0.5, \alpha = 0.1$

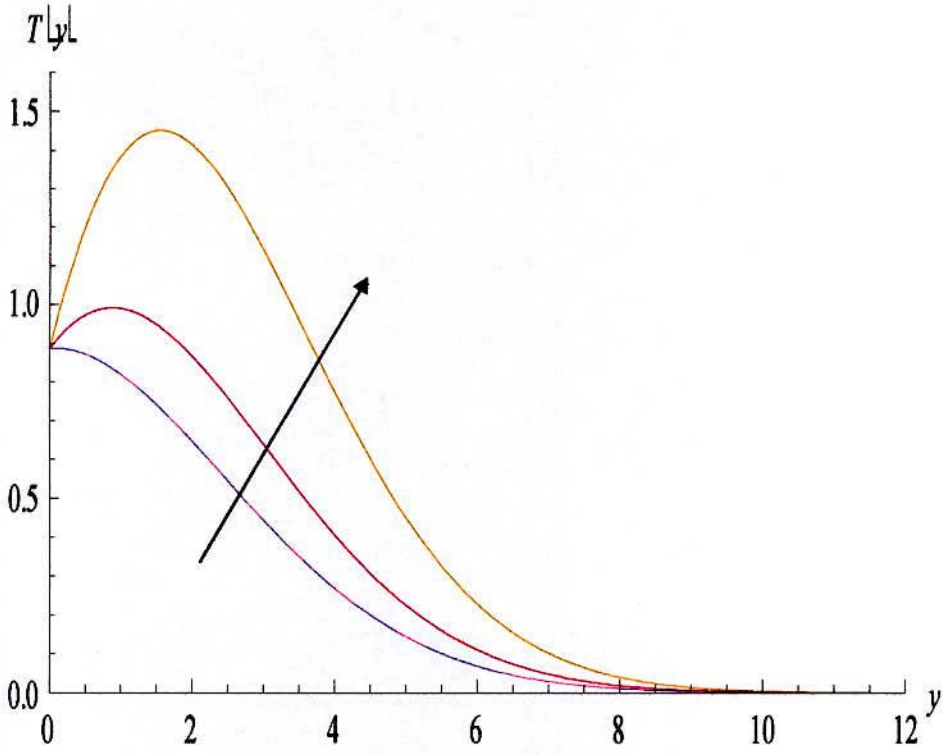

Fig.5.8 Temperature profiles for different values of α (0.3, 0.5, 0.8) with Pr =0.71, t =3.

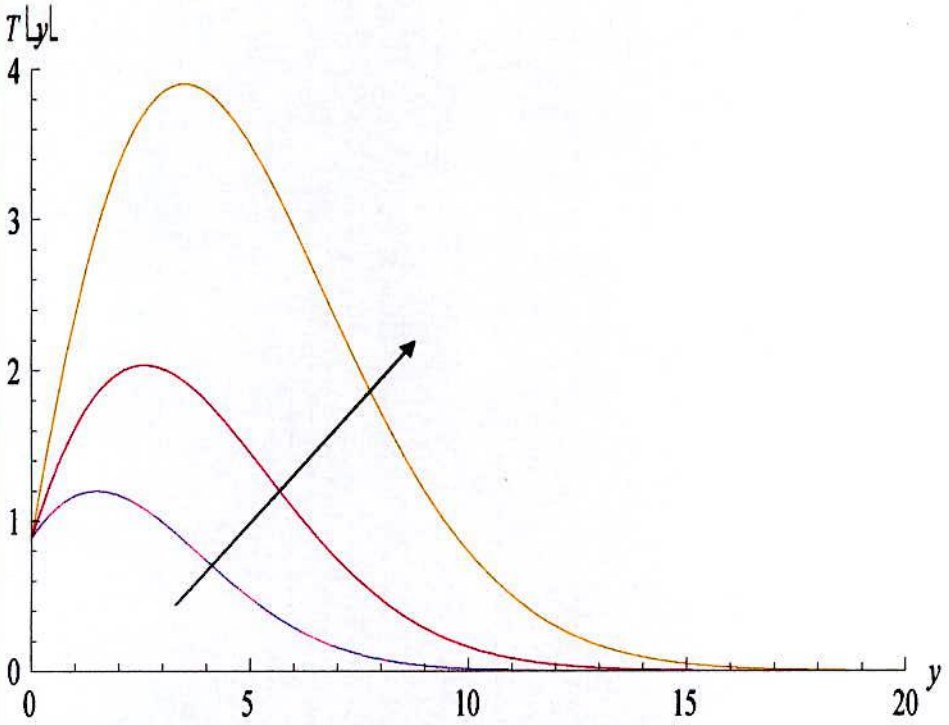

Fig.5.9 Temperature profiles for different values of t (4, 6, 8), taking $\alpha = 0.5, \Pr = 0.71$.

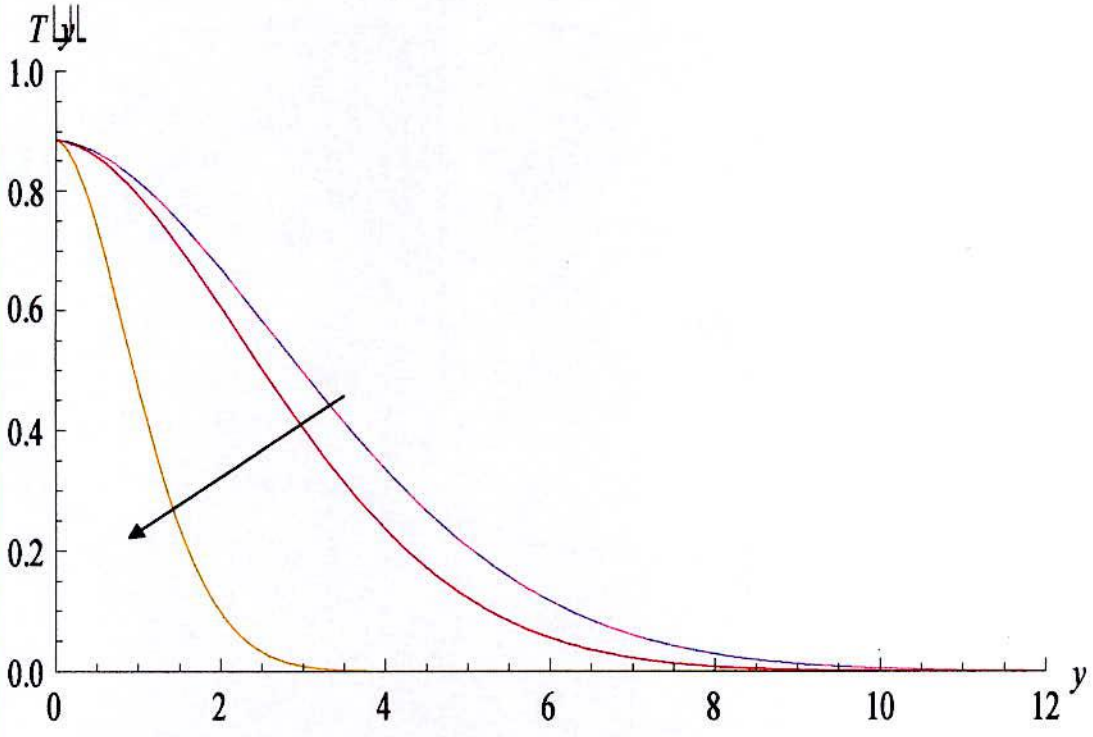

Fig.5.10 Temperature profiles for different values of Pr (0.71, 1.00, 7.01), taking $\alpha = 0.2, t = 4$ as fixed.

In figures(5.8)-(5.10) the temperature profiles for different values of the heat source parameter α, time t and Prandtl number Pr are shown respectively. From Fig(5.8) it is seen that the temperature is increasing with the increase in α and it is becoming zero near the same place away from the wall. Fig(5.9) shows that the temperature also increases with the increase in t, but the temperature is becoming zero at far away for higher values of t. From Fig(5.10) it is seen that the temperature is decreasing with the increase in Pr and it is not becoming zero at the same place away from the wall. The temperature is becoming zero at close to the wall for higher values of Pr.

Figures (5.11)-(5.13) represents the angular momentum profiles for different values of constant E, time t and material parameter λ respectively. Figure (5.11) shows that E has no impact on angular momentum, it is just indicating the starting value near the wall, as a result all the curves are finishing at the same distance from the plate. Figure (5.12) shows that the angular momentum increases and spreads more with the increase in time t. The same is observed from Fig. (5.13) for different values of λ. But the rate of increase or spreading are different for change in different parameters.

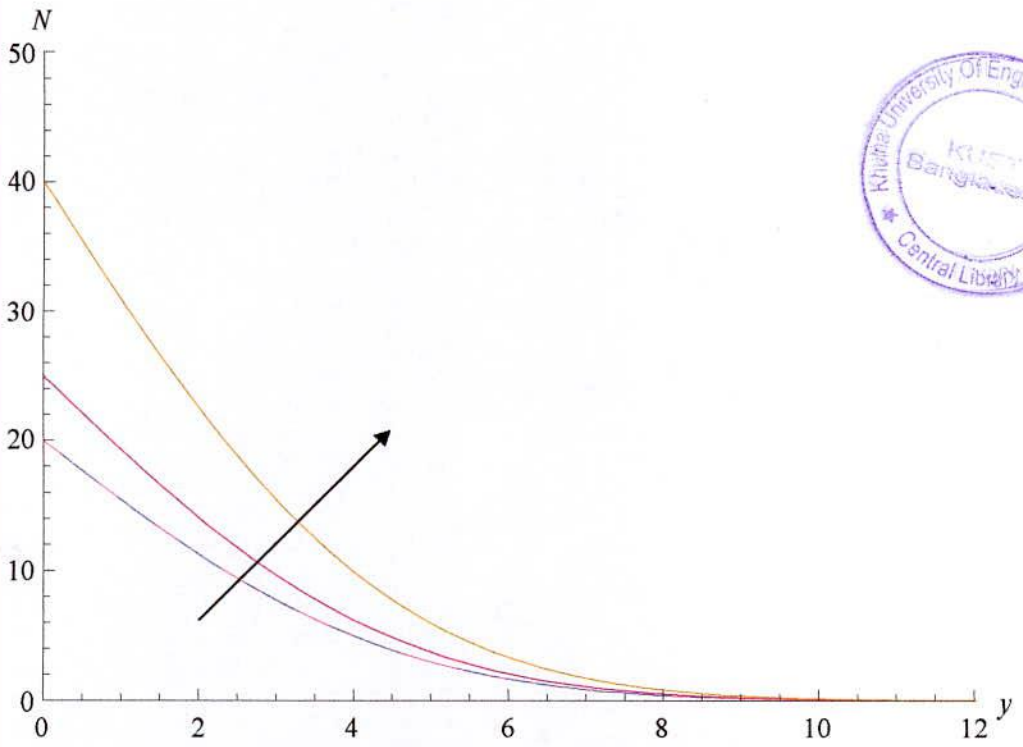

Fig.5.11 Angular momentum profiles for different values of E (20, 25, 40), with $\lambda = 3, t = 2$.

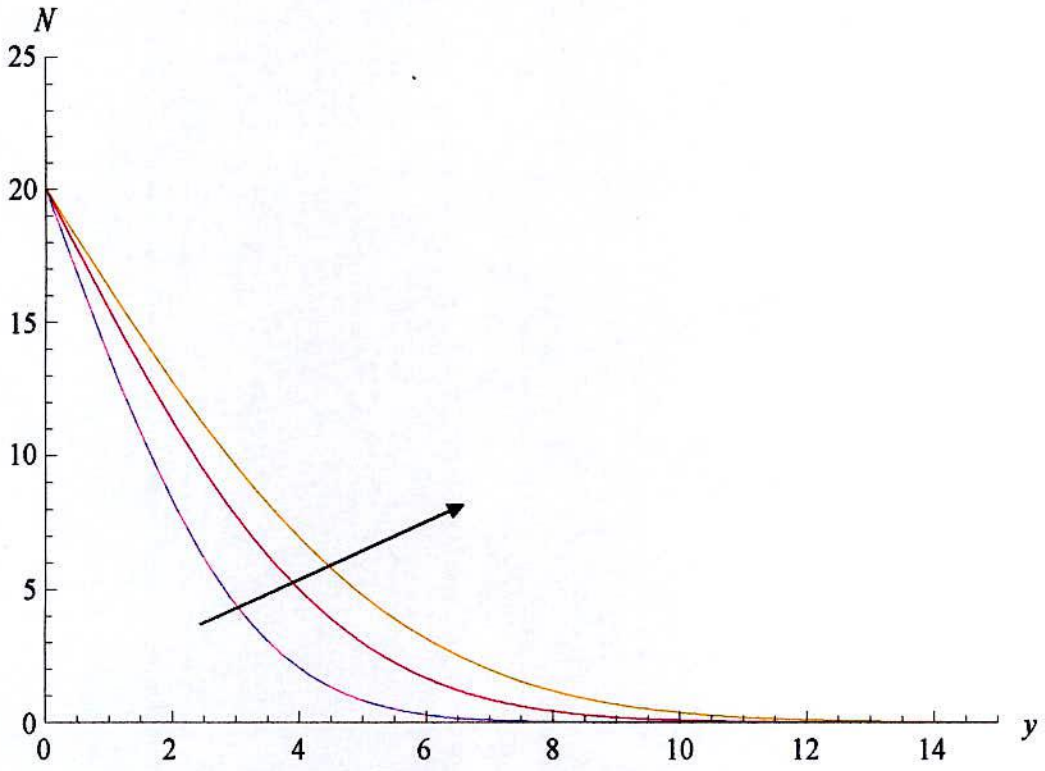

Fig.5.12 Angular momentum profiles for different values of t (1, 2, 3) with $\lambda = 3, E = 20$.

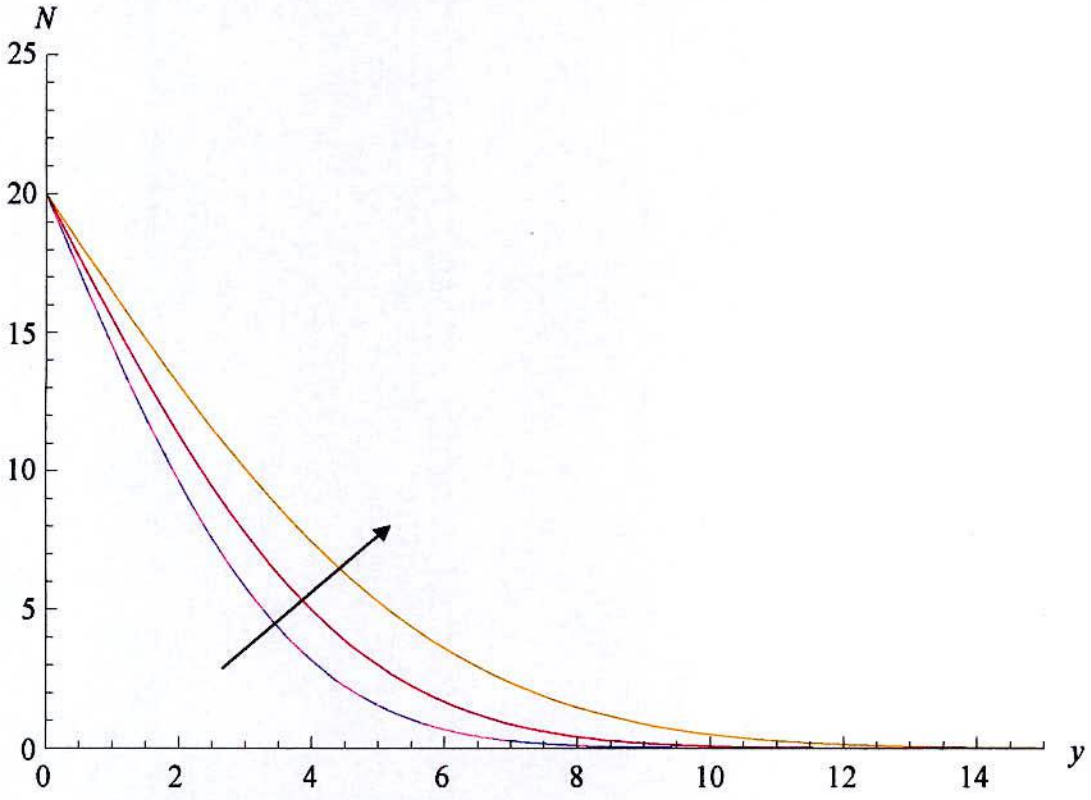

Fig.5.13 Angular momentum profiles for different values of λ (2, 3, 5), with E=20, t =2 .

References

[1] Eringen, A.C., *J. Math.* **16** (1966) 1.

[2] Zakaria, M., *Applied Mathematics and computation*, **151**(2004), 601.

[3] Eringen, A.C., *J. Math. Anal. Appl.* **38** (1972) 469.

[4] Khonsari, M.M., *Acta Mech.* **81** (1990) 235.

[5] Khonsari, M.M. and Brewe, D., *STLe Tribology Transe.* **32** (1989) 155.

[6] Hudimoto, B. and Tokuoka, T., *Int. J Eng. Sci.* **7** (1969) 515.

[7] Lockwood, F., Benchaita, M. and Friberg, S., *ASLE Tribology Trans.* **30** (1987) 539.

[8] Lee, J. D. and Eringen, A. C. , *J. Chem. Phys.* **55** (1971) 4509.

[9] Ariman, T., Turk, A. and Sylvester, N. D., J. *Appl. Mech.* **41** (1974) 1.

[10] Kolpashchikov, V., Migun, N.P. and Prokhorenko, P.P. , *Int. J. Eng. Sci.* **21** (1983) 405.

[11] Arman, T., Turk, M. and Sylvester, N. D., *Int. J. Eng. Sci.* **11** (1973) 905.

[12] Arman, T. and Sylvester,N. D., *Int. J. Eng. Sci.* **12** (1974) 273.

[13] Crane, L. J., *J. Appl. Math. Phys.* **21** (1970) 645.

[14] Chiu, C. P. and Chou, H. M., *Acta Mech.* **101** (1993) 161.

[15] Hassanien, I. A. and Gorla, R. S. R., *Acta Mech.* **84** (1990) 191.

[16] Gorla, R. S. R., *Acta Mech.* **108** (1995) 101.

[17] Ramachandran, N., Chen, T.S. and Armaly, B.F., ASME *J. Heat Trans.* **110** (1988) 373.

[18] Hassanien, I. and Gorla, R. S. R., *Int J Engg Sc* **28** (1990) 783.

[19] Devi, C.D.S., Takhar, H.S. and Nath, G., *Heat and Mass Transfer* **26** (1991) 71.

[20] Lok, Y.Y., Amin, N, Campean, D. and Pop, I., *Int J Num Meth Heat & Fluid Flow* **15** (2005) 654.

[21] Lok, Y.Y., Amin, N. and Pop, I., *Int J Therm Sc* **11** (2006) 49.

[22] Uchida, S. and Aoki, H., *J Fluid Mecha* **82**(2) (1977) 371.

[23] Ohki, M., *Bull of the JSME* **23**(179) (1980) 679.

[24] Goto, M. and Uchida, S., *J Jap Soc Aero Space Sc* **33**(9) (1990) 14.

[25] Bujurke, N. M., Pai, N. P., and Jayaraman, G., *IMA J App Math* **60**(2) (1998) 151.

[26] Majdalani, J., Zhou, C., and Dawson, C. D., *J Biomecha* **35**(10) (2002) 1399.

[27] Dauenhauer, C. E. and Majdalani, J., *Physics of Fluids* **15**(6) (2003) 1485.

[28] Majdalani, J. and Zhou, C., *Zeit Ange Math Mech* **83**(3) (2003) 181.

[29] Soundalgekar, V. M., *Proc. Roy. Soc.* A-**333**, (1973) 25.

[30] Gorla, R.S.R and Tornabane, R., *Transp. Porous Media,* **3,** (1988) 95.

[31] Raptis, A., *Int. J. Heat and Mass Trans*, **41** (1998) 2865.

[32] Kim, Y.J., *Acta Mech.,* **148** (1-4) (2001) 105.

[33] Kim, Y. J. and Fedorov, A. G., *Int. J. Heat and Mass Trans*, **46**(2003) 1751.

[34] El-Amin, M.F., *J. Mag and Mag Mat*, 270 (2004) 130.

[35] El-Hakiem, M. A., *Int. Comm. Heat Mass Transfer*, **31** (2004) 1177.

[36] Caldwell, D. R. , *J Fluid Mech*, **64**(1974) 347.

[37] Groots, S. R. T. and Mozur, P., *Non –equilibrium thermodynamics*, *North Holland, Amsterdam.*(1962)

[38] Hurle, D.T.J. and Jakeman, E., (1971), *J Fluid Mech*, **47**(1971) 667.

[39] Legros, J. C., Van hook, W. K. and Thomas, G., *Chem Phy Let*, **2**(1968) 696.

[40] Legros, J. C., Rosse, D. and Thomas, G., *Chem Phy Let*, **4**(1970) 632.

[41] Somers, F. V., *J App Mech*, **23**(1956) 295.

[42] Gill, W. N., Casel, A. D. and Zeh, D. W., *Int J Heat and Mass Tran,* **8**(1965) 113.

[43] Lowell, R. L. and Adams, J. A., *AIAA, Journal*, **5**(1967) 1360.

[44] Adams, J. A. and Lowell, R. L., *Int J Heat and Mass Tran,* **11**(1968) 1215.

[45] Lightfoot, E. N., *Chem Engg and Sc*, **23**(1968) 931.

[46] Saville, D. A. and Chuchchill, S. W., AICE *Journal,* **16**(1970) 268.

[47] Adams, J. A. and McFadden, P.W., AICE *Journal,* **12**(1966) 642.

[48] Gebhart, B. and Pera, L., *Int J Heat and Mass Tran,* **14**(1971) 2025.

[49] Pera, L. and Gebhart, B., *Int J Heat and Mass Tran,* **15**(1972) 269.

[50] Mollendrof, J. C. and Gebhart, B., *In Proceeding of the 5th International Heat Transfer Conference, Tokyo*, **No. CT 1.3**(1974).

[51] Tenner, A.R. and Gebhart, B., *Int J Heat and Mass Tran,* **14**(1971) 2051.

[52] Hubbel, R. H. and Gebhart, B., *In Proceeding of the 24th Heat Mass Transfer and Fluid Mechanics institute of Corvallis, Oregon (USA),*(1974).

[53] Boura, A. and Gebhart, B., AICE *Journal,* **22**(1976) 94.

[54] Agrawal, H. L., Ram, P.C. and Singh, S.S., *Acta Phy, Hung*, **42**(1977) 49.

[55] Agrawal, H. L., Ram, P.C. and Singh, S.S., *Canadian J Chem Engg*, **58**(1980) 131.

[56] Georgantopoulos, G.A., Koullias, J., Goudas, C. L. and Couragenis, C., *Astro Spa Sc*, **74**(1981) 359.

[57] Haldavneker, D. D. and Soundalgekar, V. M., *Acta Phy, Hung*, **43**, (3/4)(1977) 243.

[58] Soundalgekar, V. M., Gupta, S. K. and Birajdar, N. S., *Nuc Engg*, **53(3)**(1979) 339.

[59] Nanousis, N. D. and Goudas, C. L., *Astro Spa Sc*, **66(1)**(1979) 13.

[60] Raptis, A. A. and Kafoussias, N. G., *Rev. Roum. Sci. Tech. Mech. Appl.*, **27(1)**(1982) 37.

[61] Raptis, A. A. and Tzivanidis, G. J., *Astro Spa Sc*, **94(2)**(1983) 311.

[62]] Raptis, A. A., *Astro Spa Sc*, **92(1)**(1983) 135.

[63] Agrawal, H. L., Ram, P.C. and Singh, V., *Proceeding of National Academy of Science*, **57(II)**(1987) 329.

[64] Schlichting, H., *Boundary Layer Theory, Mcgraw-Hill, New York,*(1968).

[65] Rosenberg, D. U. V., *Method of Numerical Solution of partial differential equations. American Elsevier, New York,* (1969).

[66] Patenker, S. V. and Spalding,, D. V., *Heat and Mass transfer in Boundary Layer. 2nd Edition, Interext Books, London,* (1970).

[67] Spalding, D. B., GENMIX, *A general computer program for two dimensional parabolic phenomena, Program Press, Oxford, UK,*(1977),

[68] Peddinsen, J. and McNitt, R. P., *Recent Advanced Engineering Science,* **5**(1970) 405.

[69] Gorla, R. S. R., *Int J Engg Sci*, **21**(1983) 25.

[70] Takhar, H. S. and Soundalker, V. M., *Int J Engg Sci*, **23**(1985) 201.

[71] Hossain, M. A. and Ahmed, M., *Int J Engg Sci*, **33**(1990) 571.

[72] Mohammadein A. A., El-Hakiem, M. A., El-Kabier, S. M. M. and Mansour, M. A., *App Mech Engg*, **2**(1997) 187.

[73] Rees, D. A. S. and Bassom, A. P., *Int J Engg Sci*, 34(1996)113.

[74] Rees, D. A. S., *IMA, J App Math*, **61**(1997) 179.

[75] El-Amin, M. F., *J Mag and Mag Mat*, **234**(2001) 567.

[76] Rahman, M. M. and satter, M. A., ASME *J Heat and Mass Tran*, **128**(2006) 142.

[77] El-Arabawy, H. A. M., *Int J Heat and Mass Tran*, **46**(2003) 1471.